4520-6003-R0000

FINAL REPORT

for

THEORETICAL INVESTIGATION: THE SCATTERING OF LIGHT BY A PLANETARY ATMOSPHERE

15 September 1965–21 June 1966

Contract No. NAS5-9678

Prepared by
TRW SYSTEMS
One Space Park
Redondo Beach, California

for
GODDARD SPACE FLIGHT CENTER
Greenbelt, Maryland

TRW SYSTEMS

4520-6003-R0000

Final Report
for

Theoretical Investigation; the Scattering of Light by a Planetary Atmosphere

(15 September 1965 - 21 June 1966)

Contract No.: NAS5-9678

Prepared by
Robert S. Fraser
TRW Inc.
One Space Park
Redondo Beach, California

Robert S. Fraser

Robert S. Fraser
Theoretical Physics Department
Quantum Physics Laboratory

S. Altshuler

Saul Altshuler, Manager
Theoretical Physics Department

H C Corben

H.C. Corben, Director
Quantum Physics Laboratory

for

Goddard Space Flight Center
Greenbelt, Maryland

ACKNOWLEDGEMENTS

The author wishes to express his appreciation to the National Center of Atmospheric Research (NCAR) at Boulder, Colorado for the extensive computing services that they provided for this research. The services were provided without charge to the author's employer -- TRW Systems. The author is grateful to Mr. W.H. Walker of NCAR, who skillfully programmed and conducted the computations. Finally, the author is especially grateful to Dr. J.V. Dave of NCAR, who arranged for these services and provided scientific assistance.

ABSTRACT

Computed effects of specular reflection at the ground on the radiation scattered from a Rayleigh atmosphere are presented. The relative contribution to the ground albedo by each of several components of the radiation field is discussed. The characteristics of the neutral points in the degree of polarization that would be observed from the ground looking up or from above the atmosphere looking down are presented.

TABLE OF CONTENTS

LIST OF ILLUSTRATIONS

LIST OF TABLES

1. INTRODUCTION

When a planet is illuminated from the exterior, as by sunlight, the characteristics of the scattered radiation that leaves either the top or the bottom of the planet's atmosphere depend on the reflection properties of the ground, if the optical thickness of the atmosphere is not too large. One useful representation of the characteristics of ground reflection is that part of the reflected light is diffuse and the remaining part is specular.[1] The diffuse reflection characteristics can be specified by the Lambert law, which states that the reflected radiation is isotropic and unpolarized. The characteristics of the specular reflection can be related to those of the incident radiation by means of the Fresnel law. The effect of Lambert reflection on radiation scattered from a Rayleigh atmosphere has been investigated thoroughly.[2,4,7,18] Before discussing the effect of specular reflection, the models used for the computations will be specified.

The computations for three models will be discussed in this report. A model includes both an atmosphere and the ground below it. The atmosphere is identical for the three models; only the reflection characteristics of the grounds differ. The atmosphere is a plane-parallel slab of infinite extent in the horizontal direction. The radiation parameters vary only in a vertical direction, which is perpendicular to the slab's surface. A unit volume of the atmosphere scatters radiation according to the Rayleigh law. As a result of this law, radiation that is scattered from a small volume of matter at right angles to the incident beam is 100 per cent plane polarized, regardless of the polarization of the incident beam. The model atmosphere does not absorb radiation. No radiation is reflected from the ground of one model, which is called the zero ground albedo model. Then for this model of course, the characteristics of the scattered radiation that leaves the atmosphere depend only on the atmosphere. The second model is called the Fresnel model, since the ground is a smooth water surface, which reflects radiation incident on it specularly according to the Fresnel law. If radiation is transmitted through the water surface into the water, it is lost from the radiation field. The index of refraction (m) of sea water is assumed. The value used increases from 1.34 to 1.38

as the total normal optical thickness of the atmosphere (τ_1) increases from 0.02 to 2.00. Finally, the third model is called the Lambert model, since the ground of this model reflects radiation according to the Lambert law. The ground albedos of the Fresnel and Lambert models are identical when the atmospheric optical thickness and solar zenith angle are the same for both models. The source of illumination is parallel, unpolarized radiation that is incident on top of an atmosphere. The incident radiation is directed from the top to the bottom of the atmosphere. This incident radiation will be called solar radiation.

Sekera[19] computed the specific intensity and degree of polarization of the skylight falling on the ground of the Fresnel and of the zero ground albedo models. The degree of polarization and intensity were approximately the same for the two models. However, the neutral points, which refer to the directions in the sky where the light is unpolarized, were considerably different for the two models, when the atmospheric optical thickness was less than 0.50.

The National Aeronautics and Space Administration supported research to compute parameters that characterize scattered radiation which is directed outwards from the top of the atmosphere of the Fresnel model (contract No. NAS5-3891).[10] These parameters included the flux, specific intensity, degree of polarization, and neutral point positions. When parameters for the Fresnel model were compared with corresponding ones for the Lambert model, it was found that the parameters were essentially independent of the ground reflection when the optical thickness was greater than two. If the outward radiation did not come from near the horizon (at large zenith angle), the relative difference between the specific intensities and between the polarizationsfor the two models increased to large values as the optical thickness decreased to $\tau_1 = 0.02$. The outward fluxes for the two models differed by less than five per cent. The neutral points for the two models differed significantly when the optical thickness was less than 0.5. Coulson[4] had found previously that the neutral points for the Lambert model always occur in the sun's vertical plane. (The sun's vertical plane is perpendicular to the horizontal surfaces of a model, contains the zenith direction, and also passes through the sun.)

However, the neutral points for the Fresnel model disappear from the sun's vertical plane for a certain range of solar zenith angle and of optical thickness.[10]

The neutral point characteristics merited additional investigations that were not done on the previous contract, since neutral points are sensitive to the scattering properties of a planetary atmosphere and to the nature of the ground reflection.[4,9,10,11,13,14,15,18,19,20] Furthermore, the neutral point positions could be measured accurately from a satellite. Hence, NASA supported the research reported here, where the principal effort was given to finding the neutral point characteristics for the Fresnel model.

The equations for the Stokes parameters of the diffuse radiation field were obtained by the methods of Chandrasekhar. The derivation of these equations are given in reference 10. The computational methods and their accuracy are also given in that reference. Although the ground albedo for the Fresnel model was discussed in reference 10, new computed albedo data will be given here. In addition to the neutral point characteristics at the top of the atmosphere, new neutral point data for the base of the atmosphere are presented also.

2. GROUND ALBEDO

2.1 GENERAL

Mullamaa[12] has published extensive computations of the albedo of sea surfaces. He took into account the roughness of the sea and polarization effects. Mullamaa calculated the albedos of the direct sunlight, the skylight, and of both combined, but he did not give the relative contribution of each of these components to the total albedo. This information will be given for a smooth sea surface in this report. Mullamaa did not discuss the effect of polarization on the albedo of the skylight, and that will be done here. Since Mullamaa did not relate the albedo of skylight for rough and for smooth surfaces, this too will be done.

2.2 CONTRIBUTIONS OF COMPONENTS TO ALBEDO

The ground albedo, as used here, is defined as the ratio of the upward flux of radiation that is reflected from the surface of the water (or ground) to the downward flux that is incident on the surface. The upward flux does not include the upward radiation that comes from below the surface of the water, or the underwater light. The albedo defined here is sometimes referred to as "surface loss". The <u>total albedo</u> (λ_o) can be considered as the sum of the albedos of components of the radiation field, if each component albedo (λ_o^i) is weighted according to its relative contribution ${}^{\downarrow}F_i$ to the total downward flux of radiation (${}^{\downarrow}F^F$):[10]

$$\lambda_o(\tau_1; \mu_o) = \sum_i \left[{}^{\downarrow}F_i(\tau_1; \mu_o) / {}^{\downarrow}F^F(\tau_1; \mu_o) \right] \lambda_o^i(\tau_1; \mu_o) \qquad (1)$$

$$\lambda_o^i(\tau_1; \mu_o) = \frac{{}^{\uparrow}F_i}{{}^{\downarrow}F_i}$$

The flux and albedo of each component depend on the total normal optical thickness of the atmosphere (τ_1), and on the sun's zenith angle θ_o, where $\theta_o = \cos^{-1} \mu_o$. The superscript F indicates that the total flux (${}^{\downarrow}F^F$) is calculated for the Fresnel model. The flux ${}^{\downarrow}F^F$ is also the global radiation for the Fresnel model.

The radiation field is usefully separated into the direct sunlight, which is attenuated by scattering as it passes through the atmosphere, and the diffuse radiation, which is radiation that is scattered out of the direct sunlight. Fluxes and the albedo that apply to the direct sunlight will be given the subscript or superscript one. The diffuse radiation can be separated into two more components. The most important component for the Fresnel model is the one which reaches the ground without having been reflected from the ground previously. This component will be called the unreflected skylight, since it is not reflected from the water until it reaches the water surface for the first time. The fluxes and albedo of the unreflected skylight are designated by the subscript and superscript two; for example, $^{\uparrow}F_2$ denotes the upward flux of unreflected skylight that is reflected from the water surface only once. The second component of diffuse radiation has been reflected from the ground or water surface at least once, and then is scattered back down to the ground by the atmosphere. This component will be called the reflected skylight. The fluxes and albedo of the reflected skylight will be designated by the subscript and superscript three. The reflected skylight will be shown to make a small contribution to the total albedo. The unmodified word skylight refers to the diffuse radiation that includes both the unreflected and reflected components. The term skylight is synonymous with diffuse radiation. The albedo and relative flux of each component of Eq. (1) will be discussed.

The albedo of the direct sunlight at a smooth water surface is computed according to the Fresnel law. This albedo is given as a function of the angle of incidence, which is equivalent to the solar zenith angle (θ), in Fig. 1. The total specific intensity (I) of the incident radiation, which is unpolarized is assumed to be one unit for Fig. 1. The intensities of the reflected radiation are given for the parallel component, perpendicular component, and sum of the two by $I_{g,\ell}$, $I_{g,r}$, and I_g, respectively. The numerical value of I_g equals the albedo of the sunlight. Twice the values of $I_{g,\ell}$ and of $I_{g,r}$ equal the albedo if the incident radiation were totally plane polarized either parallel or perpendicular, respectively, to the sun's vertical plane.

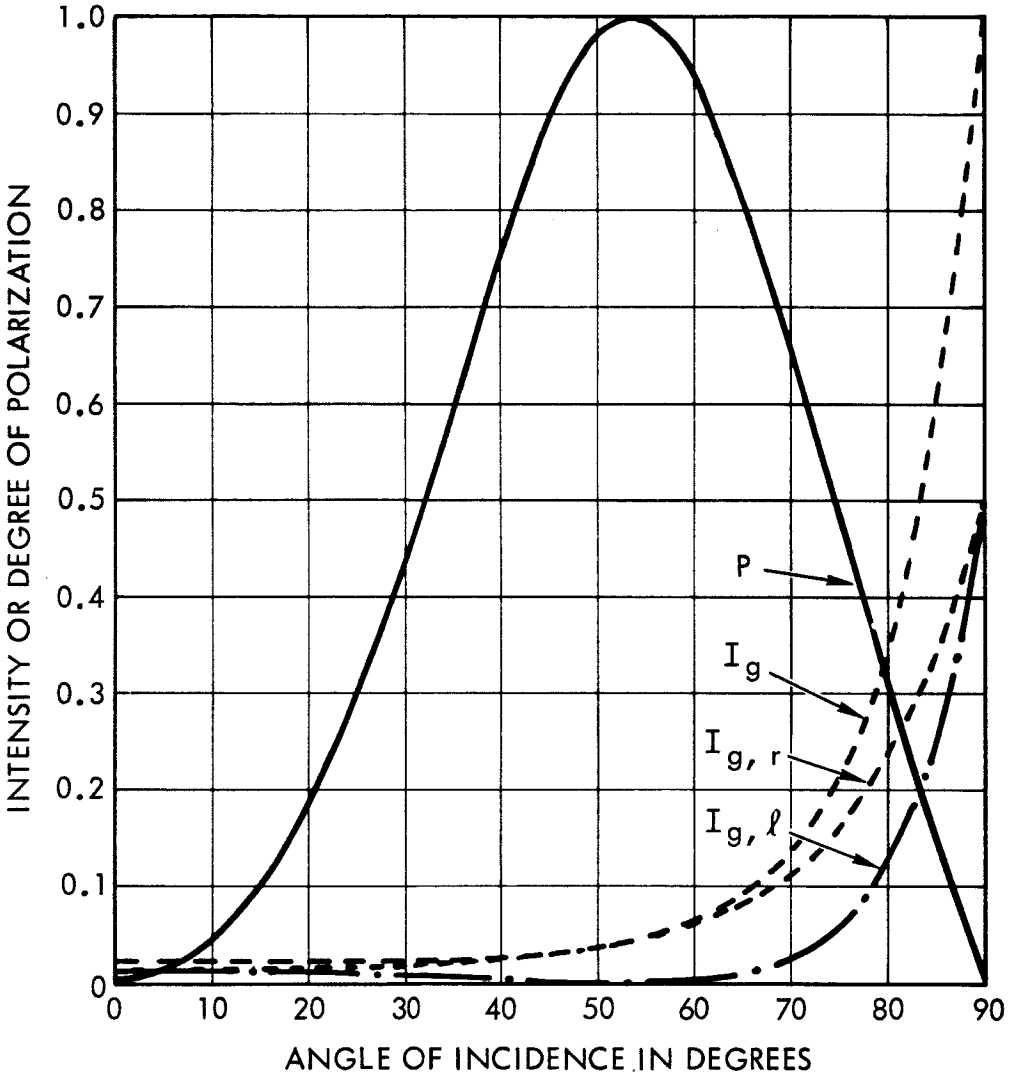

Figure 1. One-half of albedo of l-component ($I_{g,l}$), r-component ($I_{g,r}$), and albedo of neutral component (I_g) of intensity at smooth water surface of m ≐ 1.34. Incident total intensity I = 1. P is degree of polarization. Reflection according to the Fresnel law.

The ratio of the flux of direct sunlight ($^{\downarrow}F_1$) to the total flux ($^{\downarrow}F^F$) is shown in Fig. 2. This ratio is shown for each of the optical thicknesses for which the computations were made and for approximately five values of $\mu_o = \cos \theta_o$, whose limits are $0.05 \leq \mu_o \leq 1$. The data indicate that the direct solar flux makes the largest contribution to the total downward flux at the ground, if $\tau_1 \sec \theta_o$ is less than approximately one. Then of course the diffuse flux exceeds the flux of direct sunlight if $\tau_1 \sec \theta_o > 1$. Another interesting result is that the computed values have a small scatter about a line, which is located in Fig. 2 by eye.

One can show that the ratio $^{\downarrow}F_1/^{\downarrow}F^F$ depends only on $\tau_1 \sec \theta_o$, when $\tau_1 \sec \theta_o$ is small. To do this, consider the simpler Lambert model instead of the Fresnel model. The downward fluxes of global radiation at the bottom of the model atmospheres are the same within a few per cent for the two models. The ratio of the direct to the total flux is:[7]

$$\frac{^{\downarrow}F_1(\tau_1,\mu_o)}{^{\downarrow}F^L(\tau_1,\mu_o)} = \frac{2\left(1 - \lambda_o \bar{s}(\tau_1)\right) e^{-\tau_1/\mu_o}}{\left[\gamma_\ell(\tau_1, \mu_o) + \gamma_r(\tau_1, \mu_o)\right]} \tag{2}$$

The new functions introduced in this equation are defined in reference 7. Deirmendjian and Sekera[7] show that for primary scattering the following relation holds:

$$\frac{1}{(1 - \lambda_o \bar{s})} \quad \frac{\gamma_\ell + \gamma_r}{2} = e^{-\tau_1/\mu_o} + \frac{\tau_1}{2\mu_o} \tag{3}$$

If Eq. (3) is substituted into Eq. (2), then

$$\frac{^{\downarrow}F_1(\tau_1, \mu_o)}{^{\downarrow}F^L(\tau_1, \mu_o)} = \frac{1}{1 + \frac{\tau_1}{2\mu_o} e^{\tau_1/\mu_o}} \doteq 1 - \frac{1}{2}\frac{\tau_1}{\mu_o} - \frac{1}{2}\left(\frac{\tau_1}{\mu_o}\right)^2 \tag{4}$$

if $\tau_1/\mu_o \ll 1$.

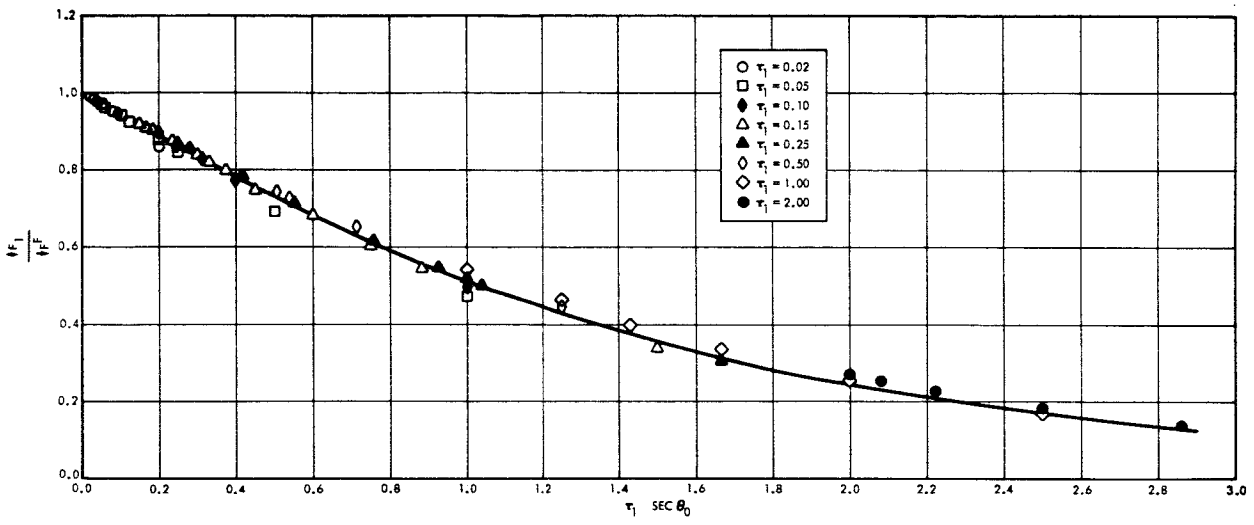

Figure 2. Ratio of direct solar flux to total flux at ground of Fresnel model as a function of τ_1 sec θ_o.

Hence, the ratio of the direct solar to the total flux depends only on the parameter $\tau_1 \sec \theta_o$, when it is small. Of course, if $\tau_1 \sec \theta_o$ is small enough, the functional dependence is linear.

The empirical fact that the ratio ${}^{\downarrow}F_1 / {}^{\downarrow}F^F$ depends essentially on the one parameter $\tau_1 \sec \theta_o$, even when it is large, instead of two parameters τ_1 and $\sec \theta_o$, is curious. The characteristics of the diffuse light falling on the ground depend on τ_1 and $\sec \theta_o$ separately. The diffuse intensity is relatively weak towards the zenith and relatively strong near the horizons at small optical thickness; the reverse is true at large optical thickness.[5,10] The polarization of the diffuse light depends strongly on θ_o and also on τ_1.[18] Nevertheless, the fluxes of diffuse radiation times $\sec \theta_o$ that leave the top or bottom of either the Fresnel or Lambert models depends essentially on $\tau_1 \sec \theta_o$, but not exactly. Where more than one value of the ratio ${}^{\downarrow}F_1/{}^{\downarrow}F^F$ is plotted for one value of $\tau_1 \sec \theta_o$, on Fig. 2, the smallest value of the ratio occurs at the smallest τ_1.

The reflected skylight makes a negligible contribution to the total albedo of the Fresnel model. The albedo of this component (λ_o^3) is less than 0.16 for the optical thickness within the limits $0.02 \leq \tau_1 \leq 2.00$. Also the relative contribution to the total downward flux is small. Figure 3 shows that the fraction of total downward flux $({}^{\downarrow}F^F)$ that is contributed by the reflected component $({}^{\downarrow}F_3)$ is less than 0.04, if the sun is at the zenith, and increases, but remains less than 0.10, when the solar zenith angle increases to $\theta_o = 84^o$. The contribution of the reflected skylight depends essentially on two factors: 1, the albedo of the direct sunlight and unreflected skylight and 2, the fraction of this reflected radiation that is scattered back to the ground by the atmosphere, which depends on the reflectivity of the atmosphere. If the solar zenith angle $\theta_o < 65^o$, less than 10 per cent of the incident flux is reflected by the water (Fig. 9). The albedo exceeds 10 per cent, if both $\theta_o > 65^o$ and $\tau_1 < 0.6$. However, under these conditions the reflectivity of the atmosphere is small, as will be demonstrated with Figs. 4 and 5.

The reflectivity of the atmosphere for illumination at the base is defined as the inverse ratio of upward flux into the base of the

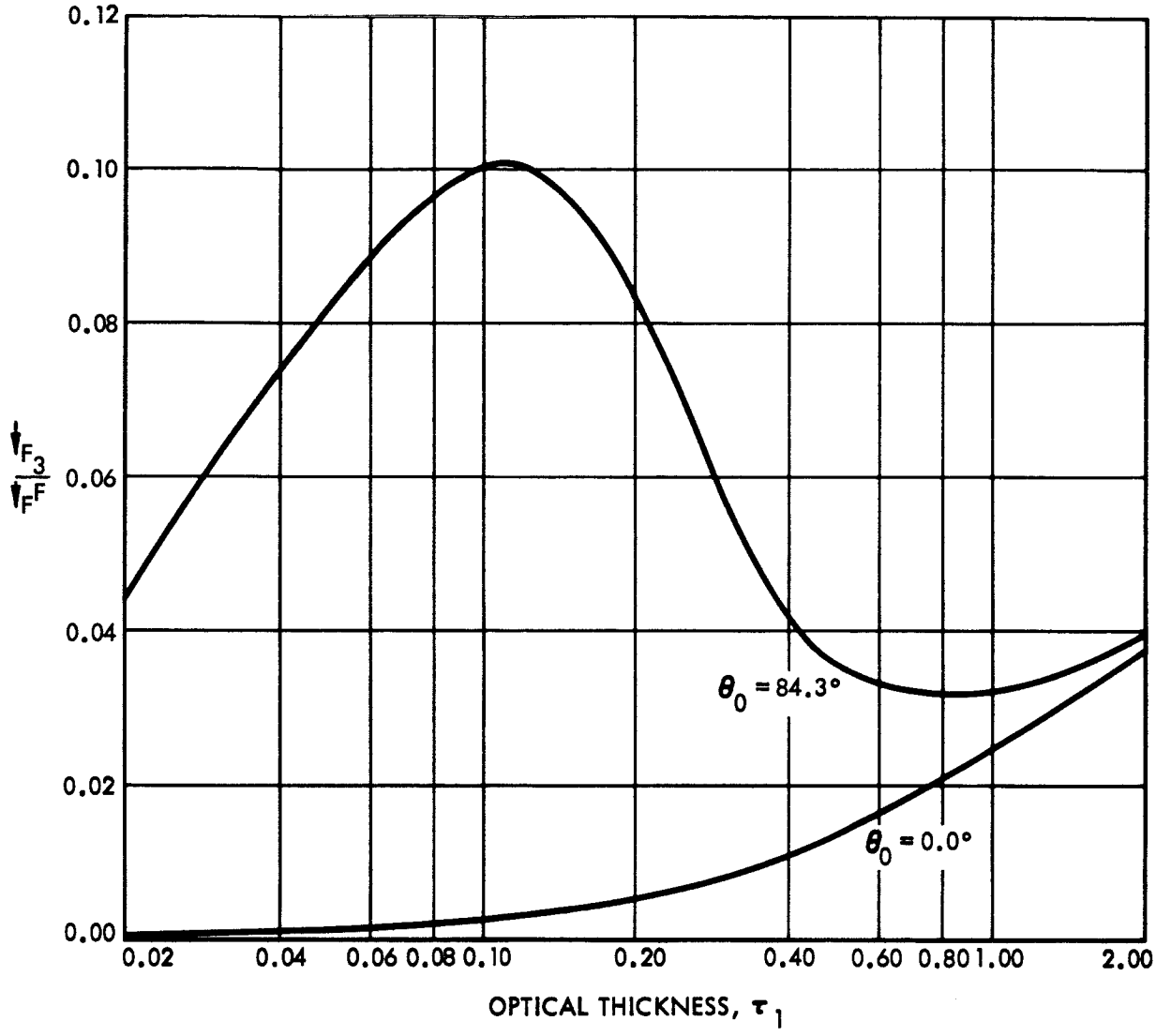

Figure 3. Ratio of downward flux of reflected skylight to total downward flux at base of atmosphere for Fresnel model.

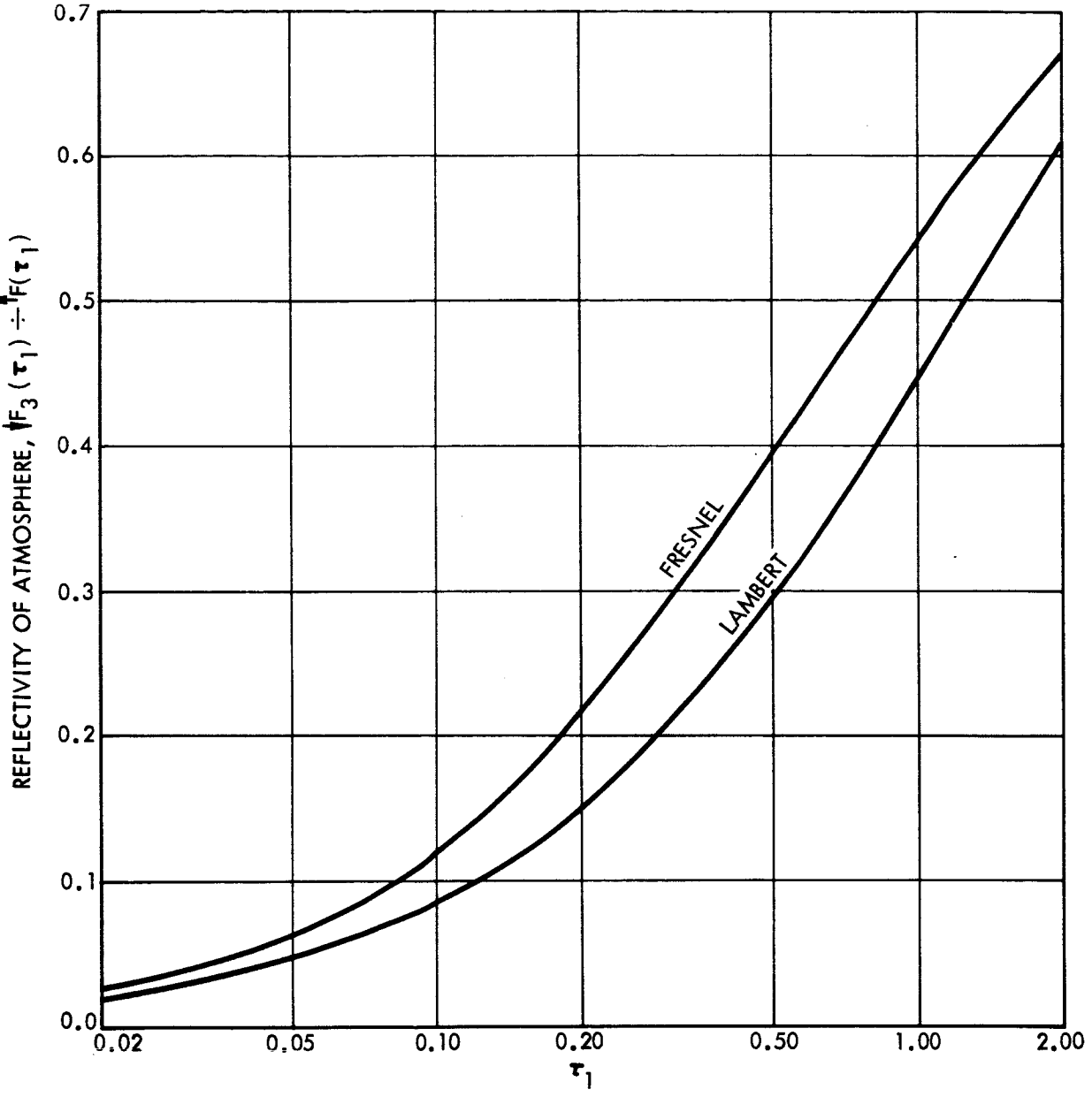
0.7
0.6
0.5
0.4
0.3
0.2
0.1
0.0
REFLECTIVITY OF ATMOSPHERE, $\frac{1}{4}F_3(\tau_1) \div \frac{1}{4}F(\tau_1)$
FRESNEL
LAMBERT
0.02
0.05
0.10
0.20
0.50
1.00
2.00
τ_1

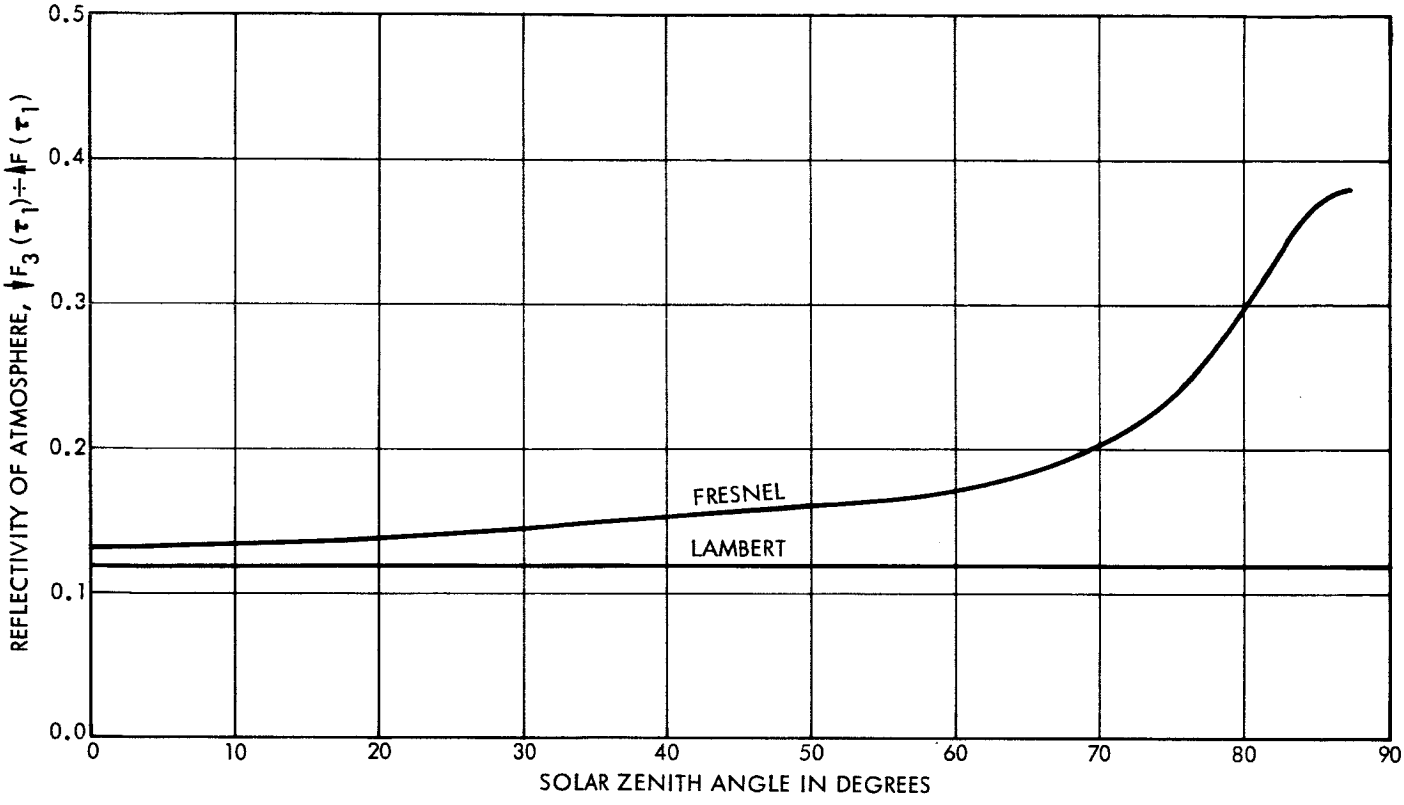

Figure 5. Reflectivity of atmosphere to illumination from below as a function of θ_o. $\tau_1 = 0.15$.

atmosphere to the flux of this radiation that is scattered back down to the ground by the atmosphere: $^{\downarrow}F_3(\tau_1; \mu_o) + \left[{}^{\uparrow}F_1(\tau_1; \mu_o) + {}^{\uparrow}F_2(\tau_1; \mu_o) + {}^{\uparrow}F_3(\tau_1; \mu_o)\right]$. The reflection of both direct sunlight and skylight are accounted for. The reflectivity of the atmosphere for the Fresnel and the Lambert models are given as a function of optical thickness and for $\theta_o = 60^o$ in Fig. 4. The atmospheric reflectivity of the Lambert model increases as τ_1 increases, since the nature of the illumination into the base of the atmosphere remains constant; that is the upward illumination is unpolarized and isotropic. The atmospheric reflectivity for both the Lambert and Fresnel models approaches one as $\tau_1 \to \infty$. The atmospheric reflectivity for the Fresnel model exceeds that of the Lambert model when $\theta_o = 60^o$, because relatively more radiation enters the bottom of the atmosphere of the Fresnel model at large zenith angle than at small zenith angle. This fact will be demonstrated later on Fig. 7. The longer the optical path of radiation through the atmosphere, the greater the probability that it will be scattered back to the water. The reflectivities for the Fresnel and the Lambert models are shown as a function of solar zenith angle for $\tau_1 = 0.15$ in Fig. 5. The Lambert reflectivity is independent of solar zenith angle. The atmospheric reflectivity for the Fresnel model increases as θ_o increases, since the intensity of radiation leaving the water at large solar zenith angle increases. Other computed data not given here show that the reflectivity of the atmosphere of the Fresnel model always exceeds that for the Lambert model when the optical thickness lies in the range $0.05 \leq \tau_1 \leq 2.00$, except when the sun is near the zenith at $\tau_1 = 0.05$ ($\theta_o < 18^o$).

In order to show the contribution of zones of the sky to the albedo of skylight, the cumulative downward and upward fluxes of skylight at the surface of the water are shown as a function of $\mu = \cos\theta$ in Figs. 6 and 7. All the total cumulative fluxes are normalized to one. Figure 6 shows the cumulative fluxes for small and for large θ_o at $\tau_1 = 0.15$. The cumulative downward flux for large zenith angle exceeds that for small θ_o, except where $\mu = 0.0$ and 1.0. Consequently, the ratio of the total intensity of skylight from near the horizons to that from the zenith is greater at the larger solar zenith angle (θ_o). It does not necessarily follow that the cumulative upward flux will also be greater at the larger θ_o, because the

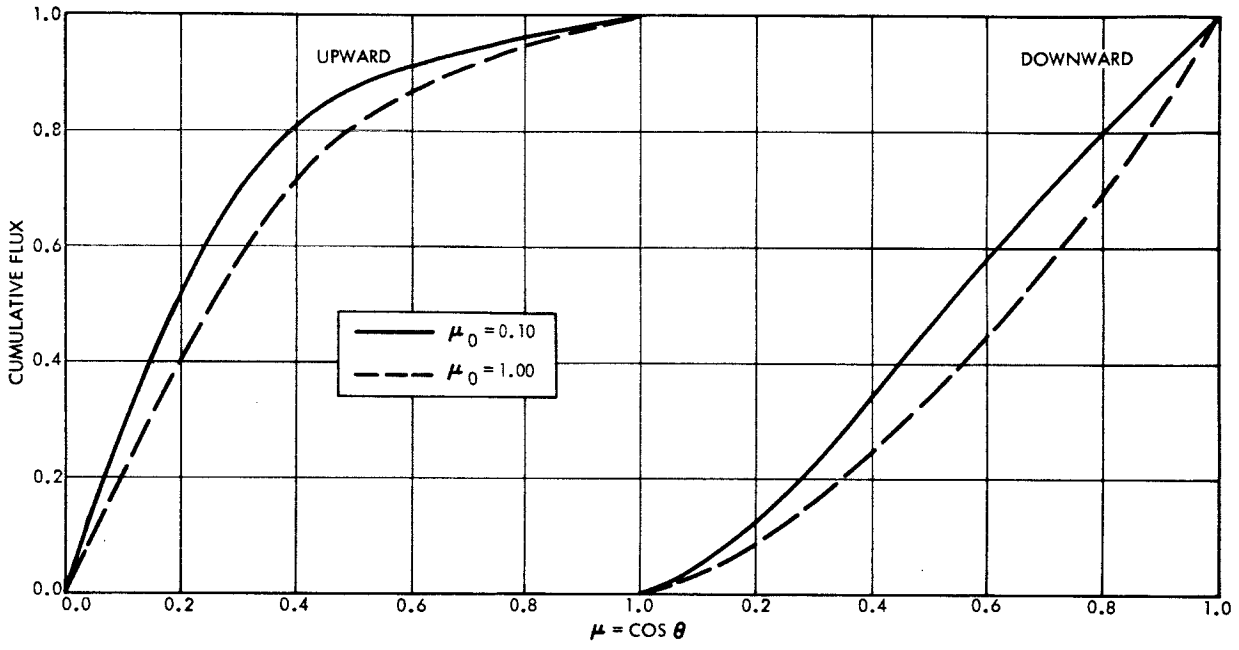

Figure 6. Cumulative relative flux of skylight at base of atmosphere. $\tau_1 = 0.15$.

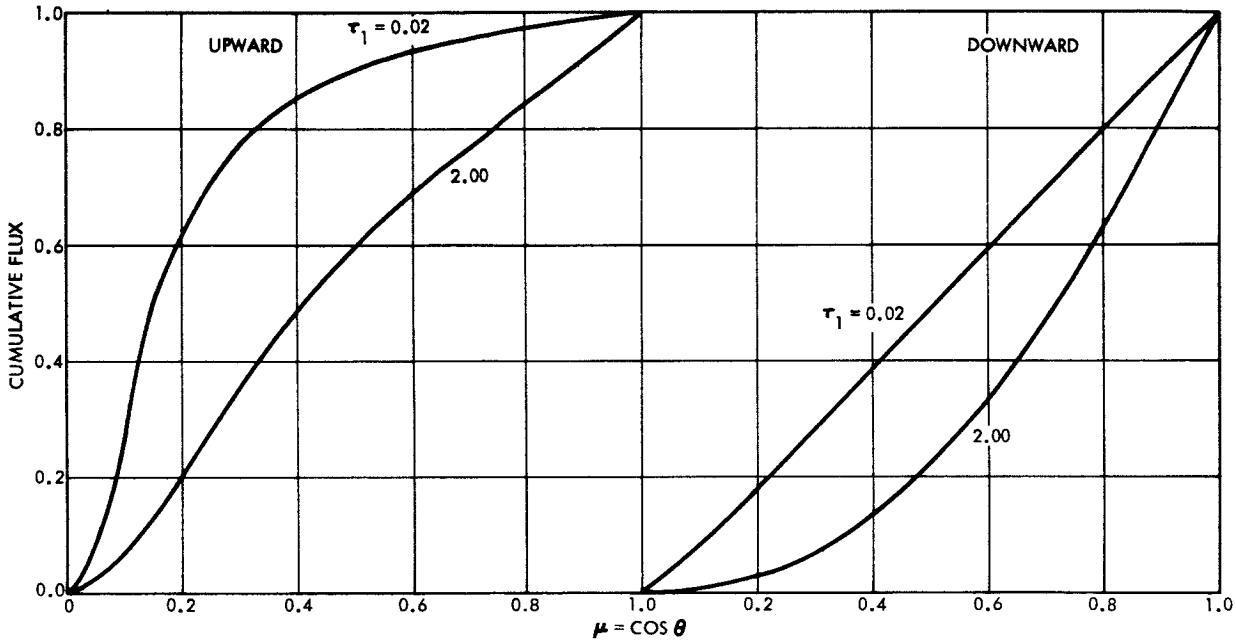

Figure 7. Cumulative relative flux of skylight at base of atmosphere. $\theta_o = 60^o$.

reflectance of the diffuse radiation depends on its polarization. However, in the case of $\tau_1 = 0.15$, the cumulative upward flux is greater at the larger θ_o. Curves of upward cumulative flux for both small and large θ_o show that at least one-half of the upward flux occurs for $\mu < 0.26$, or $\theta > 75^o$. It should be remembered that if a spherical model were used instead of a plane-parallel model, the intensity of the skylight from near the horizons would be different. The large contribution to the upward flux of diffuse radiation by reflected skylight leaving the water at large zenith angles has an important bearing on the computation of the albedo of rough sea surfaces. It is difficult to compute the reflectance of light incident at a large angle on a rough sea, because of multiple reflections on the water surface and because part of the surface is shaded by other elements. A small error in the reflection coefficient for radiation incident at large angles could cause a large error in the albedo.

The cumulative fluxes of diffuse radiation are shown for small and large optical thickness when $\theta_o = 60^o$. The larger value of the cumulative downward flux at the smaller optical thickness occurs because the sky is brighter than the zenith at $\tau_1 = 0.02$, and the opposite is true at $\tau_1 = 2.0$. Eighty per cent of the upward flux for $\tau_1 = 0.02$ but only one-half of that for $\tau_1 = 2.0$ occurs for zenith angles greater than 70^o.

The relative contribution to the ground albedo by each of three components of the radiation field is shown in Fig. 8. The value of the quantity $({}^{\downarrow}F_i \lambda_o^i) \div ({}^{\downarrow}F \lambda_o)$, which appears in Eq. (1), is given. The total albedo $\lambda_o(\tau_1)$ varies between 0.06 and 0.08, as shown. The relative contribution of the reflected skylight, is less than 0.06. Hence, the albedo is determined essentially by the direct sunlight and by the unreflected skylight. The curves for these two components cross at $\tau_1 = 0.47$; the direct sunlight dominates the total albedo at smaller optical thickness, and the skylight dominates at larger optical thickness.

The total albedo at the ground for the Fresnel model is shown in Fig. 9. The total albedo is less than 0.10 if the solar zenith angle $\theta_o < 65^o$ and also if $\tau_1 > 0.6$. The total albedo becomes large at small optical thickness and large θ_o. The total ground albedos for the Lambert

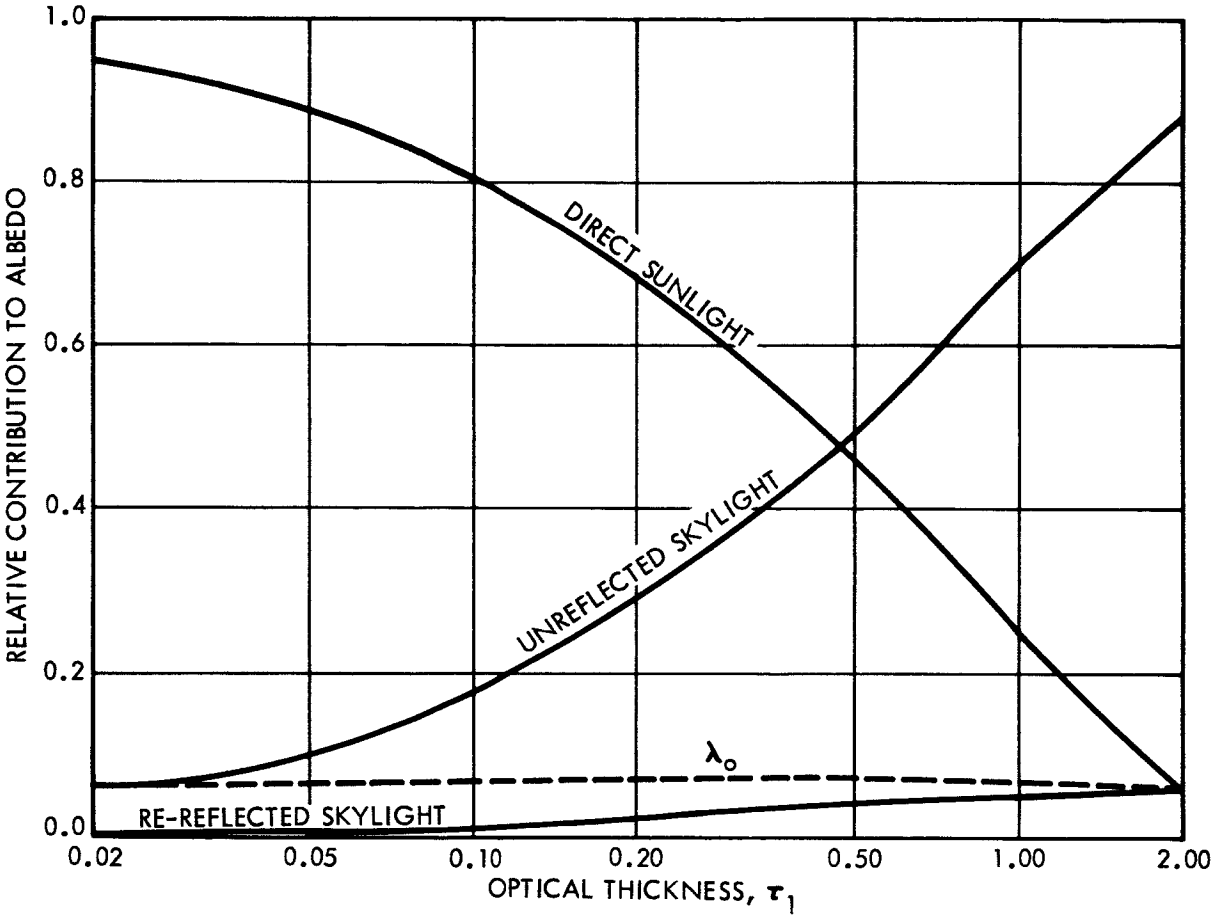

Figure 8. Relative contributions by components of radiation field to total albedo at water surface of Fresnel model. $\theta_o = 60^o$.

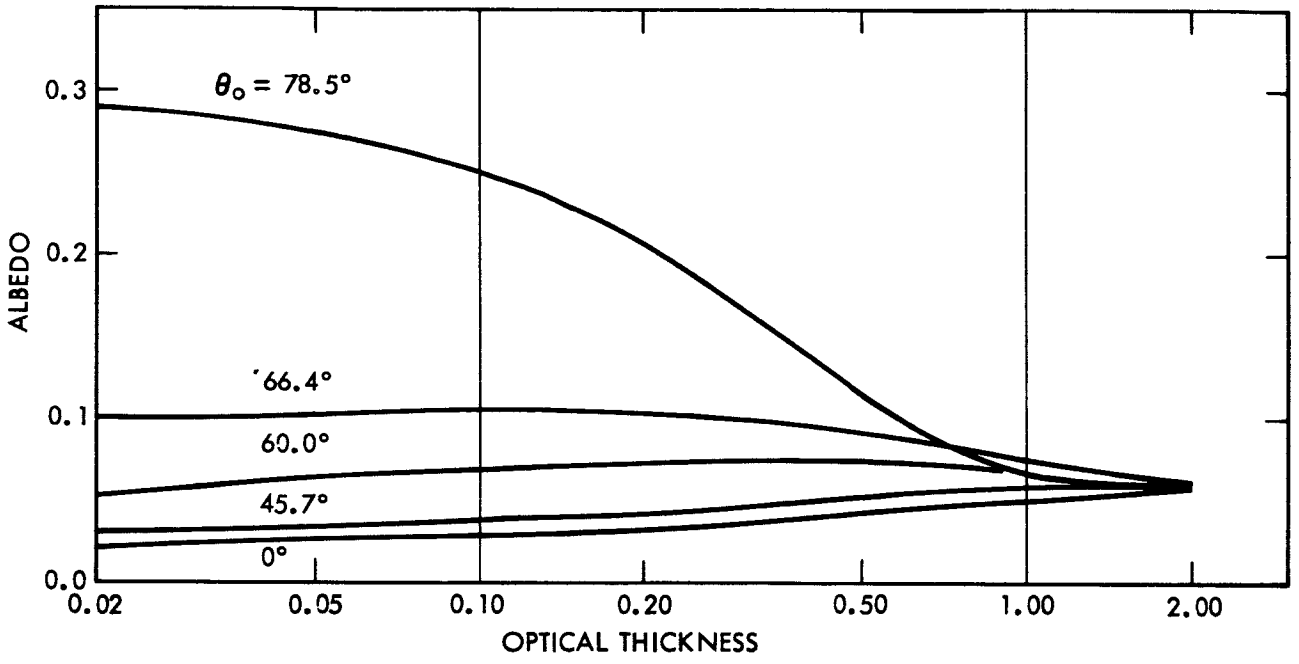

Figure 9. Total albedo at smooth water surface of Fresnel model as a function of optical thickness.

model are assigned the same values that appear on Fig. 9.

2.3 POLARIZATION

The effect of polarization on the albedo of the skylight at the water surface will be discussed for the Fresnel model in this section. Either the incident or reflected diffuse flux of radiation at the water surface is computed from the total specific intensity (I) by the following equation:

$$\uparrow\downarrow F(\tau_1; \mu_o) = \int_o^{2\pi} \int_o^1 \uparrow\downarrow I(\tau_1; \mu, \varphi; \mu_o, \varphi_o)\, \mu\, d\varphi d\mu \qquad (5)$$

where the double arrows indicate that both upward and downward radiation are represented. Since the intensity can be expressed as a harmonic series in the azimuth difference of $\varphi_o - \varphi$ the flux depends only on the azimuth-independent intensity $\uparrow\downarrow I^{(o)}(\tau_1; \mu; \mu_o)$:

$$\uparrow\downarrow F(\tau_1; \mu_o) = 2\pi \int_o^1 \uparrow\downarrow I^{(o)}(\tau_1; \mu; \mu_o)\, \mu\, d\mu \qquad (6)$$

The azimuth-independent intensity can be separated into two components parallel and perpendicular to a local vertical plane:

$$I^{(o)} = I_\ell^{(o)} + I_r^{(o)} \qquad (7)$$

When Eq. (7) is substituted into Eq. (6), the latter can be expressed as

$$\uparrow\downarrow F(\tau_1; \mu_o) = \uparrow\downarrow F_\ell(\tau_1; \mu_o) + \uparrow\downarrow F_r(\tau_1; \mu_o) \qquad (8)$$

where

$$\uparrow\downarrow F_{\ell,r}(\tau_1, \mu_o) = 2\pi \int_o^1 \uparrow\downarrow I_{\ell,r}^{(o)}(\tau_1; \mu, \mu_o)\, \mu\, d\mu \qquad (9)$$

The upward intensities are related to the downward intensities by means of the following equations:[10]

$$\uparrow I_r^{(o)}(\tau_1; \mu) = R(\mu) \downarrow I_r^{(o)}(\tau_1; \mu) \tag{10}$$

$$\uparrow I_\ell^{(o)}(\tau_1; \mu) = q^2(\mu)\, R(\mu) \downarrow I_\ell^{(o)}(\tau_1; \mu) , \tag{11}$$

where the reflection coefficients R and q^2R are defined for the Fresnel model in reference 10. If Eq. (10) and (11) are substituted into Eq. (9), the equations for the upward components of diffuse flux are:

$$\uparrow F_\ell(\tau_1; \mu_o) = 2\pi \int_o^1 q^2(\mu)\, R(\mu) \downarrow I_\ell^{(o)}(\tau_1; \mu, \mu_o)\, \mu\, d\mu \tag{12}$$

$$\uparrow F_r(\tau_1; \mu_o) = 2\pi \int_o^1 R(\mu) \downarrow I_r^{(o)}(\tau_1; \mu, \mu_o)\mu\, d\mu \tag{13}$$

The albedo of the diffuse radiation, or skylight, is defined as the ratio of the reflected to the incident downward flux of diffuse radiation. This albedo can be expressed in terms of the l- and r-components by using Eq. (8):

$$\lambda_o^d(\tau_1; \mu_o) = \frac{\uparrow F_\ell(\tau_1; \mu_o) + \uparrow F_r(\tau_1; \mu_o)}{\downarrow F(\tau_1; \mu_o)} \tag{14}$$

where the superscript d indicates the albedo of diffuse radiation. Equation (14) can be expressed in the following form:

$$\lambda_o^d(\tau_1; \mu_o) = \frac{\downarrow F_\ell(\tau_1; \mu_o)}{\downarrow F(\tau_1; \mu_o)} \lambda_o^\ell(\tau_1; \mu_o) + \frac{\downarrow F_r(\tau_1; \mu_o)}{\downarrow F(\tau_1; \mu_o)} \lambda_o^r(\tau_1; \mu_o) \tag{15}$$

where

$$\lambda_o^{\ell,r} = \uparrow F_{\ell,r} \,/\, \downarrow F_{\ell,r}$$

that is, λ_o^{ℓ} and λ_o^{r} represent the albedos of the l- and r-components, respectively, of the total diffuse flux. According to Eq. (15), the albedo of diffuse radiation, or of skylight, equals the sum of the albedos of the l- and r-components, when they are weighted by their relative contribution to the total downward flux of diffuse radiation.

An expression will be derived for the albedo of the skylight, when the polarization of the skylight incident on a smooth water surface is neglected. Let such an albedo be defined by the equation

$$\lambda_o^{d,n}(\tau_1; \mu_o) = {}^{\uparrow}F_n(\tau_1; \mu_o) \;/\; {}^{\downarrow}F_n(\tau_1; \mu_o) \tag{17}$$

where the superscript and subscript n indicate that the polarization of the skylight incident on the water is neglected. The equation for the upward flux of reflected light is

$$ {}^{\uparrow}F_n(\tau_1; \mu_o) = 2\pi \int_o^1 R(\mu) \left[\frac{1 + q^2(\mu)}{2}\right] \left[{}^{\downarrow}I_{\ell}^{(o)}(\tau_1; \mu, \mu_o) + {}^{\downarrow}I_r^{(o)}(\tau_1; \mu, \mu_o) \right] \mu d\mu \tag{18}$$

If Eqs. (12) and (13) are substituted into Eq. (18), then the expression for ${}^{\uparrow}F_n$ becomes

$$ {}^{\uparrow}F_n(\tau_1; \mu_o) = {}^{\uparrow}F(\tau_1; \mu_o) + \pi \int_o^1 R(\mu) \left[1 - q^2(\mu)\right] {}^{\downarrow}Q^{(o)}(\tau_1; \mu, \mu_o)\, \mu d\mu \tag{19}$$

where

$$ {}^{\downarrow}Q^{(o)} = {}^{\downarrow}I_{\ell}^{(o)} - {}^{\downarrow}I_r^{(o)} \gtrless 0 \quad . \tag{20}$$

Equation (19) states that if the polarization of the incident skylight is neglected, the flux of reflected light (${}^{\uparrow}F_n$) equals the flux of reflected skylight for the Fresnel model (${}^{\uparrow}F$) plus the integral that appears on the right-hand side of Eq. (19). The term in brackets in the integrand is greater than or equal to zero; $1 - q^2 \geq 0$. If the skylight is neutral,

$Q^{(o)} = 0$, and ${}^{\uparrow}F_n = {}^{\uparrow}F$. Otherwise, ${}^{\uparrow}F_n$ can be greater or less than the flux of reflected diffuse light for the Fresnel model (${}^{\uparrow}F$) because of Eq. (20).

The downward flux of diffuse light at the water surface may be related to components of the radiation field by the following equation:

$$
\begin{aligned}
{}^{\downarrow}F_n(\tau_1; \mu_o) = {}^{\downarrow}F_2(\tau_1; \mu_o) &+ {}^{\downarrow}F_{3,1}(\tau_1; \mu_o) + \\
&{}^{\downarrow}F^n_{3,2}(\tau_1; \mu_o) + \\
&{}^{\downarrow}F^n_{3,3}(\tau_1; \mu_o)
\end{aligned}
\tag{21}
$$

The components of the diffuse radiation field that were introduced in Eq. (1) are subdivided again in Eq. (21). ${}^{\downarrow}F_2$ is the flux of unreflected skylight. The sum of ${}^{\downarrow}F_3 = {}^{\downarrow}F_{3,1} + {}^{\downarrow}F^n_{3,2} + {}^{\downarrow}F^n_{3,3}$ is the flux of radiation that has been reflected from the water at least once, and then is scattered back down to the water by the atmosphere above it. ${}^{\downarrow}F_{3,1}$ and ${}^{\downarrow}F^n_{3,2}$ refer to the direct sunlight and skylight that has previously been reflected from the water just once. ${}^{\downarrow}F^n_{3,3}$ refers to the component that has been reflected from the water more than once.

The flux ${}^{\downarrow}F^n$ was not computed; but it approximately equals the flux of skylight for the Fresnel model (${}^{\downarrow}F$). The relation between the Fresnel flux and its components is

$$
\begin{aligned}
{}^{\downarrow}F(\tau_1; \mu_o) = {}^{\downarrow}F_2(\tau_1; \mu_o) &+ {}^{\downarrow}F_{3,1}(\tau_1; \mu_o) \\
&+ {}^{\downarrow}F_{3,2}(\tau_1; \mu_o) \\
&+ {}^{\downarrow}F_{3,3}(\tau_1; \mu_o)
\end{aligned}
\tag{22}
$$

where ${}^{\downarrow}F_{3,2}$ and ${}^{\downarrow}F_{3,3}$ correspond to ${}^{\downarrow}F^n_{3,2}$ and ${}^{\downarrow}F^n_{3,3}$, respectively, but have different values, in general. ${}^{\downarrow}F_{3,2} + {}^{\downarrow}F_{3,3}$ and ${}^{\downarrow}F^n_{3,2} + {}^{\downarrow}F^n_{3,3}$ make small contributions to Eqs. (21) and (22), respectively, since the albedo of the

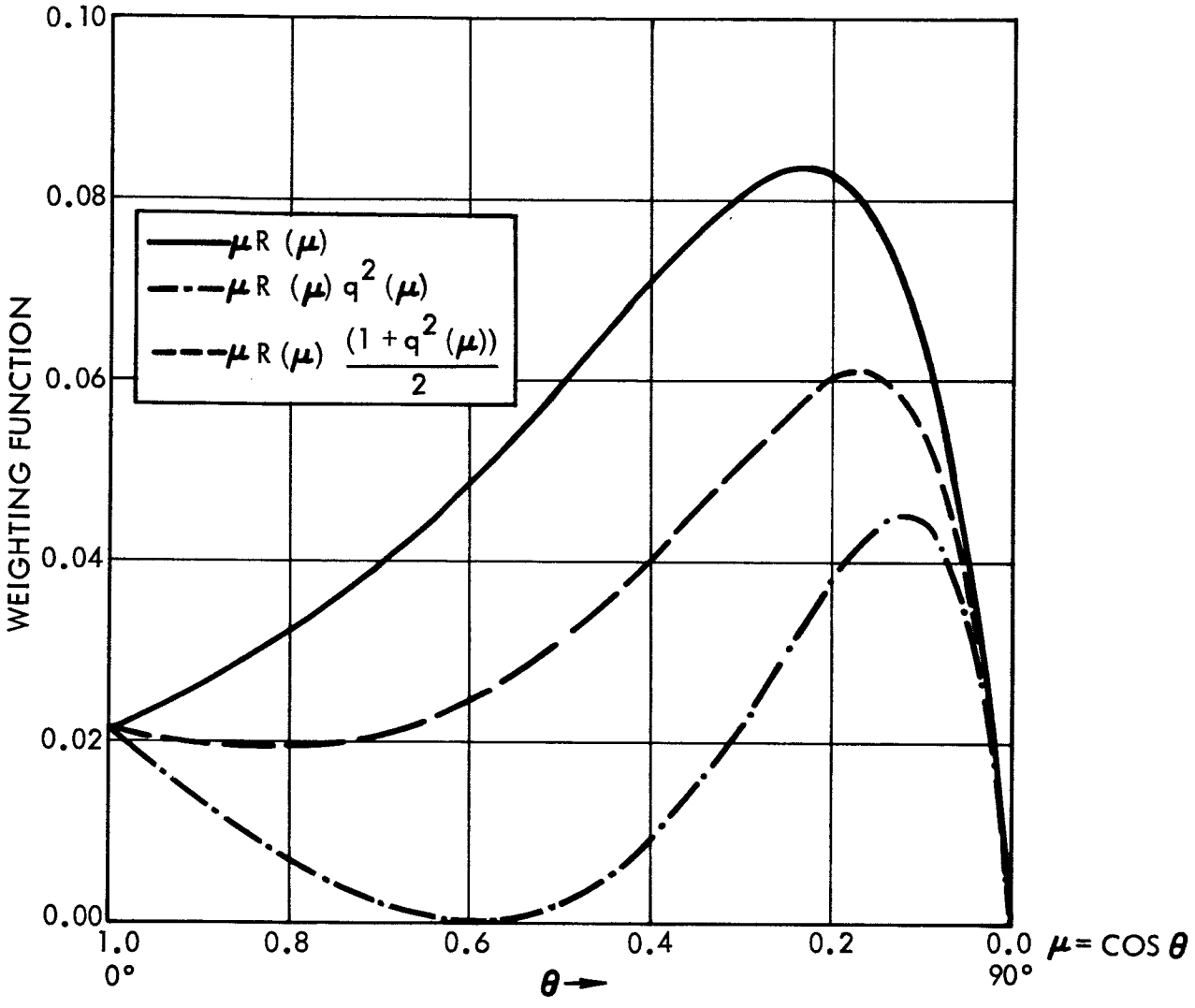

Figure 10. Weighting functions for reflection according to Fresnel law. m = 1.344.

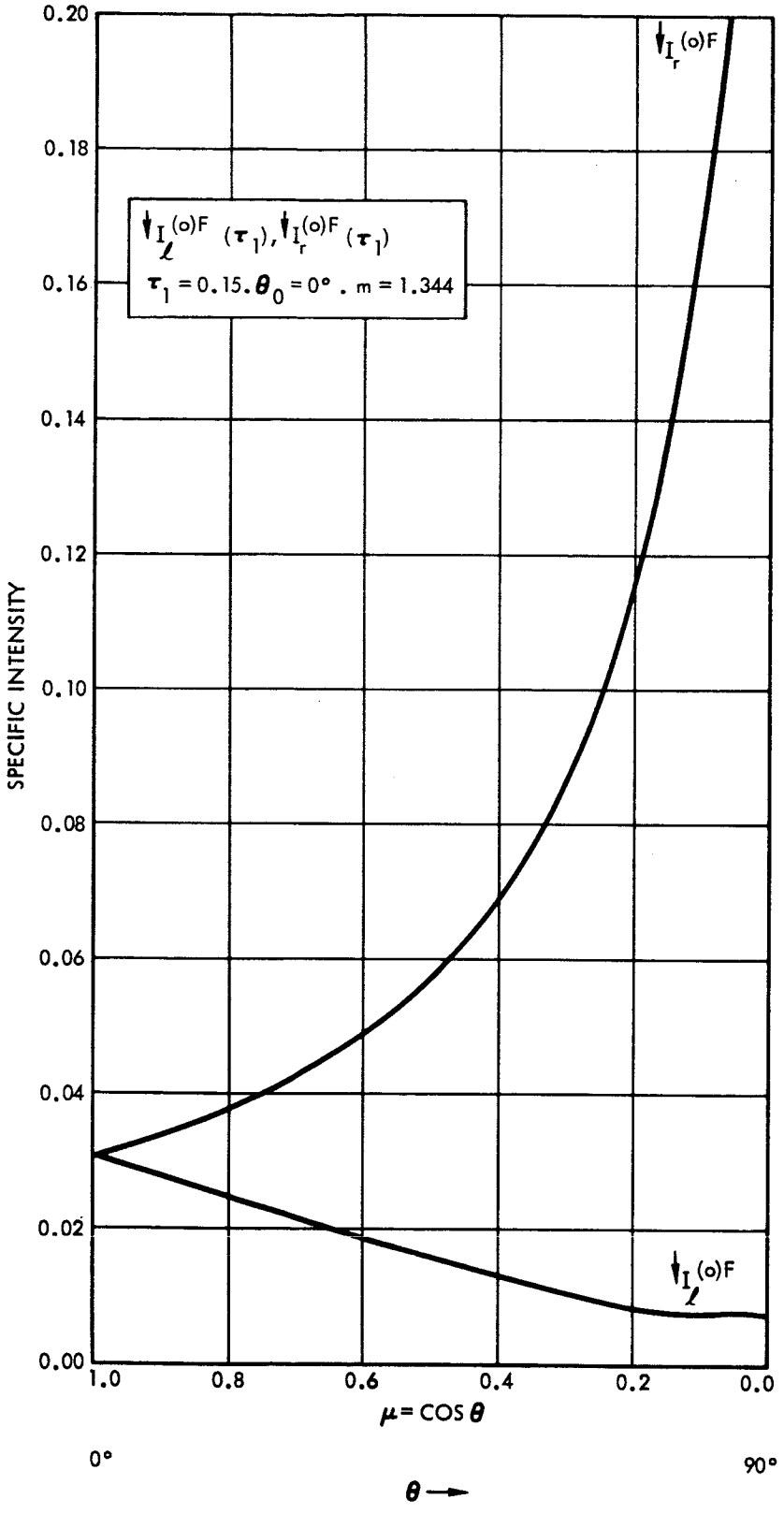

Figure 11. Azimuth independent l- and r-components of intensity of skylight at base of atmosphere of Fresnel model. $\tau_1 = 0.15$. $\theta_o = 0^o$.

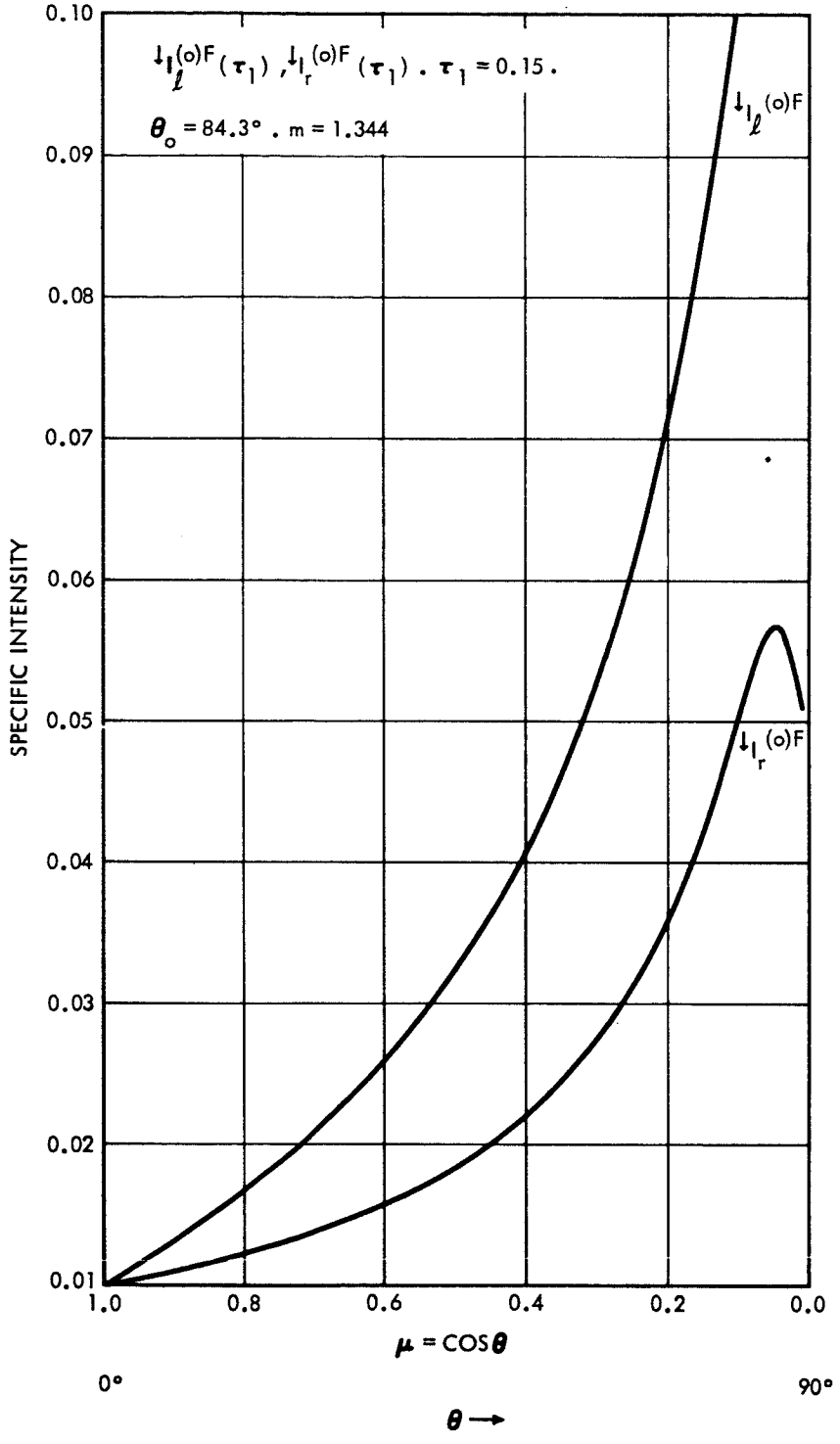

Figure 12. Azimuth independent l- and r-components of intensity of skylight at base of atmosphere of Fresnel model. $\tau_1 = 0.15$. $\theta_o = 84.3°$.

diffuse light is less than 20% for $\tau_1 \geq 0.02$, and part of that reflected radiation is lost from the top of the atmosphere. Hence, ${}^{\uparrow}F_n$ will be replaced by ${}^{\downarrow}F$ in Eq. (17) to obtain the following approximate expression for the albedo of skylight when its polarization is neglected:

$$\lambda_o^{d,n}(\tau_1; \mu_o) \doteq {}^{\uparrow}F_n(\tau_1; \mu_o)/{}^{\downarrow}F(\tau_1; \mu_o) \tag{23}$$

The reflection coefficients times cos θ, or the weighting factors for the incident intensities that appear in the integrands of Eqs. (12), (13), and (18) are given in Fig. 10. The weighting factor for the r-component is largest and least for the l-component. The neutral weighting factor equals the average of the other two. The incident intensity at large zenith angle ($\theta \doteq 80^{\circ}$) is weighted most heavily.

The l- and r-components of the azimuth independent intensity of skylight falling on the ground are given in Figs. 11 and 12. The skylight includes both the unreflected and multiply reflected components. However, the multiply reflected component makes a relatively small contribution. When the sun is at the zenith (Fig. 11), the l-component decreases from the zenith to the horizon, whereas the r-component increases strongly. One expects such a distribution of intensities from considerations of primary scattering. When the sun is near the horizon (Fig. 12), on the other hand, the l-component increases from the zenith to the horizon, and the r-component does not increase as much.

The albedos of the different components of diffuse radiation are given in Fig. 13. The albedo is smallest for the l-component and largest for the r-component. The total albedo when polarization is taken into account (λ_o^d) lies closer to the r-albedo at small solar zenith angle and closer to the l-albedo at large θ_o, because the relative downward flux is greatest (least) for the r-component at small (large) θ_o, as can be deduced from Figs. 11 and 12. The albedo $\lambda_o^{d,n}$ is computed from Eq. (23) when the polarization of the skylight is neglected. If $\lambda_o^{d,n}$ is compared with λ_o^d, $\lambda_o^{d,n}$ is 22 per cent too small when $\theta_o = 0^{\circ}$ and about 13 per cent too large when $\theta_o = 85^{\circ}$. The reason that $\lambda_o^{d,n} < \lambda_o^d$ when θ_o is small is that $Q^{(o)} < 0$ (Fig. 11); and as a conse-

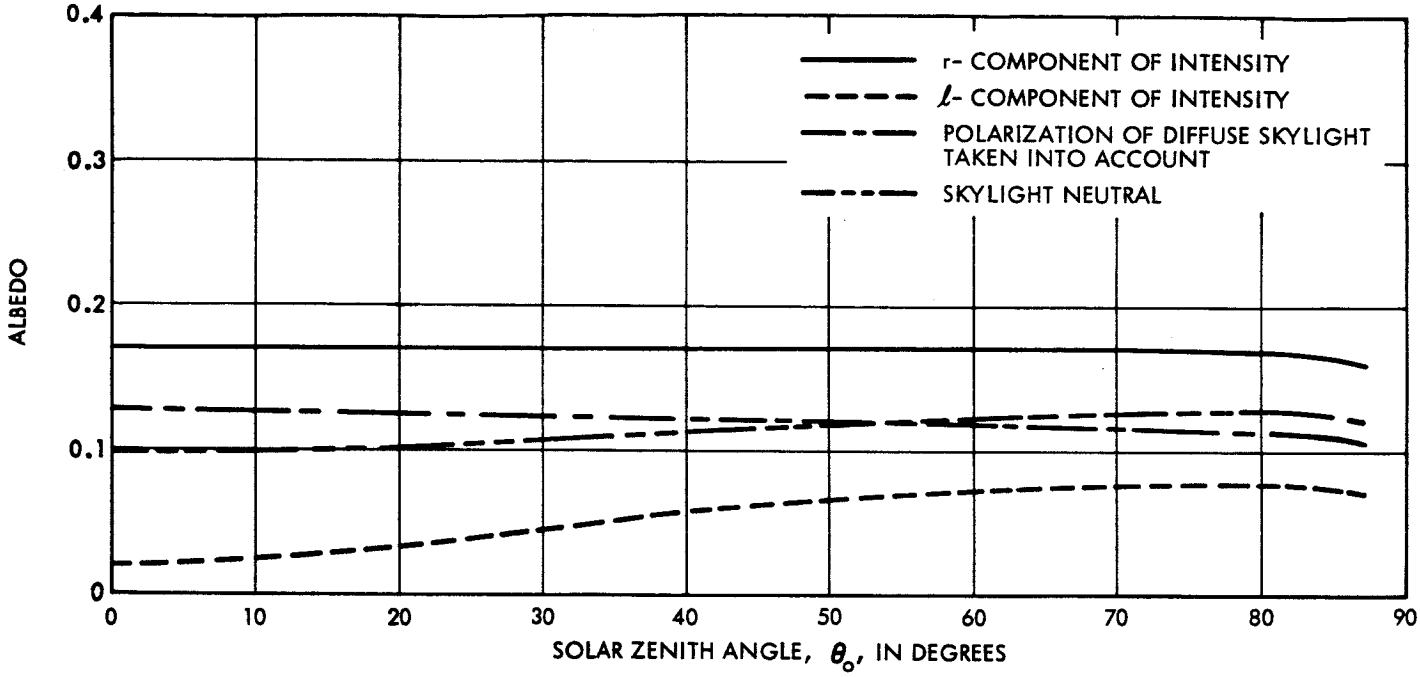

Figure 13. Albedo of polarized components of skylight as a function of θ_o for Fresnel model. $\tau_1 = 0.15$.

quence, ${}^{\uparrow}F_n < {}^{\uparrow}F$ (Eq. 19). On the other hand, $\lambda_o^{d,n} > \lambda_o^d$ when θ_o is large, because $Q^{(o)} > 0$ (Fig. 12) and ${}^{\uparrow}F_n > {}^{\uparrow}F$ (Eq. (19)).

The albedos λ_o^d and $\lambda_o^{d,n}$ are shown as a function of optical thickness in Fig. 14. The absolute difference in the two albedos is less than 0.005 when $\theta_o = 60^o$. The difference increases to as much as 0.03 when the sun is at the zenith. However, the larger difference has a small effect on the total albedo of both the diffuse skylight and direct sunlight (λ_o).

In order to see what effect neglect of the polarization of skylight has on the total albedo of both direct and diffuse light, separate Eq. (1) for the total albedo into two terms:

$$\lambda_o = \frac{{}^{\downarrow}F_1}{{}^{\downarrow}F} \lambda_o^1 + \frac{{}^{\downarrow}F}{{}^{\downarrow}F} \lambda_o^d \tag{24}$$

where the first term on the right-hand side of this equation applies to the direct sunlight and the second term applies to the diffuse light. Define an albedo Λ_o that is computed by neglecting the polarization of the skylight, which can be done by substituting the approximate albedo of Eq. (23) into Eq. (24):

$$\Lambda_o = \frac{{}^{\downarrow}F_1}{{}^{\downarrow}F} \lambda_o^1 + \lambda_o^{d,n} \frac{{}^{\downarrow}F}{{}^{\downarrow}F} \tag{25}$$

Let the two albedos λ_o^d and $\lambda_o^{d,n}$ be related as follows:

$$\lambda_o^d = \lambda_o^{d,n} + \varepsilon \tag{26}$$

An expression for the relative difference in the albedo is obtained by substituting Eq. (26) into Eq. (24), subtracting Eq. (25), and dividing by λ_o:

$$\frac{\lambda_o - \Lambda_o}{\lambda_o} = \frac{\varepsilon}{\lambda_o} \frac{{}^{\downarrow}F}{{}^{\downarrow}F} \tag{27}$$

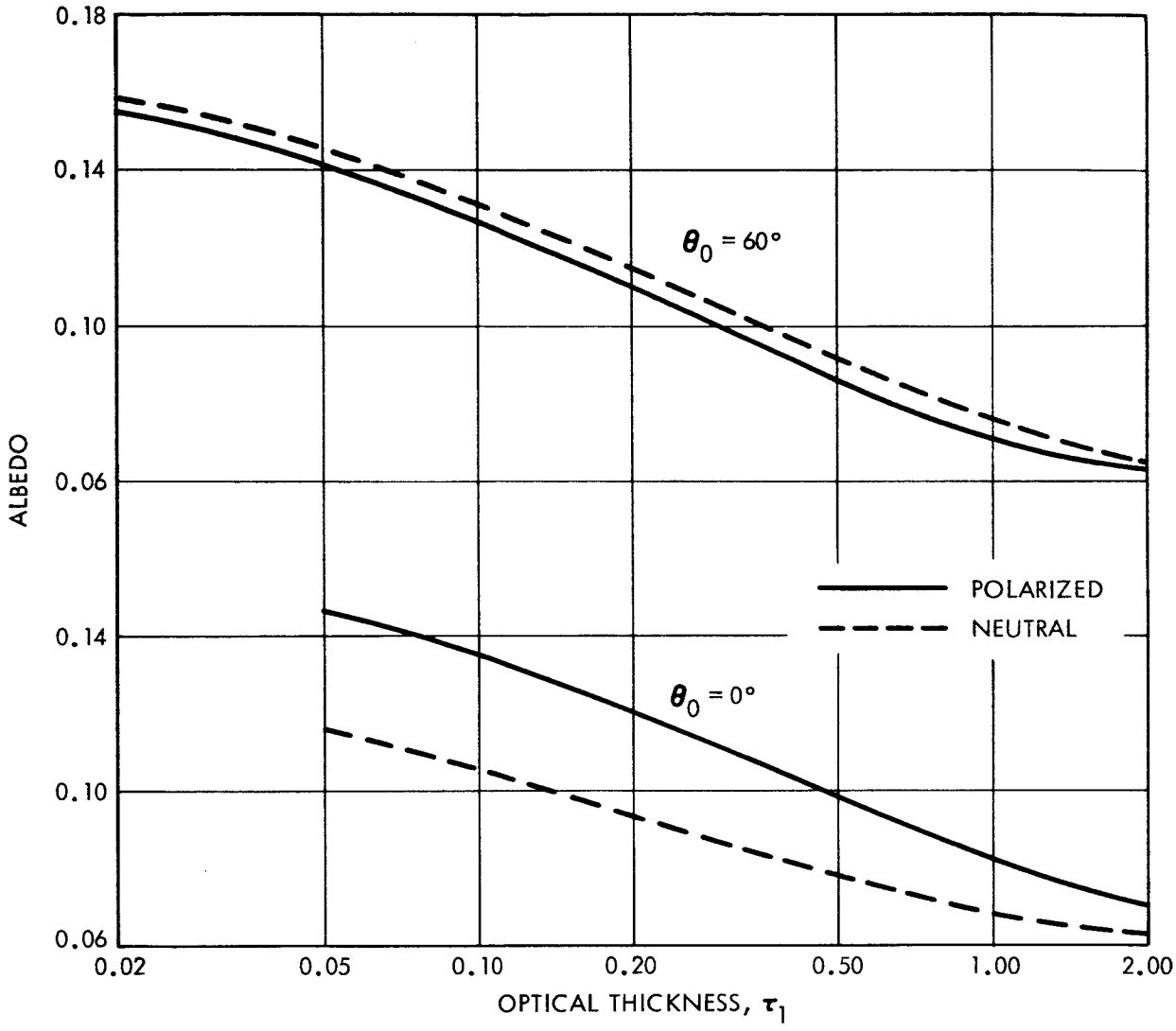

Figure 14. Albedo of polarized and neutral skylight as a function of optical thickness for Fresnel model.

Equation (27) was used to compute the relative differences in the albedo that appear in Table I. The relative difference is largest at optical thicknesses of $\tau_1 = 0.50$ and 1.00, where the relative difference is less than 15 per cent.

TABLE I

Relative difference in total albedos when polarization of skylight is taken into account and when it is neglected; Eq. (27).

τ_1	θ_o	$\frac{\lambda_o - \Lambda_o}{\lambda_o}$
0.02	75.5°	- 0.012
	60.0	- 0.001
	25.8	0.012
0.05	84.3	- 0.011
	60.0	- 0.003
	8.1	0.034
0.25	81.4	- 0.054
	60.0	- 0.018
	0.0	0.099
0.50	60.0	0.036
	8.1	0.122
1.00	84.3	- 0.144
	60.0	- 0.053
	0.0	0.129
2.00	84.3	- 0.037
	60.0	- 0.036
	0.0	0.092

The total albedo λ_o is less than 0.1 where the relative difference exceeds 10 per cent (see Fig. 9). When the data in Table I and Fig. 9 are combined, the absolute error in the computed albedo that neglects the polarization of the skylight is less than 0.01 ($\varepsilon {}^{\downarrow}F / {}^{\downarrow}F < 0.01$).

2.4 COMPARISONS WITH OTHER DATA

Mullamaa[12] did not compute the albedo of skylight for the Fresnel model, which has a smooth water surface. In order to relate Mullamaa's computations of albedo of skylight at a rough-sea surface and those for the Fresnel model, let the skylight be separated into two components: the unreflected (${}^{\uparrow}F_2$) and reflected (${}^{\uparrow}F_3$) skylight. The albedo of skylight has been introduced by Eq. (14), which can be rewritten in terms of the two components that are indicated by Eqs. (21) and (22):

$$\lambda_o^d = \frac{\left({}^{\uparrow}F_2 + {}^{\uparrow}F_3\right)}{{}^{\downarrow}F} = \frac{{}^{\downarrow}F_2}{{}^{\downarrow}F}\,\lambda_o^2 + \frac{{}^{\downarrow}F_3}{{}^{\downarrow}F}\,\lambda_o^3$$

Mullamaa neglected the reflected skylight; that is ${}^{\downarrow}F_3 = 0$. As a result, λ_o^2 is the Mullamaa albedo data for rough sea surfaces in Fig. 15. The albedo λ_o^d is used for a smooth sea surface in Fig. 15. The relative difference between the two albedo data λ_o^d and λ_o^2 for a smooth sea surface are shown to be less than a few per cent in Table II.

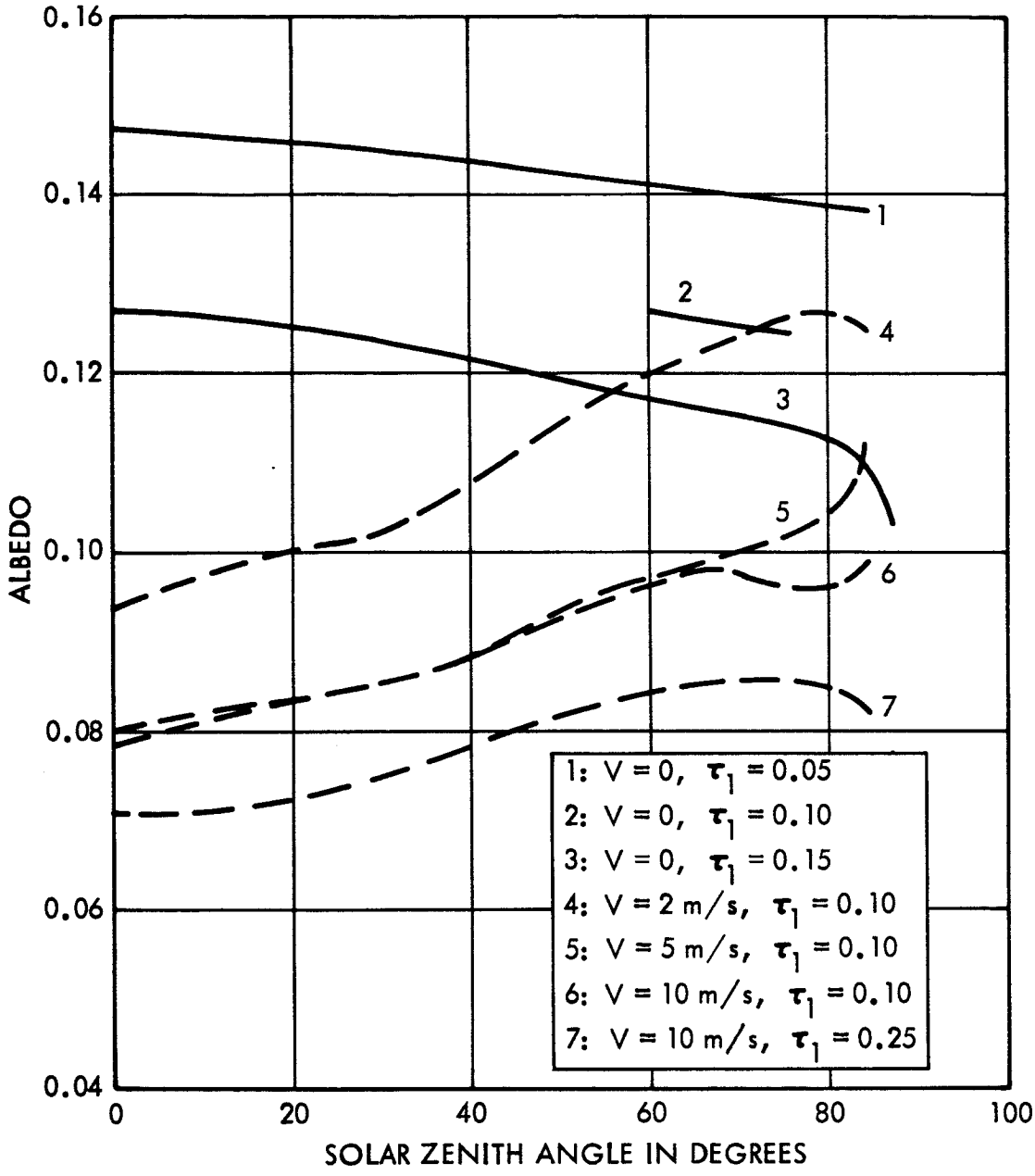

Figure 15. Computed albedo of skylight at rough[12] and smooth sea surfaces as a function of θ_o.

TABLE II

Albedo of unreflected skylight (λ_o^2) and of skylight (λ_o^d) for Fresnel model.

τ_1	θ_o											
	0.0°		25.8°		45.6°		60.0°		75.5°		84.3°	
	λ_o^2	λ_o^d	λ_o^2	λ_o^d	λ_o^2	λ_o^d	λ_o^2	λ_o^d	λ_o^2	λ_o^d	λ_o^2	λ_o^d
0.05	0.148	0.148	0.146	0.146	0.143	0.143	0.141	0.141	0.139	0.140	0.137	0.139
0.10							0.126	0.127	0.123	0.125		
0.15	0.127	0.127	0.124	0.124	0.120	0.120	0.116	0.117	0.113	0.114	0.108	0.110

The albedos of skylight at smooth and at rough sea surfaces is shown in Fig. 15. The two sets of data will be compared for $\tau_1 = 0.10$. The albedo of the smooth sea surface was not computed for $\theta_o < 60^o$ at $\tau_1 = 0.10$. Hence, curves one and three for $\tau_1 = 0.05$ and 0.15, respectively, are given since these curves bracket the one for $\tau_1 = 0.10$. Curve 4 shows the albedo when the wind speed near the surface is 2 ms^{-1}. In this case the standard deviation of the slopes of the water surface is 5^o. A comparison of curves 2 and 4 shows that a slight roughening of the surface makes a significant difference in the albedo of the skylight. The albedo of the smooth surface is 0.04 higher when $\theta_o = 0^o$, and the albedos of the rough and smooth surfaces are comparable when $\theta_o = 70^o - 80^o$. If the wind speed increases from v = 2 ms^{-1} to v = 5 ms^{-1}, then the albedo decreases about 0.02 for all θ_o. An increase of wind speed to v = 10 ms^{-1} causes only a slight additional change in the albedo.

The total albedo of both skylight and direct sunlight will be compared for wind-roughened and smooth seas. Mullamaa[12] computed an effective albedo A_Q, which included the upward flux of underwater light through the sea surface. If the same correction for the underwater light is made for the Fresnel model, the <u>effective</u> albedo λ_o^e can be expressed in terms of the total albedo λ_o by

the expression

$$\lambda_o^e = \frac{\lambda_o + 0.024}{1.024} \qquad (28)$$

The relative difference γ between the albedos for rough and smooth seas is

$$\gamma = \frac{A_Q - \lambda_o^e}{A_Q} \qquad (29)$$

Equation (29) was used to compute the relative differences that are given in Table III. The absolute value of the difference is less than 0.25 if either $\theta_o < 66.4^o$ or if $\tau_1 = 0.50$. When the relative difference is less than 0.25, the effective albedo is less than about 10 per cent. In this case the absolute error in the effective albedo is less than 0.025. Since the albedo of a smooth surface is much easier to compute than the albedo of a rough sea surface, it would be advantageous to assume a smooth surface for some studies.

TABLE III

Relative difference between effective albedo of wind-roughened and smooth seas. The tabulated values are computed from Eq. (29). A_Q is taken from ref. 12, Table A10; wind speed v = 10 ms^{-1}.

	Sun's zenith angle in degrees						
τ_1	0.0	23.1	36.9	53.1	66.4	78.5	84.3
0.02	0.00	-0.02	0.14	0.09	-0.19	-0.56	-0.72
0.05	-0.02	-0.04	0.02	0.06	-0.20	-0.54	-0.38
0.10	-0.06	-0.06	0.07	0.04	-0.23	-0.50	-0.55
0.25	-0.14	-0.14	0.02	-0.01	-0.21	-0.39	-0.32
0.50	-0.19	-0.18	-0.05	-0.04	-0.15	-0.22	-0.06

Neumann and Hollman[16] have computed the effective albedo from measured upward and downward fluxes at the sea surface and related it to the measured ratio of diffuse to total downward flux of radiation at the sea surface. Their measurements were not restricted to times when no clouds were visible in the sky. Also, the measured upward flux that they used to compute the albedo included both the radiation reflected from the surface and the underwater light.

The straight lines that they fitted to effective albedos that were computed from measured fluxes are reproduced as dashed lines in Fig. 16. The continuous lines give the computed albedo data for the Fresnel model, where the underwater light was excluded. When the solar zenith angle is small ($\theta_o \doteq 24^o$), the measured and computed data indicate that the underwater component is weak. However, the data indicate that the underwater component becomes large at large solar zenith angles. The data on Fig. 16 can be used to compute the upward flux of underwater light through the sea surface.

The fraction of the downward flux of radiation that is transmitted through the water surface and then is reflected back up through the surface from the depths of the sea is given by the following expression:

$$\beta = \frac{{}^{\uparrow}U}{(1 - \lambda_o')\,{}^{\downarrow}F^m} \tag{30}$$

where ${}^{\uparrow}U$ is the upward flux of the radiation from below the water surface and passes through the surface, λ_o' is the total albedo, or surface loss, and ${}^{\downarrow}F^m$ is the measured downward flux of radiation at the top of the sea surface. All these quantities depend on the sun's zenith angle, radiation wavelength, state of the sky, roughness of the sea, and nature of the sea water. The measured albedo data on Fig. 16, which is contained in reference 16, will be used for computing β. However, reference 16 does not give the values of λ_o' and ${}^{\downarrow}F^m$ that appear in Eq. (30). Hence, these quantities will be approximated.

The measured downward flux of radiation at the water surface will be approximated by the computed value for the Fresnel model $\left({}^{\downarrow}F^F(\tau_1; \mu_o)\right)$. The measured flux can be expressed as the sum of components, as was done in Eq. (1):

$${}^{\downarrow}F^m(\tau_1; \mu_o) = {}^{\downarrow}F_1(\tau_1; \mu_o) + {}^{\downarrow}F_2^m + {}^{\downarrow}F_3^m + \alpha\, {}^{\uparrow}U \tag{31}$$

where the successive quantities on the right-hand side of the equation represent fluxes of direct sunlight, unreflected skylight, reflected skylight, and the fraction (α) of the underwater light that is scattered back to the water by the atmosphere. Only the flux of direct sunlight (${}^{\downarrow}F_1$) depends just on θ_o and τ_1.

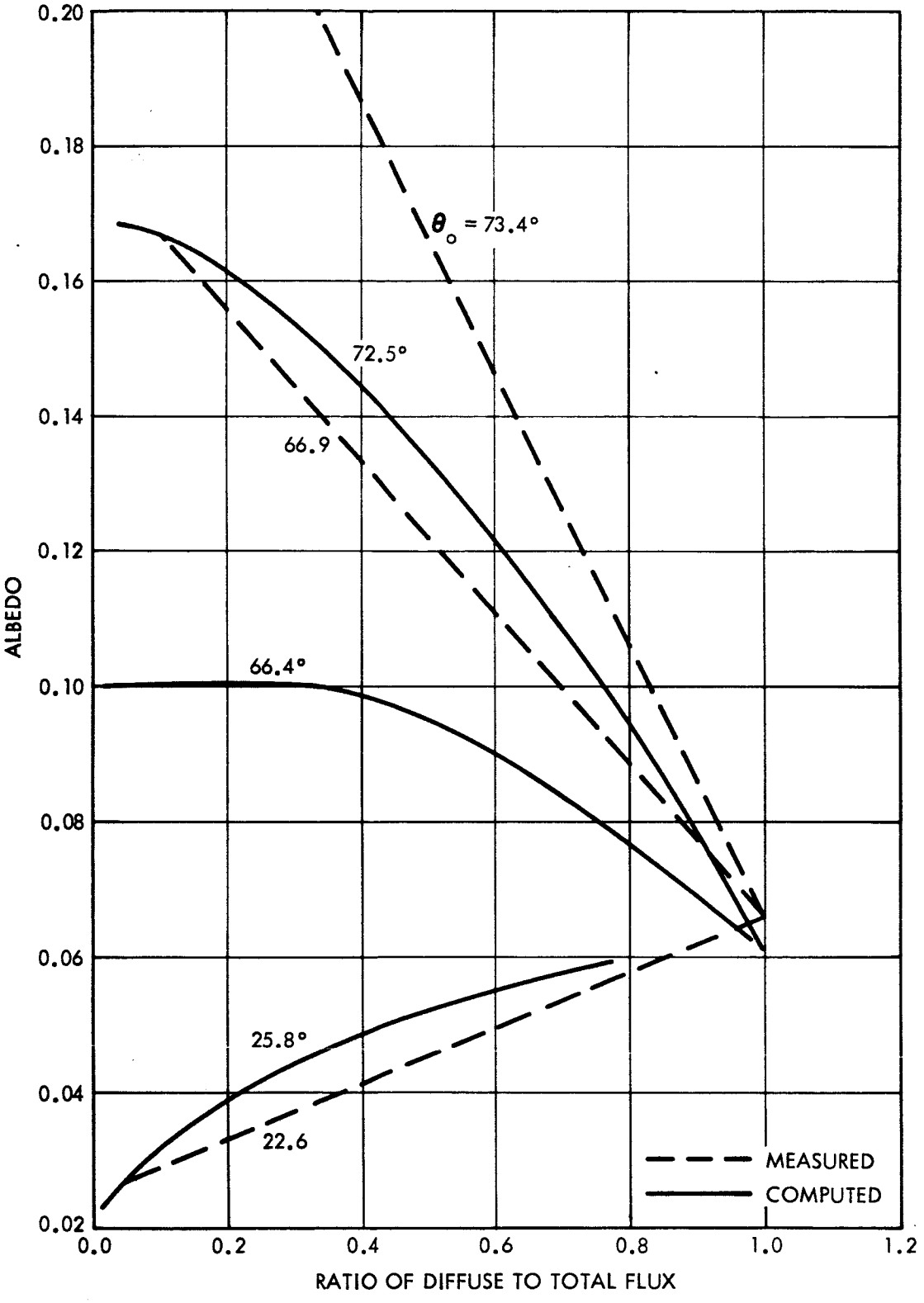

Figure 16. Measured[16] and computed total albedo at sea surfaces as function of ratio of downward skylight to total flux at sea surface.

The flux of unreflected skylight ($^{\downarrow}F_2^m$) depends on the aerosol content of the atmosphere and on θ_o. Aerosol particles have an appreciable effect on the downward flux of skylight at the ground.[8] The data in reference 8 indicate the relative difference in the flux of unreflected skylight at the ground for turbid and Rayleigh atmospheres of the same moderate optical thickness may be as much as 0.2; that is $|{}^{\downarrow}F_2^m - {}^{\downarrow}F_2| \div {}^{\downarrow}F < 0.2$. An estimate of the importance of the downward flux of reflected skylight $^{\downarrow}F_3^m$ is given by the ratio $^{\downarrow}F_3$ to the total flux downward flux ($^{\downarrow}F^F$) for the Fresnel model. The data on Fig. 3 show that ${}^{\downarrow}F_3/{}^{\downarrow}F^F \leq 0.1$. Therefore, the flux of reflected skylight ($^{\downarrow}F_3^m$) that is associated with the measured fluxes would also make about the same contribution to the total downward flux ($^{\downarrow}F^m$) in Eq. (31). Measured values of the flux of underwater light ($^{\uparrow}U$) are about 0.05 of the total downward flux ($^{\downarrow}F^m$)[6,17]; also, the reflection coefficient of the atmosphere for the underwater light is not more than one ($0 \leq \alpha \leq 1$). Hence, the total relative difference between the downward fluxes for the earth's atmosphere and for a Rayleigh atmosphere is given by the following expression:

$$|{}^{\downarrow}F^m - {}^{\downarrow}F^F| \leq |{}^{\downarrow}F_2^m - {}^{\downarrow}F_2| + |{}^{\downarrow}F_3^m - {}^{\downarrow}F_3| + \alpha\,{}^{\uparrow}U$$

$$< 0.2\,{}^{\downarrow}F + 0.1\,{}^{\downarrow}F^m + 0.05\,{}^{\downarrow}F^m$$

$$\frac{|{}^{\downarrow}F^m - {}^{\downarrow}F^F|}{{}^{\downarrow}F^m} < 0.2\,\frac{{}^{\downarrow}F}{{}^{\downarrow}F^m} + 0.15 \qquad (32)$$

The rough error estimates that have just been made have been substituted into this expression. Accordingly, the relative error varies from 0.15 if the flux of diffuse light is zero ($^{\downarrow}F = 0$) to 0.35 if no direct sunlight reaches the water surfaces, or $^{\downarrow}F = {}^{\downarrow}F^m$. The measured downward flux at the water surface will be equated to the value that is computed for the Fresnel model plus a correction ε_1, which will be neglected:

$${}^{\downarrow}F^m(\tau_1; \mu_o) = {}^{\downarrow}F^F(\tau_1; \mu_o) + \varepsilon_1 \doteq {}^{\downarrow}F^F \qquad (33)$$

The measured upward flux of radiation at the water surface is equal to the sum of the surface loss $\lambda_o' \, {}^{\downarrow}F^m$ and the flux of underwater light:

$$ {}^{\uparrow}F^m(\tau_1; \mu_o) = \lambda_o' \, {}^{\downarrow}F^m(\tau_1; \mu_o) + {}^{\uparrow}U \tag{34} $$

The albedo λ_o' depends on the sea's roughness; but as has previously been stated in the discussion of Mullamaa's computations, the albedo of a sea surface is insensitive to the roughness, if $\theta_o < 60^o$, $v < 15$ ms^{-1}, and $\tau_1 \leq 0.50$. Hence, the true albedo λ_o' will be equated to the albedo of the Fresnel model λ_o plus a correction ε_2, which will be neglected:

$$ \lambda_o' = \lambda_o + \varepsilon_2 \doteq \lambda_o \tag{35} $$

If Eq. (35) is substituted in Eq. (34), an approximate expression for the total upward flux at the water surface is

$$ {}^{\uparrow}F^m(\tau_1; \mu_o) = \lambda_o(\tau_1; \mu_o) \, {}^{\downarrow}F^m(\tau_1; \mu_o) + {}^{\uparrow}U \tag{36} $$

The effective albedo, which is computed from measured fluxes, is defined as

$$ \lambda_o^m = \frac{{}^{\uparrow}F^m}{{}^{\downarrow}F^m} \tag{37} $$

If Eqs. (33) and (36) are substituted in Eq. (37), the expression for the measured albedo becomes

$$ \lambda_o^m(\tau_1; \mu_o) = \frac{\lambda_o \, {}^{\downarrow}F^F + {}^{\uparrow}U}{{}^{\downarrow}F^F} \tag{38} $$

This equation yields the following expression for the flux of underwater light:

$$ {}^{\uparrow}U = (\lambda_o^m - \lambda_o) \, {}^{\downarrow}F^F \tag{39} $$

When Eqs. (33), (35) and (39) are substituted in Eq. (30), an approximate expression for the ratio of the upward to downward fluxes that pass through the water surface is

$$\beta = \frac{\lambda_o^m - \lambda_o}{1 - \lambda_o} \tag{40}$$

This relation was used to compute the values of β that appear in Table IV. Table IV contains values of β that are computed from albedo measurements of Neumann and Hollman at Long Island Sound.[16] Their measured values of the albedo (λ_o^m) have already been presented in Fig. 16. The values of λ_o depend on the optical thickness of the Fresnel model. The optical thickness

TABLE IV

The ratio β of Eq. (40).

θ_o	ratio of diffuse to total downward flux		
	0.2	0.7	1.0
22.6°	(0.003)	(0.002)	0.006
44.9	0.012	0.003	0.006
55.8	0.009	0.004	0.006
66.9	0.056	0.014	0.006
73.4	0.063	0.023	0.006

of the Fresnel model was determined for a particular pair of the solar zenith angle θ_o and of the ratio of diffuse to total flux from Fig. 2. Two-tenths is the smallest ratio of diffuse to total flux for which β was computed in Table IV, since this ratio is the smallest value for which the albedo λ_o^m was measured at large solar zenith angle. The values of β in parenthesis were computed using Mullamaa's[12] values of albedo for a wind-roughened sea surface (wind speed $v = 10\ ms^{-1}$). The corresponding values of albedo (λ_o) for the Fresnel model of smooth water are slightly higher and result in negative values of β. If Mullamaa's albedo data (λ_o) for wind-roughened surface

($v = 10\ ms^{-1}$) are used to determine β when the ratio of diffuse to total flux is 0.2, the resulting values of β are higher than those that are not in parenthesis. For example, if $\theta_o = 73.4^o$, $\lambda_o = 0.16$ for the rough sea surface; and as a consequence, $\beta = 0.08$. The tabulated data indicate that β increases with increasing solar zenith angle, when the ratio of diffuse to total flux equals 0.2 and 0.7. Also, when the ratio of diffuse to total flux is either 0.2 or 0.7, β is smallest at a given θ_o when the ratio of diffuse to total flux is largest. When no direct sunlight reaches the water, $\beta = 0.006$.

3. NEUTRAL POINTS

3.1 BASE OF ATMOSPHERE

3.1.1 General

The diffuse radiation falling on the ground or leaving the top of the atmosphere of a Lambert or Fresnel model is polarized. The degree of polarization is zero in a few discrete directions. These directions are referred to as neutral points, since the polarization vanishes there. The degree of polarization (P) of a pencil of radiation is defined in terms of the Stokes parameters I, Q, U, and V as

$$P(\tau;\ \mu,\ \varphi) = \frac{\left[Q^2(\tau;\ \mu,\ \varphi) + U^2(\tau;\ \mu,\ \varphi) + V^2(\tau;\ \mu,\ \varphi)\right]^{1/2}}{I(\tau;\ \mu,\ \varphi)} \qquad (41)$$

$$\begin{aligned} Q &= I_{\ell} - I_r \\ U &= Q \arctan 2\chi \end{aligned} \qquad (42)$$

The angle χ is measured clockwise from the 1-axis, which lies in the meridional plane, to the plane of polarization.

A neutral point occurs if, and only if, $Q = U = 0$, since $V \equiv 0$ for the Lambert and Fresnel models. Neutral points occur for a few discrete pairs of μ, φ at a given solar zenith angle and optical thickness. The computations were made only for discrete values of μ, φ, which in general, did not coincide with the neutral point directions. Hence, in this research the neutral points were determined by the graphical intersection of the U- and Q- lines that represented the zero values.

The parameter $U = 0$ in the vertical plane of the sun for either case of the diffuse light falling on the ground or flowing outwards from the top of the atmosphere, if the inclination of the plane of polarization is symmetrical with respect to the vertical plane, as it is for both the Lambert and Fresnel models. In these cases it is customary to define the degree of polarization in the sun's vertical plane as

$$P = \frac{I_r - I_\ell}{I_r + I_\ell} \tag{43}$$

The plane of polarization is either perpendicular or parallel to the sun's vertical plane, and the degree of polarization is said to be either positive or negative, respectively. The neutral points in the sun's vertical plane occur where P = 0, of course.

A new, more general definition of the Babinet and Brewster points will be given in order to simplify the discussion of them for the Fresnel model. A schematic representation of these neutral points for the Lambert model is given in the right-hand side of Fig. 17. These two points lie in the sun's vertical plane. The neutral point that is observed between the sun and the zenith is called the Babinet point. The neutral point that is observed between the sun and the near horizon is called the Brewster point. However, as the sun rises above the horizon, the computed Babinet position for the Fresnel model moves from above the sun, crosses it, and then appears below it, when the optical thickness of the atmosphere is less than about 0.25 ($\tau_1 < 0.25$). On some occasions this Babinet point is the only neutral point between the sun and the near horizon. When the Brewster point appears, it is always below the sun; and in addition, the Brewster point always lies between the horizon and the Babinet point. A more general definition of these neutral points can be made with respect to the sign of the polarization, instead of using the sun as the reference. The new definition will be that the degree of polarization is positive between the zenith and the Babinet point; the degree of polarization will also be positive between the horizon and the Brewster point. As a result, the polarization is negative between the two points, when the Brewster point is present. If no Brewster point is present, the polarization is negative between the Babinet point and the near horizon. This new definition does not change the identification of previously measured neutral points and of those computed for the Lambert model.

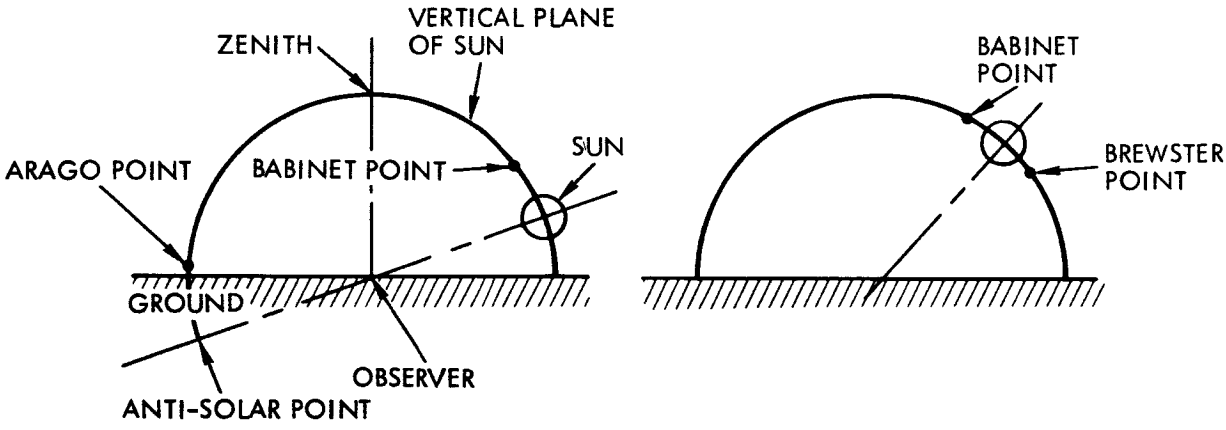

Figure 17. Schematic representation of neutral points at base of atmosphere of Lambert model.

The diagram on the left-hand side of Fig. 17 indicates the two neutral points that occur in the Lambert model, when the solar zenith angle is large. The two points lie in the vertical plane of the sun. A Babinet point lies above the sun in Fig. 17; but according to the new definition just given for it, it can occur below the sun in the Fresnel model, since the Babinet point occurs where the positive polarization that extends from the zenith becomes negative. An Arago point lies about 20° above the anti-solar point; the exact position depends on the model, optical thickness, and solar zenith angle. As the solar zenith angle decreases, the Arago approaches the horizon nearest to it, and reaches the horizon when the solar zenith angle is roughly $\theta_o = 70^{\circ}$.

3.1.2 Computed Data

The computed neutral points for the Lambert model follow the schematic representation. These neutral points lie in the sun's vertical plane. Neutral point positions for the Lambert model are given by the dashed curves on Fig. 18. The Lambert data have been given before.[18] The ordinate gives the distance of the Babinet and Brewster points from the sun and of the Arago point from the anti-solar point. The origin of the ordinate for each set of curves that are associated with a particular optical thickness (τ_1) increases by 10° for each increase of the optical thickness. In order to explain the neutral point characteristics in more detail for the Lambert model, consider the dashed Lambert curves for $\tau_1 = 0.50$. When the solar zenith angle is 84°, only the Babinet and Arago points are present in the sky. The Babinet point is about 27° above the sun, and the Arago point is about 30° above the anti-solar point. As the solar zenith angle decreases, the Babinet point approaches the sun and coincides with it when the sun reaches the zenith. The Arago point disappears below the horizon when the solar zenith angle is 64°. A Brewster point appears at the horizon below the sun at the same solar zenith angle when the Arago point disappears.

Data on the neutral points for the Fresnel model are also given on Fig. 18. Some of these data have been given before.[19] At $\tau_1 = 1.00$ the neutral point distances are slightly smaller for the Fresnel model than for the Lambert model. Also, the Babinet and Brewster points for the Fresnel model

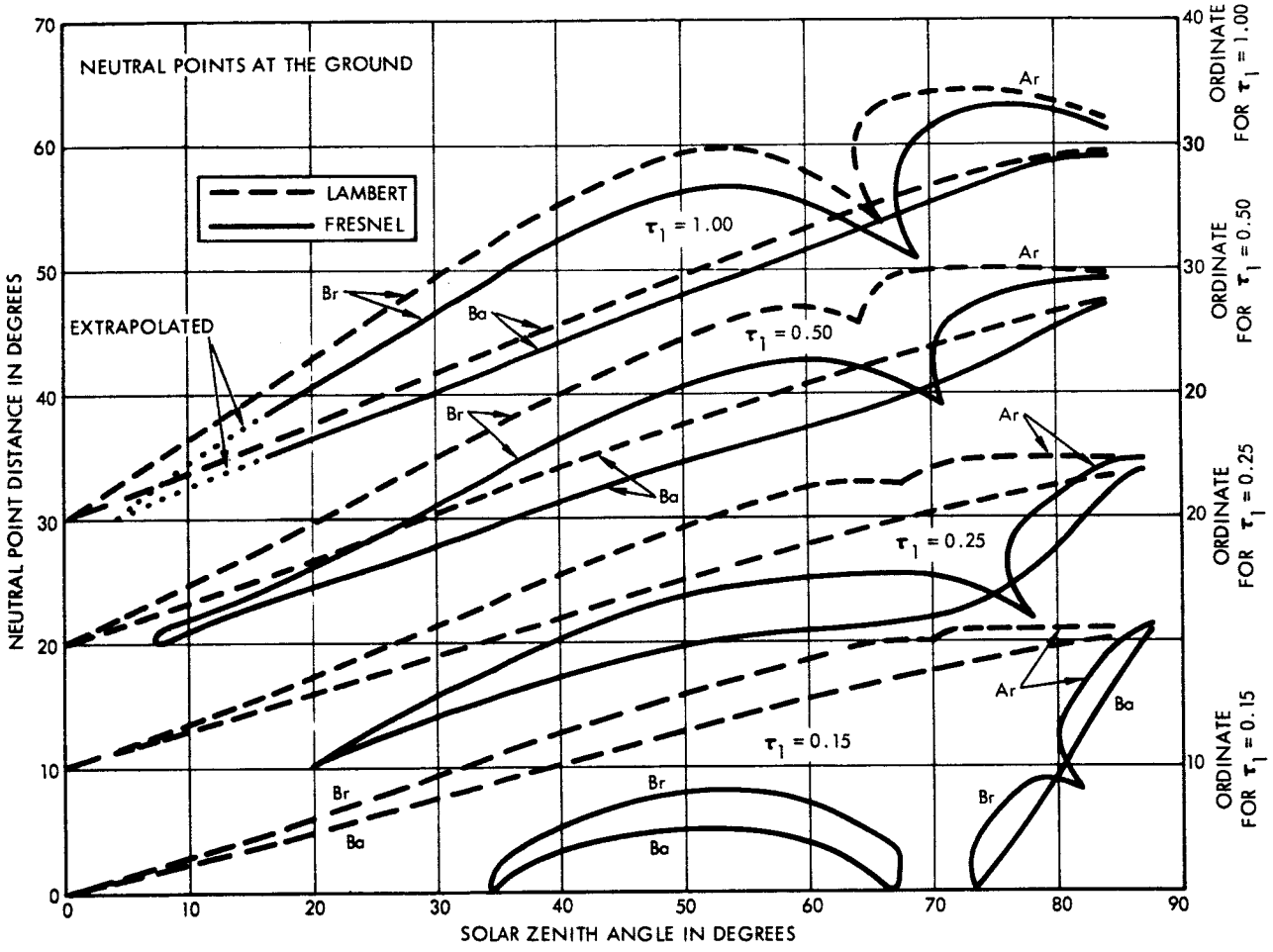

Figure 18. Neutral point positions at base of atmosphere in sun's vertical plane as a function of θ_o. The origin of a set of curves is displaced 10^o along the ordinate for suceeding values of τ_1.

may move into the direction of the sun before the sun reaches the zenith. The differences in the neutral point distances for the two models increases at the smaller optical thickness of $\tau_1 = 0.50$. The Babinet and Brewster points for the Fresnel model do not appear in the sun's vertical plane, if the solar zenith angle is less than 7°. The neutral point differences continue to increase as the optical thickness decreases to $\tau_1 = 0.25$. The next smaller optical thickness at which the computations were made for the Fresnel model was for $\tau_1 = 0.15$. This is the largest value for which computations were made that the Babinet and Brewster points disappear from the sun's vertical plane at large solar zenith angle. When $\tau_1 = 0.15$, the neutral points disappear from the sun's vertical plane when θ_o is between 67° and 73°. The Babinet and Brewster points also disappear from the vertical plane when the solar zenith angle is less than 34° and $\tau_1 = 0.15$. The next smaller value of optical thickness for which computations were made for the Fresnel model was $\tau_1 = 0.10$. At this and smaller optical thickness only the Babinet and Arago points appear and only at large solar zenith angle. The disappearance of the Babinet and Brewster points for the Fresnel model from the sun's vertical plane at small solar zenith angle, but before the sun reaches zenith, is shown here for the first time.

Figure 18 shows that the Brewster and Arago points appear on their respective horizons simultaneously. This event can be demonstrated analytically for either the Fresnel or Lambert models and for either the base or top of the atmosphere. To take one case consider the Fresnel model and the base of the atmosphere. A neutral point occurs in the sun's vertical plane where $Q = 0$ (Eqs. (42) and (43)). The equation for Q can be obtained from reference 10, Eqs. (3.4), (3.6), (3.14), and (3.33):

$$
\begin{aligned}
{}^{\downarrow}Q^*(\tau_1; -\mu, \mu_o, \Delta\varphi) = {} & I_\ell^{(o)}(\mu, \mu_o; 1) + D_\ell^{(o)}(\mu, \mu_o; 1) - \\
& I_r^{(o)}(\mu, \mu_o; 1) - D_r^{(2)}(\mu, \mu_o; 1) + \\
& \mu \left[\mu_o I_\ell^{(1)}(\mu, \mu_o) + D_\ell^{(1)}(\mu, \mu_o)\right] \cos \Delta\varphi - \qquad (44) \\
& (1 + \mu^2) \left[(1 - \mu_o^2)\, I_r^{(2)}(\mu, \mu_o) + D_r^{(2)}(\mu, \mu_o)\right] \times \\
& \cos 2\Delta\varphi \,, \quad \Delta\varphi = \varphi_o - \varphi
\end{aligned}
$$

where the arrow on Q merely indicates that Q applies to downward flowing radiation, and the asterisk on Q indicates that radiation is reflected from the ground and accounted for. The τ_1 dependence is omitted from the functions on the right-hand side of Eq. (44). At the horizon $\theta = 90^o$ or $\mu = 0$, in which case Eq. (44) becomes

$$\begin{aligned} {}^{\downarrow}Q^*(\tau_1;\, 0,\, \mu_o\,,\, \Delta\varphi\,) \;=\; & I_{\ell}^{(o)}(0,\, \mu_o;\, 1) \;+\; D_{\ell}^{(o)}(0,\, \mu_o;\, 1) \;- \\ & I_r^{(o)}(0,\, \mu_o;\, 1) \;-\; D_r^{(o)}(0,\mu_o;\, 1) \;- \\ & \left[(1 - \mu_o^2)\; I_r^{(2)}(0,\mu_o) \;+\; D_r^{(2)}(0,\mu_o)\right] \cos\, 2\,\Delta\varphi \end{aligned} \tag{45}$$

The azimuth $\varphi_o - \varphi = 0, \pi$ in the sun's vertical plane for radiation coming from below the sun and from the horizon above the antisolar point, respectively. Accordingly, Eq. (45) shows that ${}^{\downarrow}Q^*(\tau_1;\, \mu = 0,\, \mu_o,\, \varphi_o - \varphi = 0) = {}^{\downarrow}Q^*(\tau_1;\, \mu = 0,\, \mu_o,\, \varphi_o - \varphi = \pi)$; that is, ${}^{\downarrow}Q^*$ is identical at the two points where the sun's vertical plane intersects the horizon. In particular, ${}^{\downarrow}Q^*(\tau_1;\, \mu = 0,\, \mu_o,\, \varphi_o - \varphi = 0) = 0$, when the Brewster point is at the horizon; simultaneously, the Arago point is at the other horizon, since ${}^{\downarrow}Q^*(\tau_1;\, \mu = 0, \mu_o,\, \varphi_o - \varphi = \pi) \;=\; 0$.

The largest value of the optical thickness for which the neutral point positions were computed was $\tau_1 = 2.00$. The neutral points for $\tau_1 = 2.00$ depart from the regular pattern established on Fig. 18 and are shown separately on Fig. 19. Neutral point characteristics for a model with zero ground albedo and with $\tau_1 > 1.0$ have been given by Dave and Furukawa.[5] The purpose of Fig. 19 is to show that the neutral point characteristics are approximately the same for the Fresnel and Lambert models at $\tau_1 = 2$, and presumably for all larger τ_1.

A different representation of the Babinet and Brewster point distances is given on Fig. 20. The zenith angle of these two neutral points are given as a function of θ_o. The dashed line also gives the solar zenith angle. The shape of the curve for $\tau_1 = 0.15$ and near the solar zenith angle of $\theta_o = 67^o$ does not quite agree with the curve shown on Fig. 18. The curve is uncertain

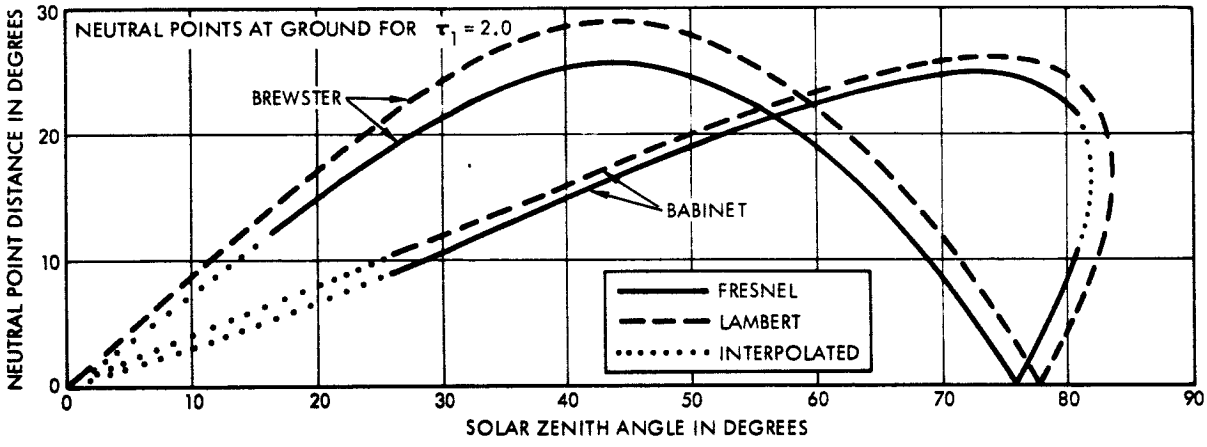

Figure 19. Neutral point positions at base of atmosphere in sun's vertical plane as a function of θ_o for $\tau_1 = 2.0$.

since no data were computed for a solar zenith angle between 66.4° and 67.6°. However, the representation on Fig. 20 seems to be more accurate: the curve above and below the knee apply to the Babinet and Brewster points, respectively.

When the Babinet and Brewster points merge and then disappear from the sun's vertical plane, a single neutral point appears on each side of the sun's vertical plane. These two points are of course symmetrical with respect to the sun's vertical plane. The zenith angle of these two points is slightly different from that of the sun (θ_o) and is given in Table VI. The azimuth of the neutral points outside of the sun's vertical plane is shown in Fig. 21. The neutral point for $\tau_1 = 0.50$ disappears from the sun's vertical plane only when the solar zenith angle is less than 8°. No computational data were available for this case. The neutral points for $\tau_1 = 0.25$ appear outside of the sun's vertical plane only when $\theta_o < 20^{\circ}$. As shown before, the neutral points for $\tau_1 = 0.15$ appear outside of the sun's vertical for two separated ranges of the solar zenith angle. The azimuthal distance is 2.2° when $\theta_o = 70^{\circ}$ but is much larger at smaller solar zenith angle. The next value of optical thickness for which the azimuthal positions of the neutral points were computed was $\tau_1 = 0.05$. In this case a neutral point appears on each side of the sun's vertical plane when the solar zenith angle is between 0° and 87°. Hence, Fig. 21 shows that as the optical thickness decreases, the neutral points appear outside of the sun's vertical plane at increasingly greater azimuth and for an increasing range of solar zenith angle.

The interpolated portions of the curves on Fig. 21 for small θ_o are uncertain. The neutral point azimuths were computed for $\theta_o = 0^{\circ}$ and 8.1°, but not for intermediate values. The azimuthal value at $\theta_o = 8.1$ is uncertain. The difficulty of obtaining an accurate value can be explained by showing the degree of polarization in the vicinity of the neutral point θ_o is small (Fig. 22). The degree of polarization vanishes somewhere within the dashed curve that is labeled 0.0001. This curve has an azimuthal range of about 2°. The neutral point, which is determined by the intersection of the zero lines of U and Q, could occur anywhere within the dashed polarization curve, since the data were computed for increments of 0.01 in μ and of 2° in $\varphi_o - \varphi$.

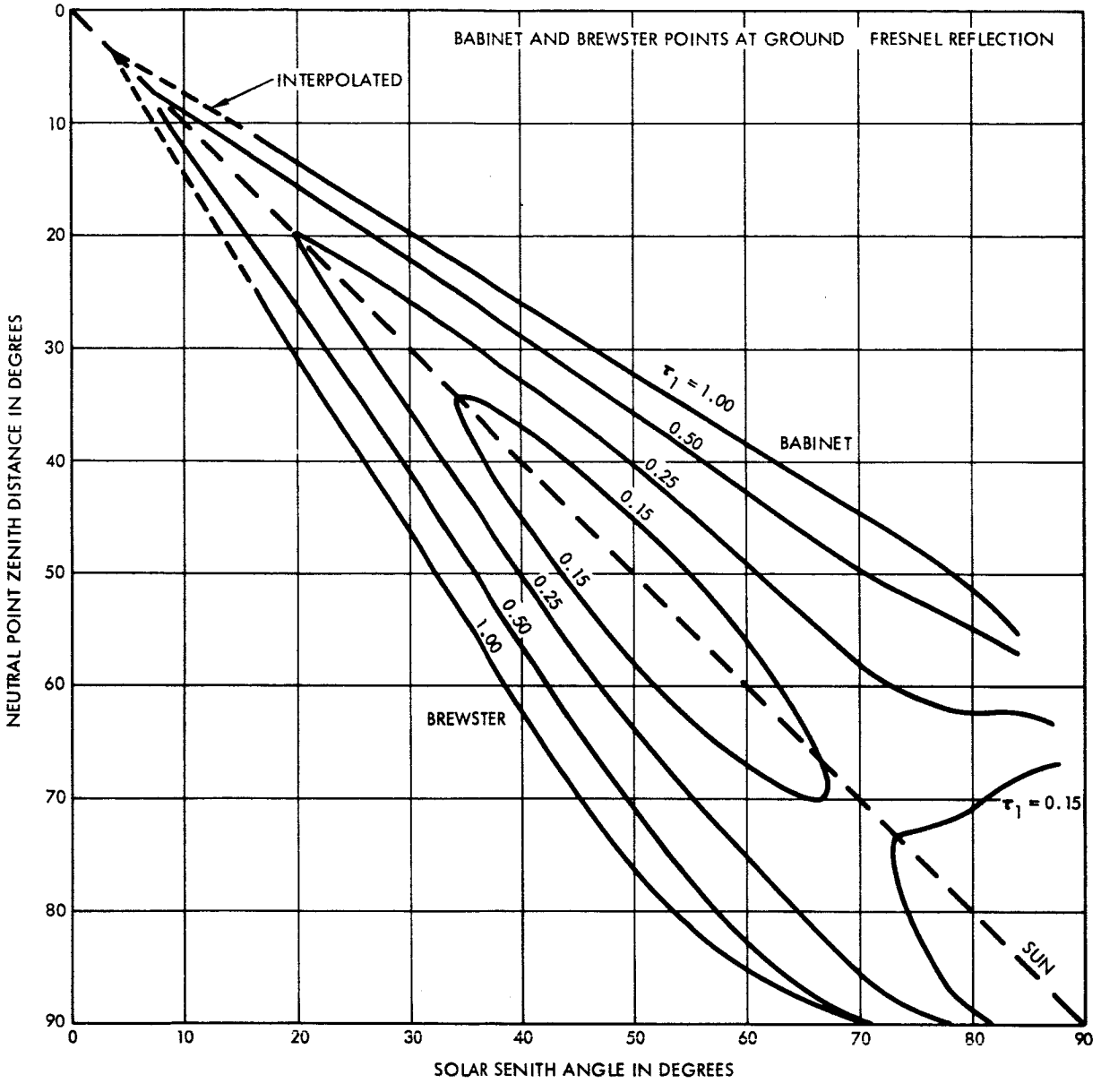

Figure 20. Zenith angle of Babinet and Brewster points at base of atmosphere for Fresnel model.

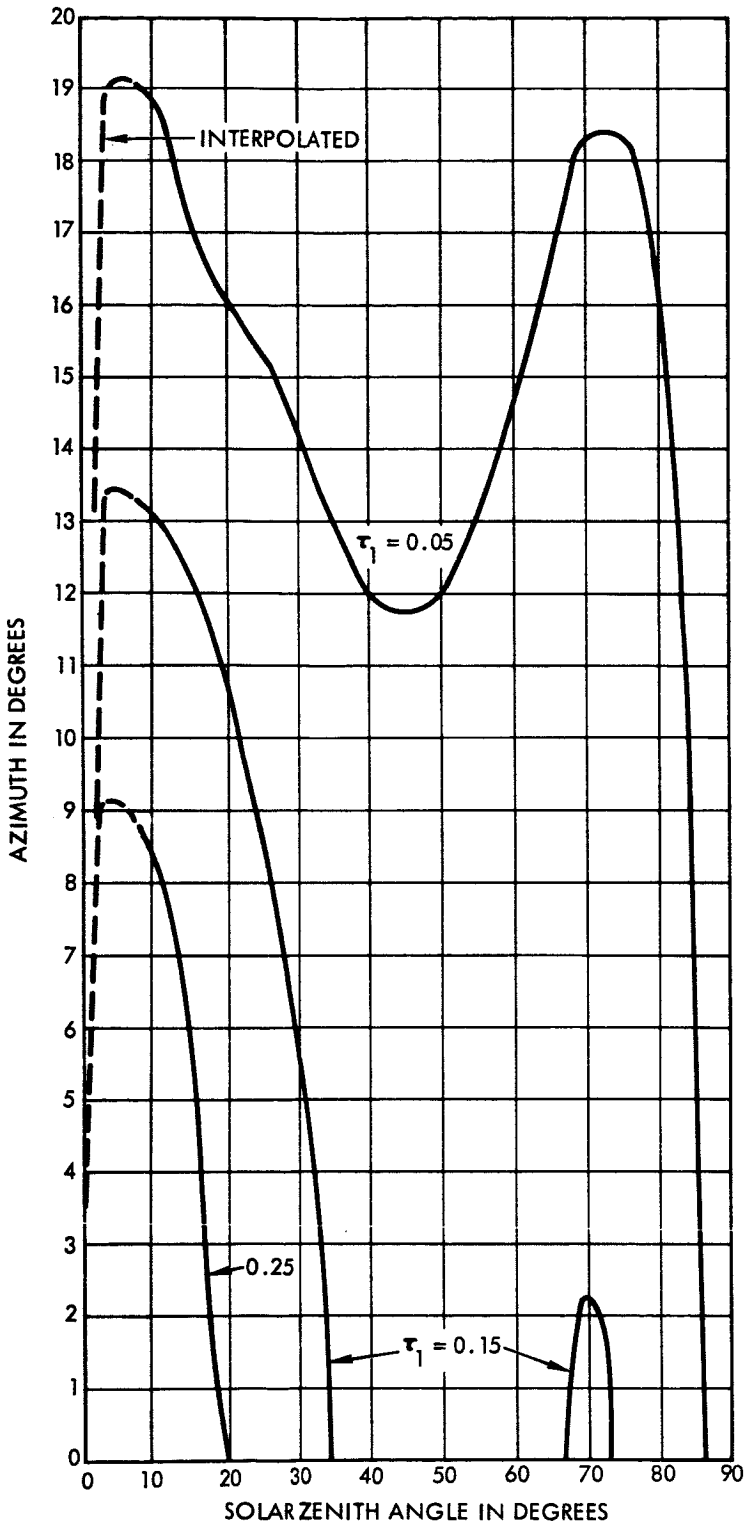

Figure 21. Azimuthal distance of neutral points from sun's vertical plane at base of atmosphere.

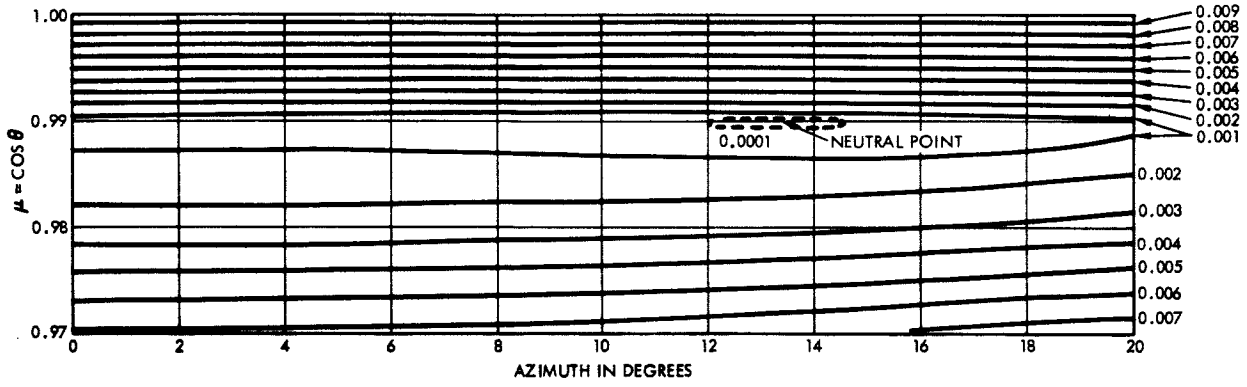

Figure 22. Degree of polarization in vicinity of neutral point at base of atmosphere of Fresnel model. $\tau_1 = 0.15$. $\theta_o = 8.1^o$.

Hence, the azimuthal position of the neutral point for $\tau_1 = 0.15$ is computed with a possible error of about 2° when $\theta_o = 8.1^\circ$.

When the solar zenith angle is small, a better measure of the neutral point position is the angle between the sun and the neutral point. Since the neutral point lies close to the almucantor, the angle between the sun and neutral point approximately equals the angular distance that is measured along the solar almucantor between the sun's vertical plane and the vertical plane through the neutral point. The angle between the neutral point and the sun is given in Table V.

TABLE V

Angle (Θ) between sun and neutral point that is outside of sun's vertical plane at base of atmosphere. $\varphi_o - \varphi$ is the azimuthal difference. $\tau_1 = 0.15$. $m = 1.344$.

θ_o	$\varphi_o - \varphi_1$	Θ
0.0°	0.0	0.0
8.1	13.3	1.8
11.5	12.9	2.6
14.1	12.9	3.1
20.0	10.7	3.7
25.8	8.3	3.7
30.7	5.2	2.6
32.9	3.2	2.1
34.9	lies in the sun's vertical plane	

The degree of polarization and the parameters Q and U are now discussed in order to show how these parameters change as the neutral points move outside of the sun's vertical plane. This information is given for an optical thickness of $\tau_1 = 0.15$. First consider the case for $\theta_o = 80.2^\circ$, when the neutral points lie in the sun's vertical plane. The degree of polarization of the diffuse radiation falling on the ground of the Fresnel model is shown on Fig. 23. The degree of polarization data for this figure is computed from Eq. (41). As a

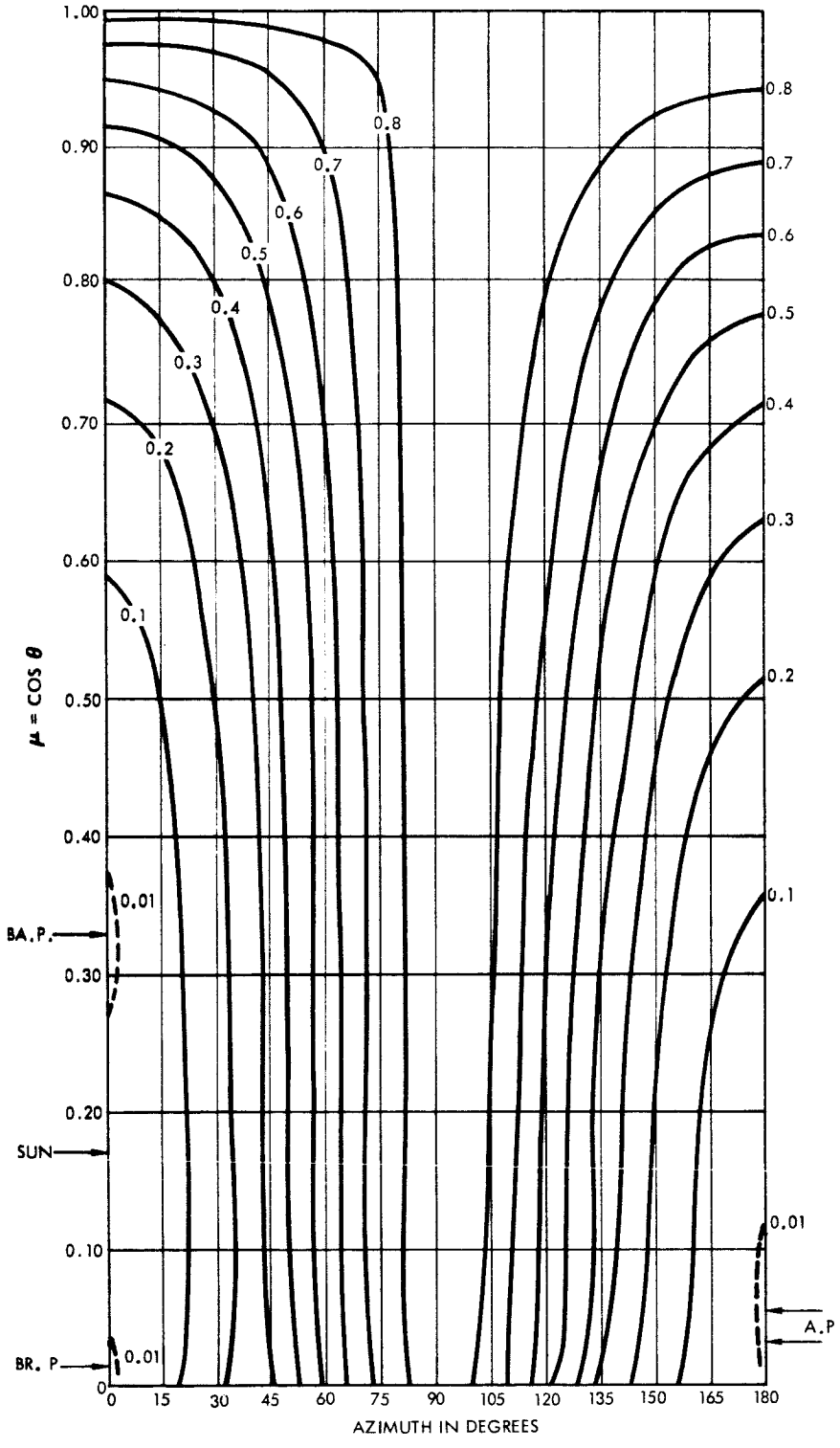

Figure 23. Degree of polarization at base of atmosphere of Fresnel model. $\tau_1 = 0.15$. $\theta_o = 80.2^o$.

result the values are greater than or equal to zero. The Brewster point appears near the horizon; the Babinet point appears at $\mu = 0.33$, $\varphi_o - \varphi = 0^o$, or 9^o above the sun; a double Arago point appears near the horizon and at an azimuth of 180^o. The maximum degree of polarization in the sun's vertical plane is 0.87 and occurs about 9^o from the zenith, or at $\mu = 0.99$ and $\varphi_o - \varphi = 180^o$. The minimum polarization for an arbitrary μ occurs at the sun's vertical plane.

The effect that specular reflection at the ground has on the degree of polarization is shown on Fig. 24. The degree of polarization for the Fresnel model is subtracted from that of a model with zero ground albedo. The effect of the Fresnel reflection is to change the degree of polarization less than an absolute value of 0.07. No unusual changes appear in the vicinity of the neutral points. It should be noted, however, that if the degree of polarization in the sun's vertical plane were given by Eq. (43) instead of Eq. (41), the effect of Fresnel reflection at the ground would be to increase the polarization of the skylight in the vicinity of the Babinet and Brewster points.

The Stokes parameter Q is shown in Fig. 25 for the model of zero ground albedo. Neutral points occur where the zero line of Q intersects the sun's vertical plane. No Brewster point occurs in this figure. The minimum values of Q occur in the sun's vertical plane, and the maximum values occur at an azimuth of about 90^o.

The effect of Fresnel reflection at the ground on Q is shown in Fig. 26. The general features are the same on both Figs. 25 and 26. However, when Fresnel reflection is present, the Babinet and Arago points are shifted towards their respective horizons. Also, a Brewster point and second Arago point appear.

The change in Q caused by Fresnel reflection at the ground is shown on Fig. 27. The change is less than 0.03 in. absolute value.

The Stokes parameter U is shown for the zero ground albedo model on Fig. 28. $U = 0$ in the sun's vertical plane. Another zero line intersects the sun's vertical plane slightly above the sun and again at the zenith at an azimuth of $\varphi_o - \varphi = 90^o$. Note also that this zero line is restricted to

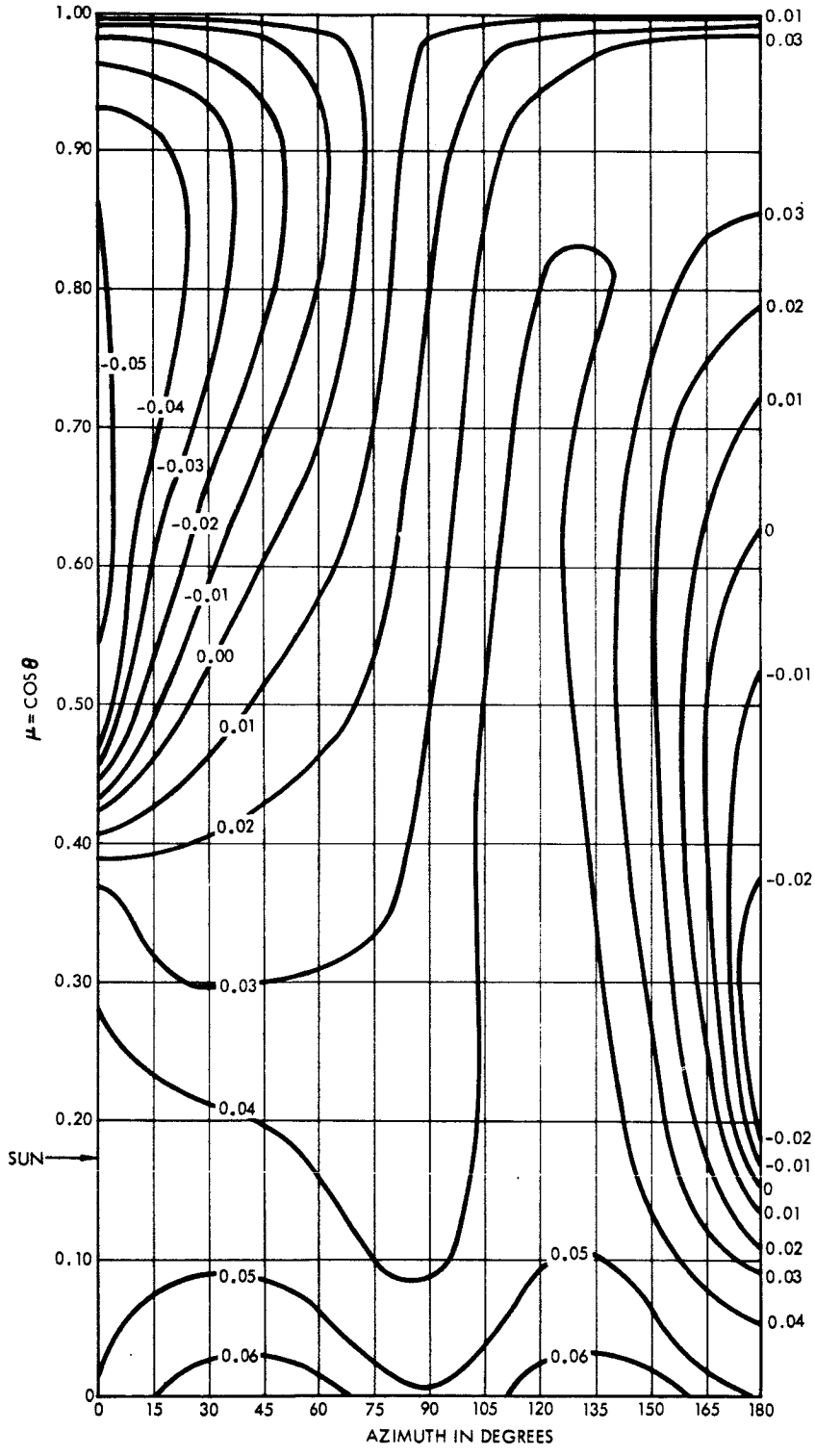

Figure 24. Degree of polarization at base of atmosphere of zero ground albedo model minus that of Fresnel model. $\tau_1 = 0.15$. $\theta_o = 80.2^o$.

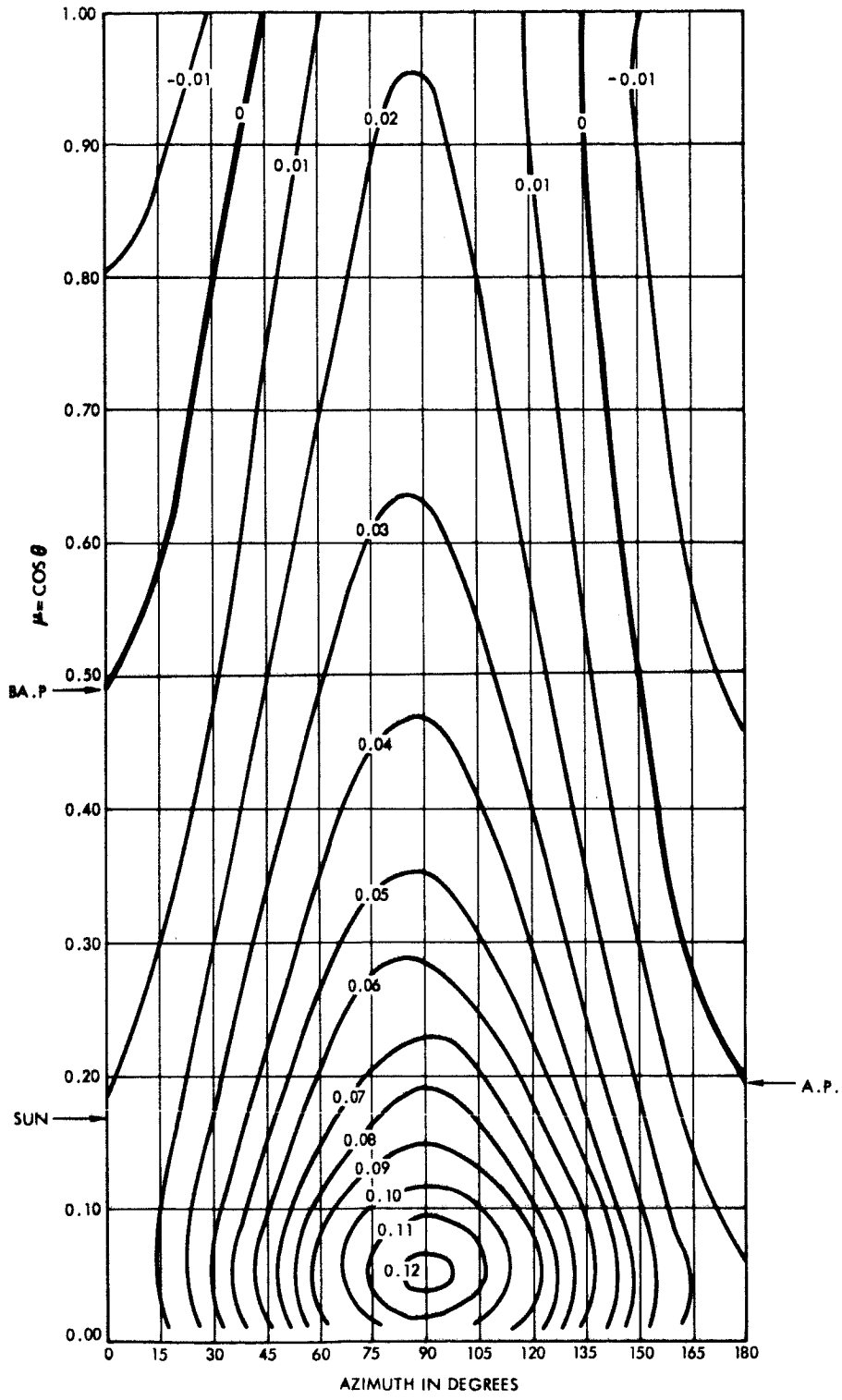

Figure 25. $\downarrow Q$ at base of atmosphere for zero ground albedo model $(\lambda_o(\tau_1) = 0)$. $\tau_1 = 0.15$. $\theta_o = 80.2^\circ$.

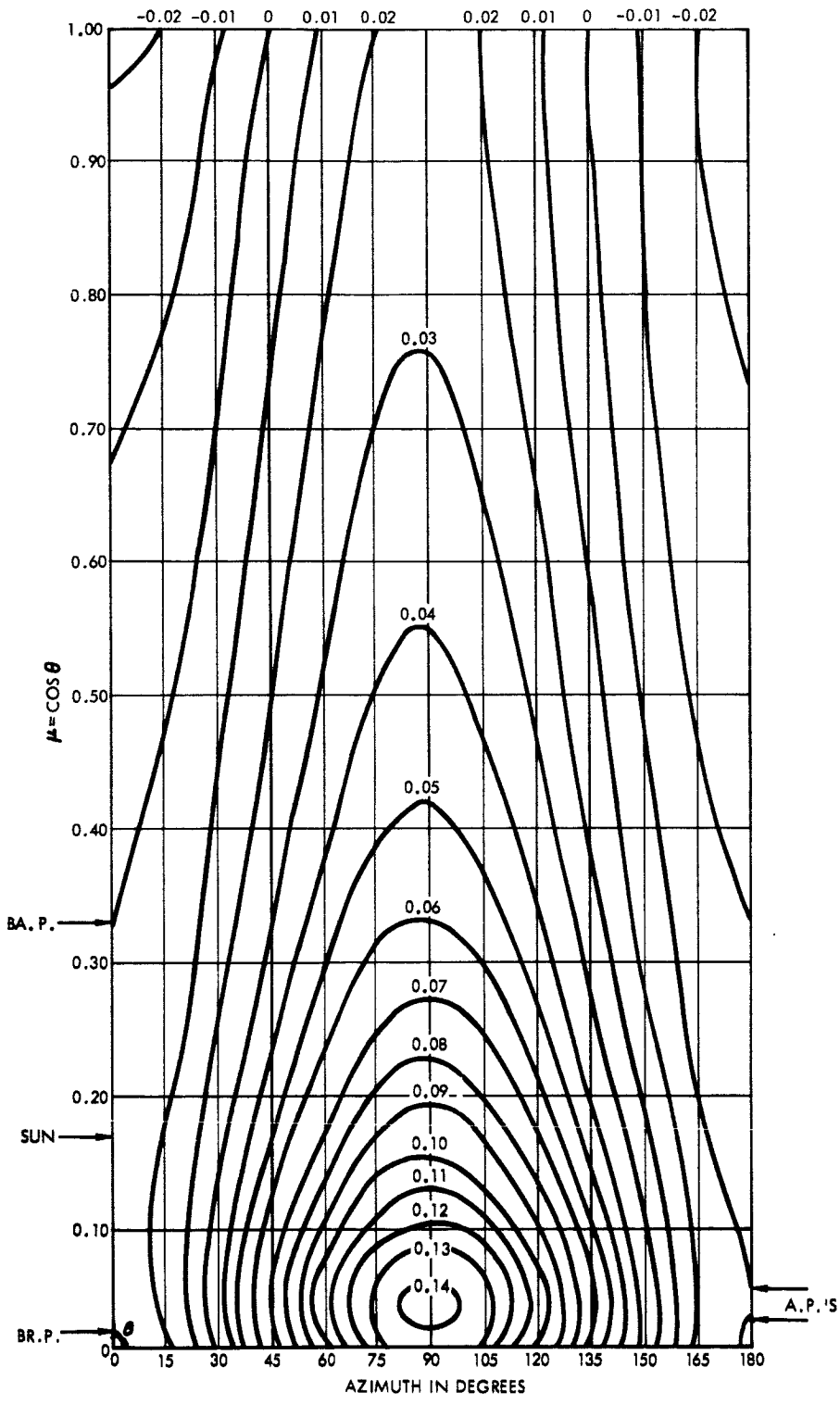

Figure 26. $^{\downarrow}Q$ at base of atmosphere for Fresnel model. $\tau_1 = 0.15$. $\theta_o = 80.2^{\circ}$.

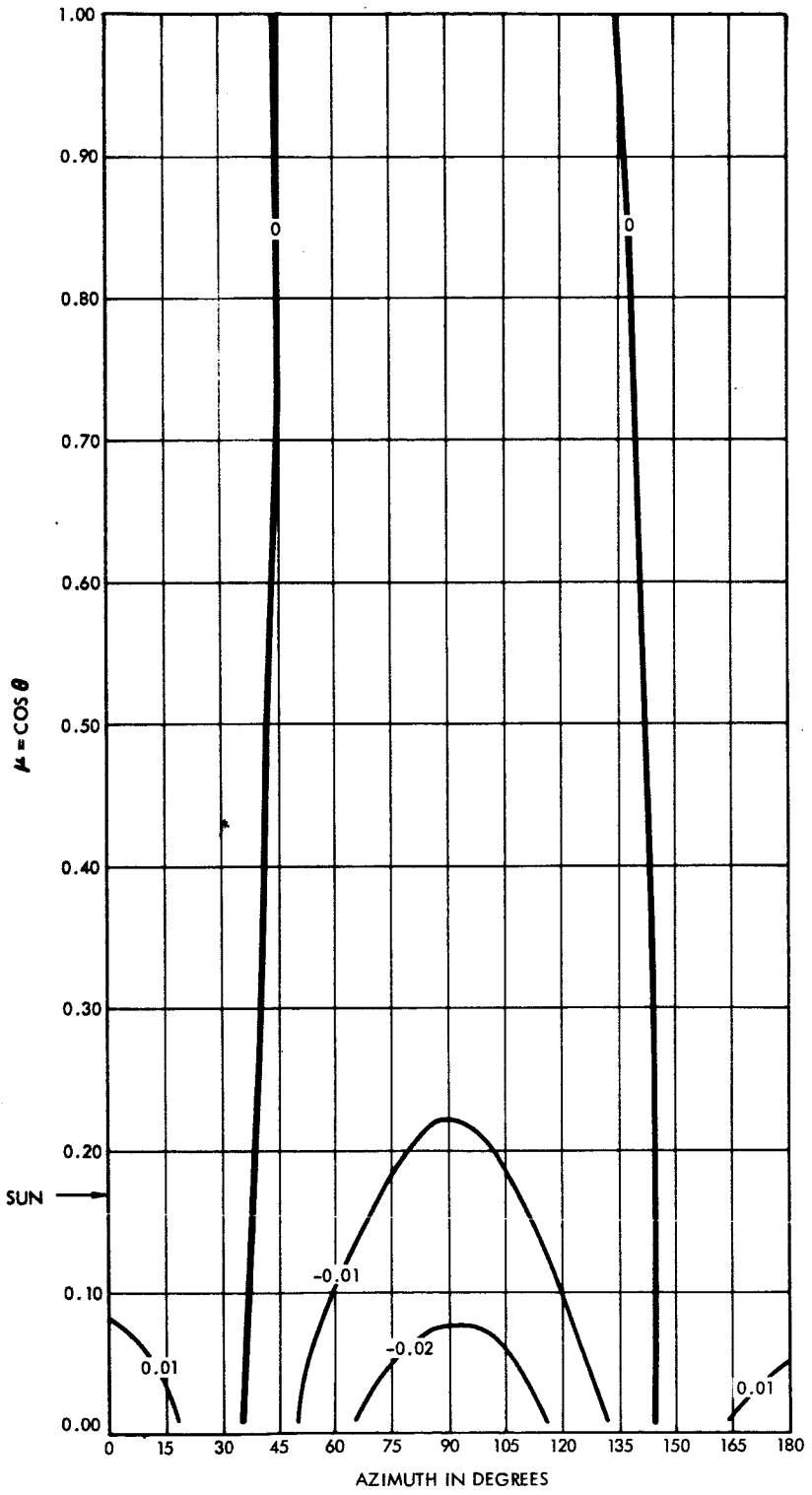

Figure 27. ^{1}Q at base of atmosphere for zero ground albedo model minus that of Fresnel model. $\tau_1 = 0.15$. $\theta_o = 80.2^{o}$.

an azimuth less than 90°.

The effect of Fresnel reflection is to make a small absolute change in U, as shown on Fig. 29. A zero line lies in the sun's vertical plane. A second zero line has an azimuth less than 90°, but it now intersects the sun vertical plane a few degrees below the sun.

Attention is now shifted to a smaller solar zenith angle, when the neutral points do not lie in the sun's vertical plane. The U-data for the Fresnel model is given on Fig. 30. A zero line still lies in the sun's vertical plane. Another zero line intersects the sun's vertical plane between the sun and the horizon. No zero line lies outside of the sun's vertical for an azimuth greater than 90°. Hence, no neutral point will occur outside of the sun's vertical plane in that half of the sky between the zenith and the ground for which the azimuth $\varphi_{o} - \varphi > 90^{\circ}$. The only neutral point on the figure occurs at an azimuth of 2.3° and at a zenith distance of 2.1° below the almucantor. Of course, a second neutral point would occur symmetrically at an azimuth of -2.3°.

The Q-data for the same conditions are shown in Fig. 31. The zero line no longer intersects the sun's vertical plane. The zero line comes closest to the vertical plane where the neutral point occurs. The zero line does not approach closer than 20° in azimuth to that half of the sun's vertical plane that has the azimuth of 180°.

Successive positions of the $Q = 0$ and $U = 0$ lines in the vicinity of the neutral points are shown for increments in the position of the sun in Fig. 32. The sun is taken as the center of the coordinate system. The zero lines of Q and U are given as a function azimuth and $\mu - \mu_{o}$. If $\mu - \mu_{o} > 0$, then the corresponding zenith angle is smaller than that of the sun. The smallest value of μ_{o} for which data are given is $\mu_{o} = 0.28$, which corresponds to $\theta_{o} = 73.7^{\circ}$. In this case a Babinet point occurs slightly above the sun at $\mu - \mu_{o} \doteq 0.01$ and a Brewster point occurs below the sun at $\mu - \mu_{o} \doteq -0.08$. It is important to note that the zero lines of U approach the sun's vertical plane at nearly a constant distance below the sun at $\mu - \mu_{o} \doteq -0.04$. Later, it will be shown that the zero line of U has a different behavior on top of the atmosphere. As μ_{o}

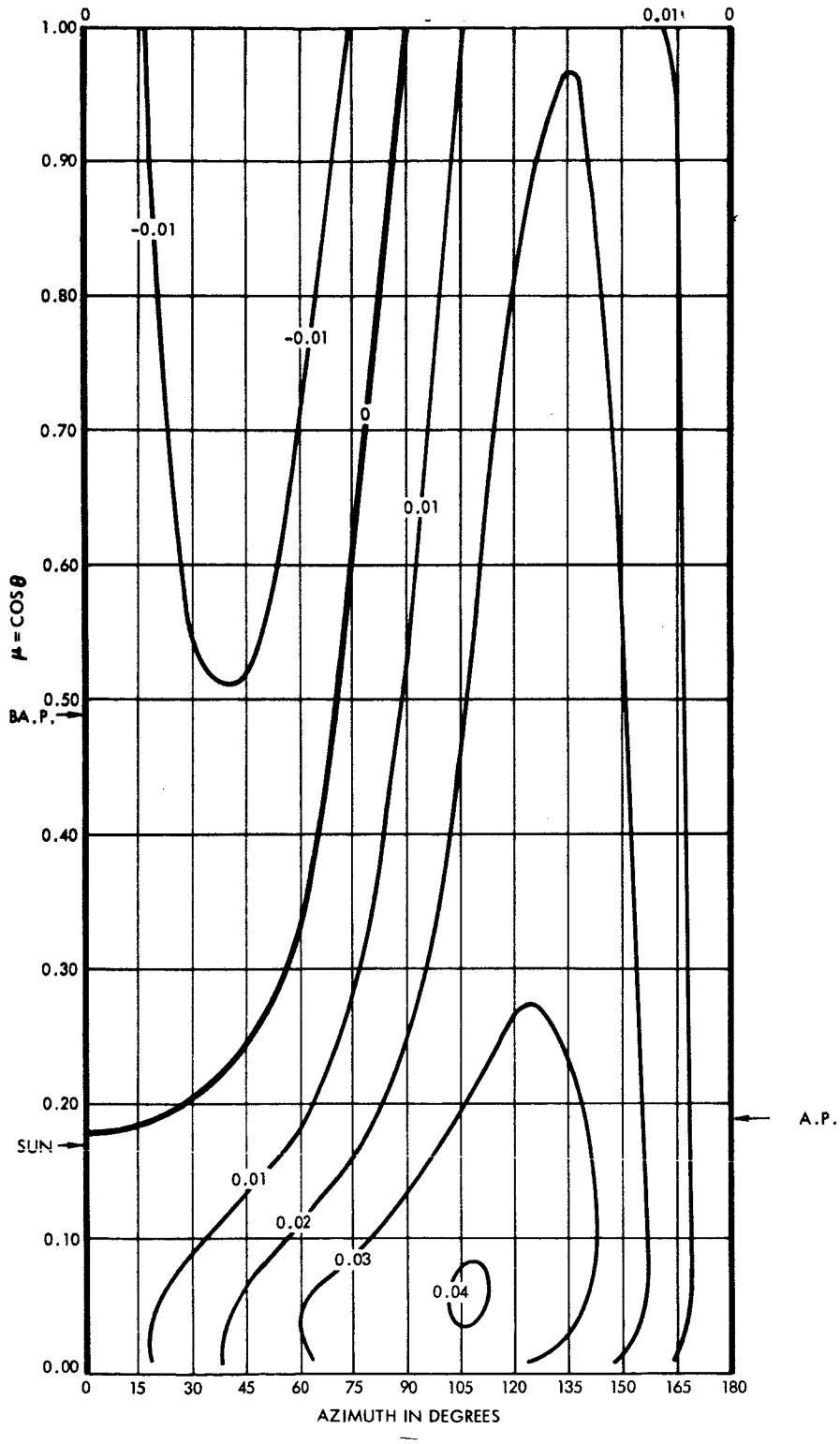

Figure 28. $\downarrow U$ at base of atmosphere for zero ground albedo model. $\tau_1 = 0.15$. $\theta_o = 80.2^\circ$.

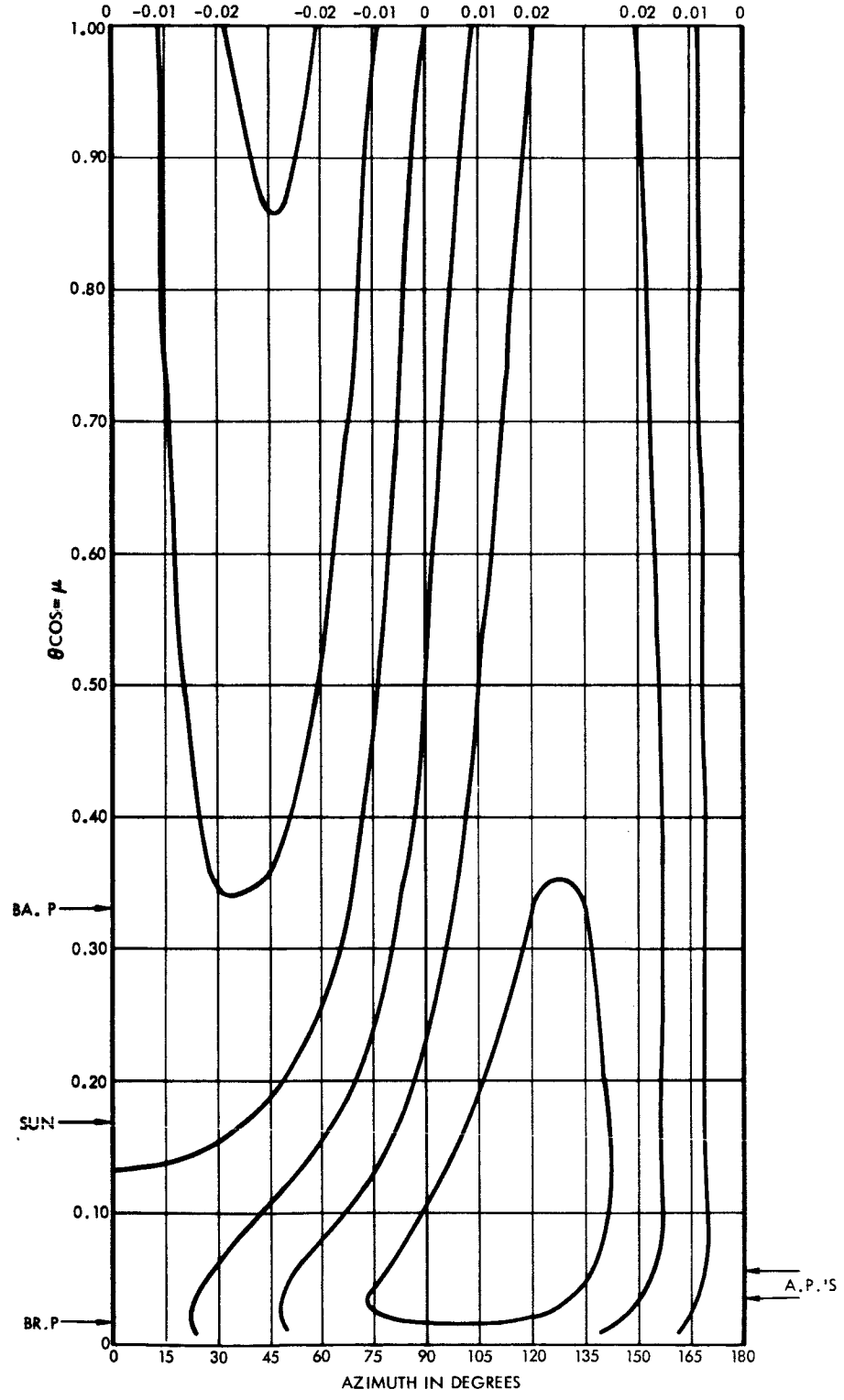

Figure 29. $^{\downarrow}U$ at base of atmosphere of Fresnel model. $\tau_1 = 0.15$. $\theta_o = 80.2^o$.

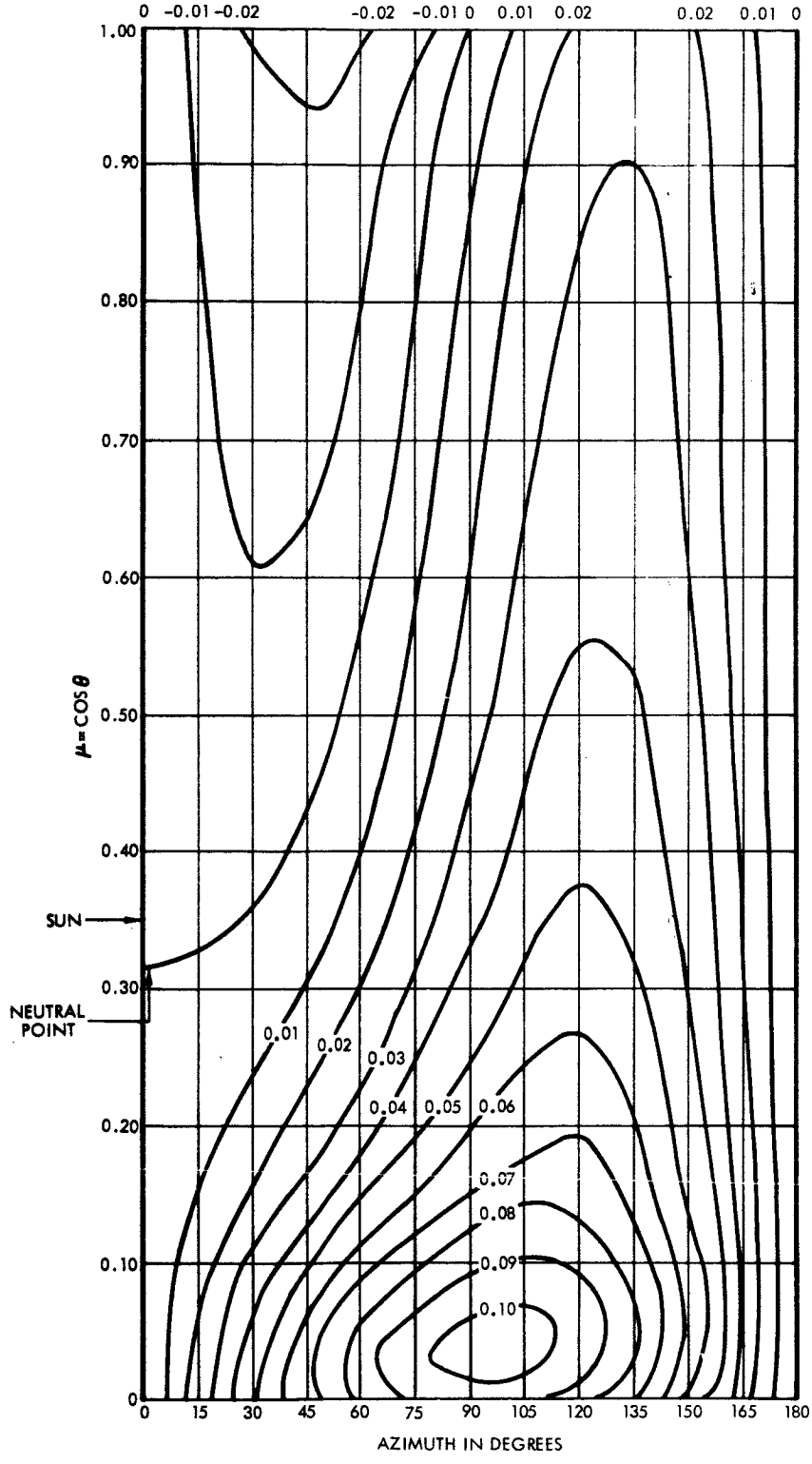

Figure 30. U at base of atmosphere of Fresnel model. $\tau_1 = 0.15$. $\theta_o = 69.5°$.

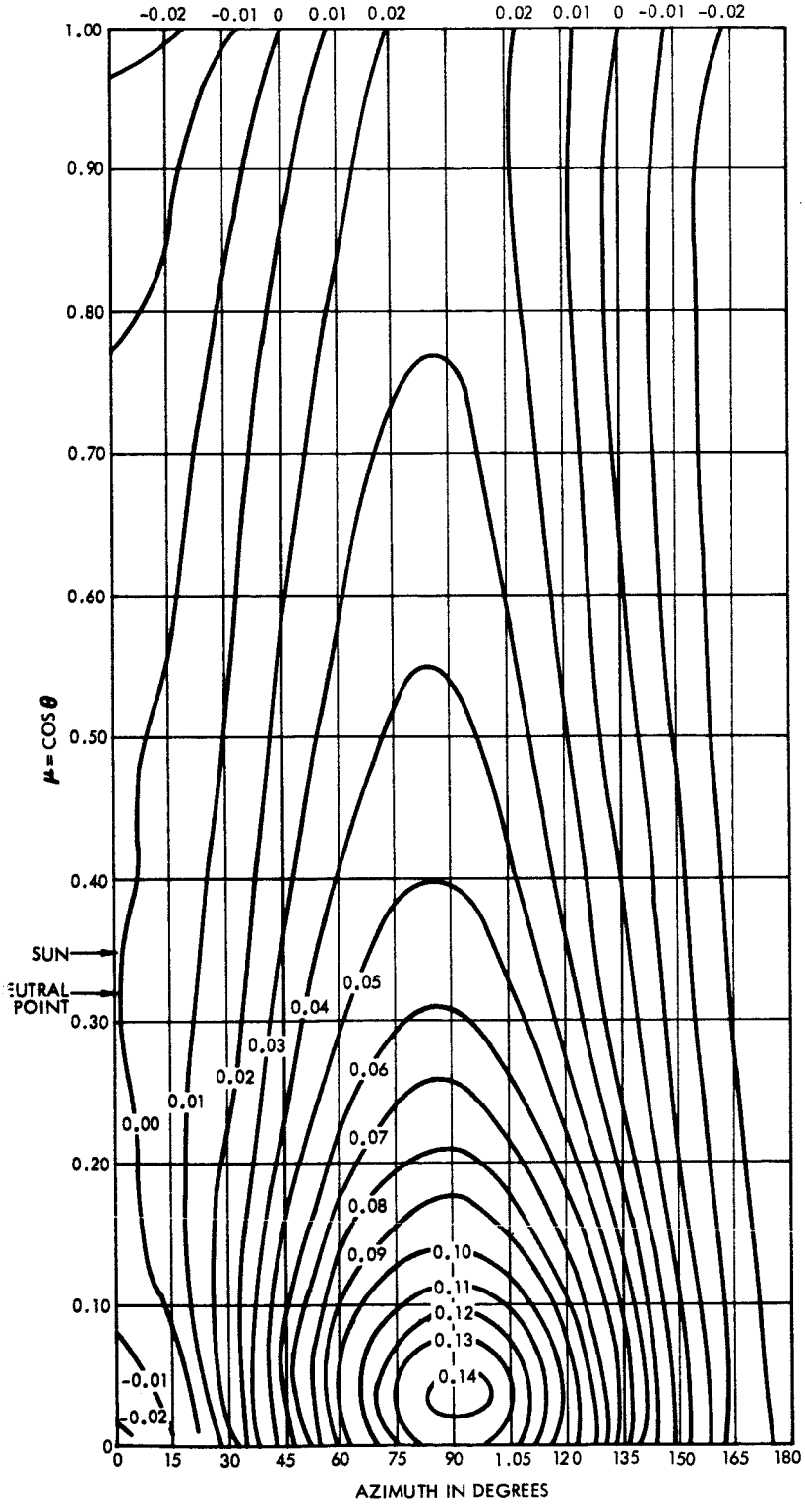

Figure 31. $^{1}_{4}Q$ at base of atmosphere of Fresnel model. $\tau_1 = 0.15$. $\theta_o = 69.5$.

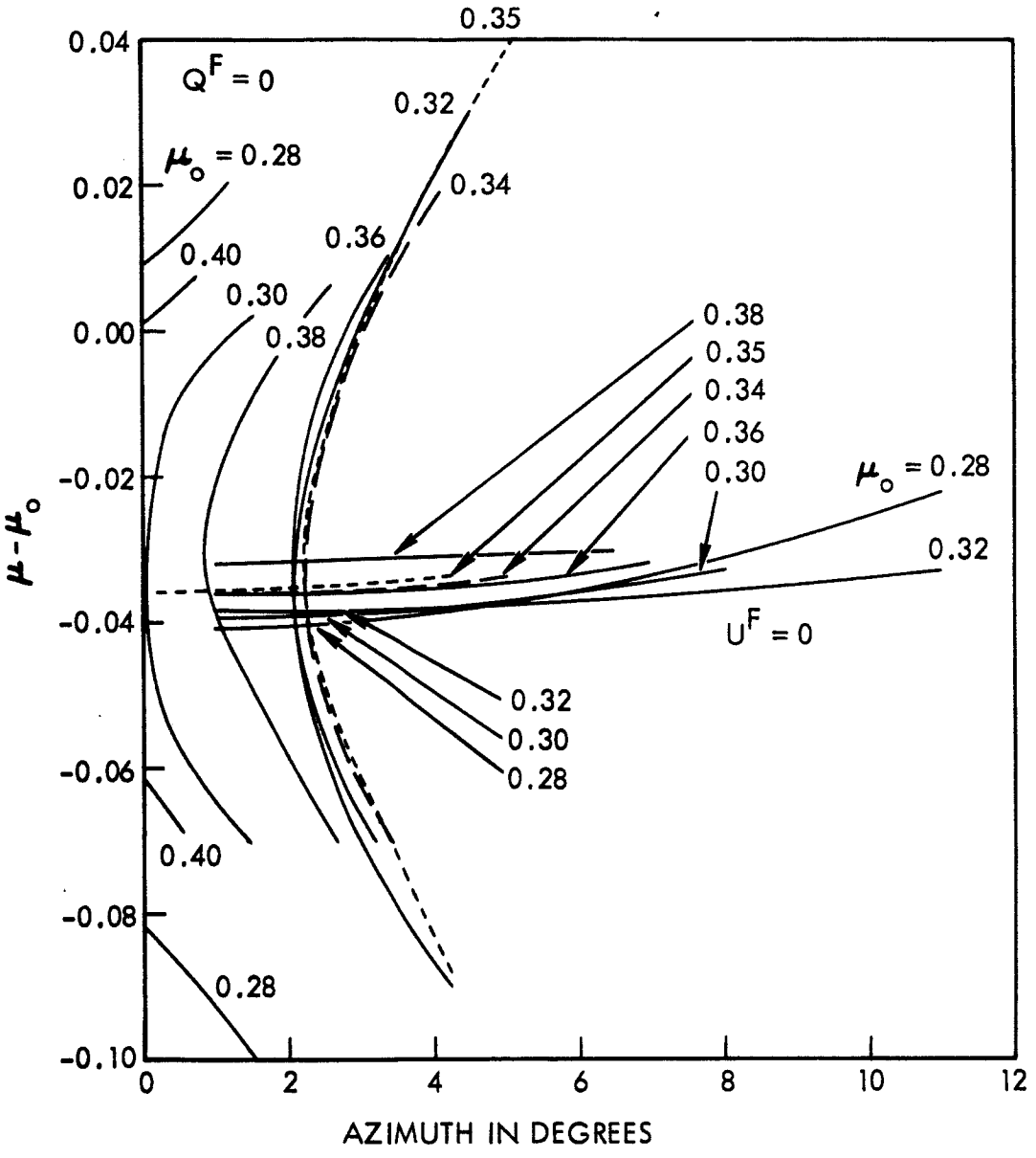

Figure 32. Position of lines of $^{\downarrow}Q = 0$ and $^{\downarrow}U = 0$ at base of atmosphere as neutral point moves in and out of sun's vertical plane. Fresnel model. $\tau_1 = 0.15$.

increases for 0.28 to 0.30, the two neutral points merge and move slightly outside of the sun's vertical plane. The neutral point remains at nearly the same position with respect to the sun for the range of μ_o between 0.32 and 0.36. As μ_o increases above 0.36, the neutral point approaches the sun's vertical plane. At $\mu_o = 0.40$ a Babinet point occurs just above the sun, and a Brewster point occurs below the sun at $\mu - \mu_o \doteq -0.06$.

The degree of polarization of the skylight in the vicinity of a neutral point that lies outside the sun's vertical plane is shown on Fig. 33. The degree of polarization changes 0.0007 at a constant zenith angle between the sun's vertical plane and the neutral point. Such a small change would be difficult to observe instrumentally. However, the change in polarization is much larger at smaller optical thickness. For example, at approximately the same solar zenith angle of $\theta_o = 72.5^\circ$ and for $\tau_1 = 0.05$, the degree of polarization changes 0.05 at a constant zenith angle between the sun's vertical plane and the neutral point. In this case the neutral point lies at an azimuth of about 18° from the sun's vertical plane.

The computed coordinates of the neutral points for the Fresnel model are given in Table VI.

The sensitivities of various radiation parameters to a change in the reflection characteristics of the ground are shown on Fig. 34. The measure of sensitivity is to take the value of a parameter for the Lambert model minus the value of the same parameter for the Fresnel model and divide by the value for the Lambert model. The absolute value of the relative difference in the total intensity of radiation from the zenith is less than 3 per cent if either the solar zenith angle is less than 53° or if the optical thickness exceeds 0.3 (bottom portion of Fig. 34). However, the relative difference in the intensity becomes large when the sun is both near the horizon ($\mu_o = 0.1$) and when the optical thickness is small. The reason for the large relative difference in this case is that the atmosphere is strongly illuminated from below, and a much larger fraction of this upward flux is scattered back down to the ground for the Fresnel model than for the Lambert model. To illustrate with a particular example, let $\mu_o = 0.1$ and $\tau_1 = 0.05$. In this case the albedo at the ground is 0.42. The upward flux

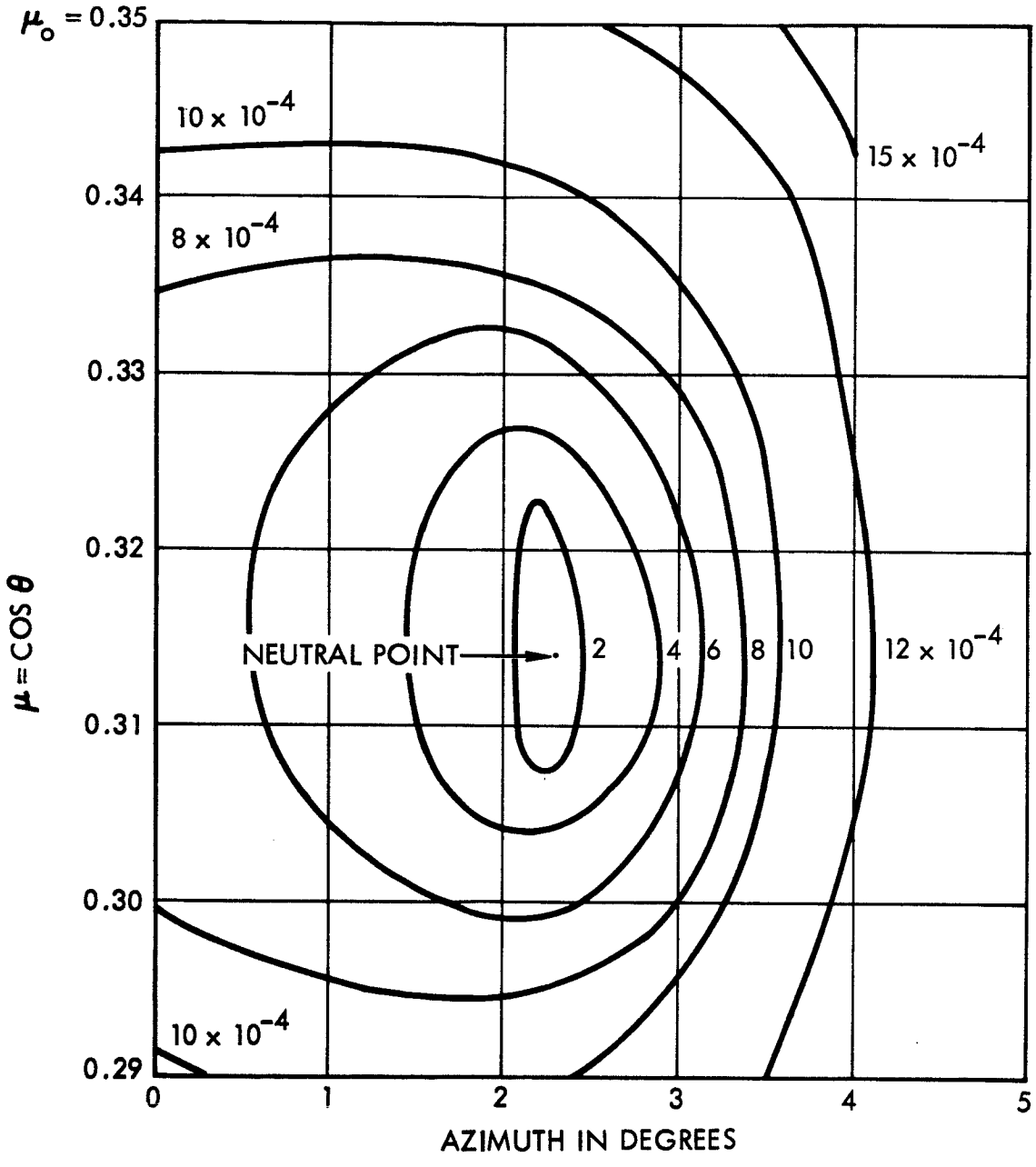

Figure 33. Degree of polarization at base of atmosphere in vicinity of neutral point exterior to sun's vertical plane. Fresnel model. $\tau_1 = 0.15$.

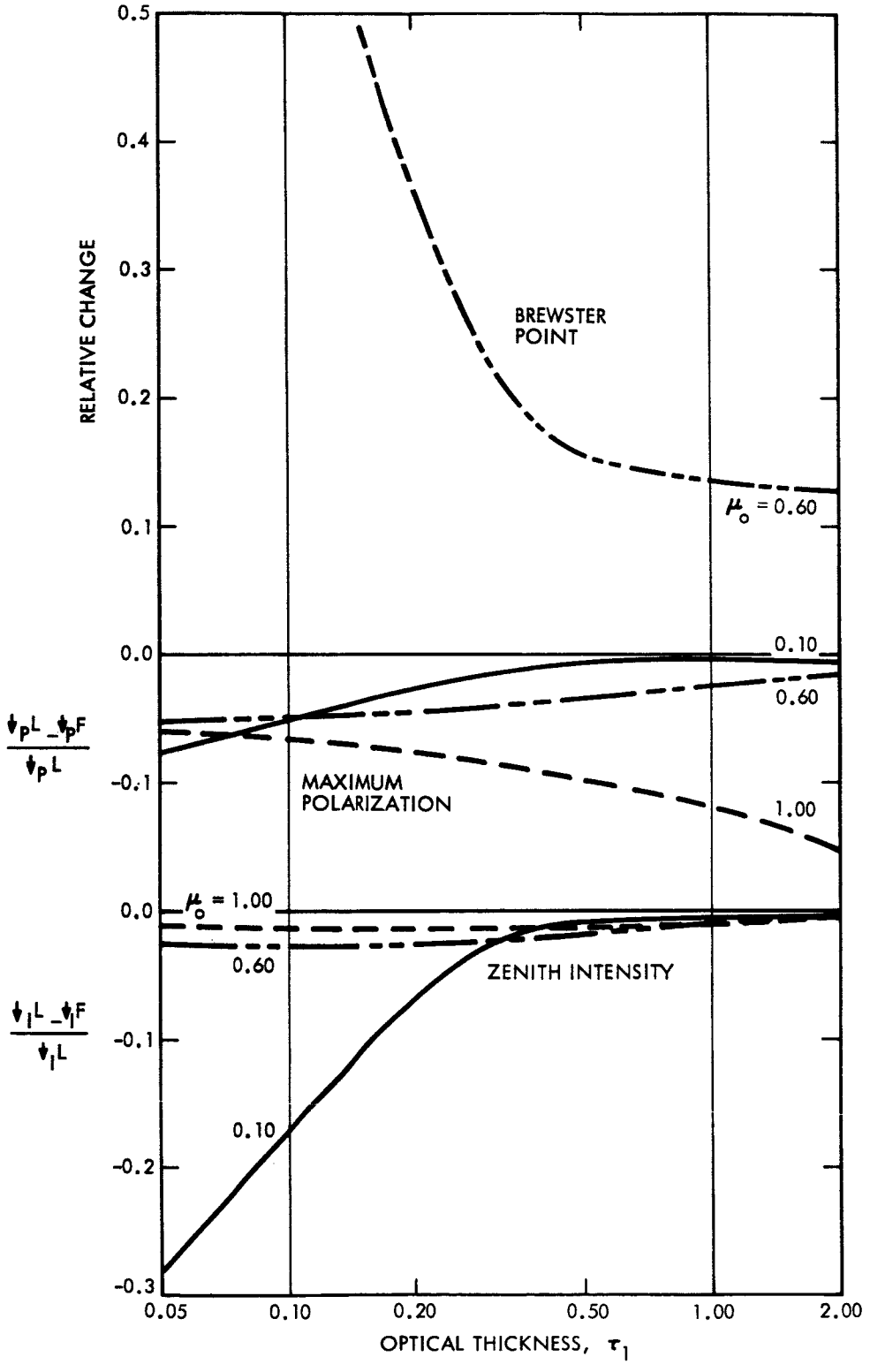

Figure 34. Relative change at base of atmosphere in a neutral point, maximum degree of polarization in the sun's vertical plane and total intensity at zenith for Lambert and Fresnel models.

TABLE VI

Computed neutral point positions at bottom of atmosphere of Fresnel model. Index of refraction is m = 1.34. The word none or a blank means that the neutral point does not exist. A dash means that the neutral point exists, but that its position was not computed. The value in parenthesis at $\tau_1 = 0.15$, $\theta_o = 75.52$ was obtained by extrapolation.

optical thickness τ_1	solar zenith angle, θ_o	ground albedo, $\lambda_o(\tau_1)$	neutral points in sun's vertical plane					
			Brewster		Babinet		Arago	
			θ	$\theta_o - \theta$	θ	$\theta_o - \theta$	θ	$\theta_o + \theta$
0.05	87.13°	0.420	none		-	-	-	-
			neutral points outside of sun's vertical plane					
			θ	$\theta_o - \theta$	$\varphi_o - \varphi$			
	84.26	0.418	87.6°	- 2.3°	9.0°			
	78.46	0.276	82.0	- 3.5	17.1			
	75.52	0.215	78.8	- 3.3	18.2			
	72.54	0.167	75.5	- 3.0	18.4			
	66.42	0.102	69.2	- 2.8	17.0			
	60.00	0.065	61.7	- 1.7	14.7			
	53.13	0.045	54.6	- 1.5	12.6			
	45.57	0.033	46.9	- 1.3	11.8			
	36.87	0.028	37.8	- 0.9	12.6			
	25.84	0.025	26.4	- 0.6	15.2			
	18.19	0.025	18.5	- 0.3	16.4			
	8.11	0.024	8.2	- 0.1	19.0			
	0.00	0.024	0.0	0.0	0.0			
0.15			neutral points in sun's vertical plane					
			Brewster		Babinet		Arago	
			θ	$\theta_o - \theta$	θ	$\theta_o - \theta$	θ	$\theta_o + \theta$
	87.71°	0.134	none		67.0°	20.8°	70.9°	158.6°
	87.13	0.164	"		-	-	71.6	158.7
	84.26	0.257	"		68.1	16.1	76.6	160.9

τ_1	θ_o	$\lambda_o(\tau_1)$	Brewster θ	Brewster $\theta_o - \theta$	Babinet θ	Babinet $\theta_o - \theta$	Arago θ	Arago $\theta_o + \theta$
0.15	83.11	0.264	none		-	-	79.1	162.2
	80.79	0.253	89.4	- 8.6	70.2	10.6	84.6	165.4
							89.1	169.9
	80.21	0.248	89.0	- 8.8	70.8	9.4	86.8	167.0
							88.0	168.2
	79.63	0.241	-	-	-	-	none	
	78.46	0.228	87.4	- 9.0	71.7	6.8		
	77.88	0.220	86.7	- 8.8	71.9	6.0		
	77.29	0.213	85.8	- 8.5	72.1	5.2		
	75.52	0.191	(82.5)	(- 7.0)	72.7	2.8		
	74.34	0.176	-	-	73.0	1.4		
	73.7	0.170	78.5	- 4.8	73.2	0.5		
	72.54		none		none			

<u>neutral points outside of sun's vertical plane</u>

θ	$\theta_o - \theta$	$\varphi_o - \varphi$
75.0	- 2.4	0.1
73.7	- 2.3	2.0
72.3	- 2.2	2.2
71.6	- 2.1	2.3
71.0	- 2.1	2.1
70.3	- 2.0	1.7
69.6	- 2.0	0.9
none		

τ_1	θ_o	$\lambda_o(\tau_1)$	Brewster θ	Brewster $\theta_o - \theta$	Babinet θ	Babinet $\theta_o - \theta$
	66.42	0.104	70.1	- 3.7	66.4	0.05
	65.17	0.096	-	-	64.0	1.2
	60.00	0.071	67.1	- 7.1	56.1	3.9
	58.67	0.066	-	-	54.4	4.3
	53.13	0.051	61.3	- 8.1	48.0	5.1
	51.68	0.048	-	-	46.6	5.1

τ_1	θ_o	$\lambda_o(\tau_1)$	Brewster θ	Brewster $\theta_o - \theta$	Babinet θ	Babinet $\theta_o - \theta$
0.15	45.57	0.040	52.7	- 7.1	41.1	4.5
	43.95	0.038	-	-	39.8	4.2
	36.87	0.034	40.5	- 3.6	35.0	1.9
	34.92	0.033	37.1	- 2.2	34.3	0.6
	32.86		none		none	
			neutral points outside of sun's vertical plane			
			θ	$\theta_o - \theta$	$\varphi_o - \varphi$	
	32.86	0.032	33.5	- 0.6	3.2	
	30.68	0.032	31.2	- 0.5	5.2	
	28.36	0.031	28.8	- 0.4	6.8	
	25.84	0.031	26.2	- 0.4	8.3	
	19.95	0.030	20.2	- 0.2	10.7	
	14.07	0.030	14.1	0.0	12.7	
	11.48	0.030	11.5	0.0	12.9	
	8.11	0.030	8.1	0.0	13.3	
	0.00	0.030	0.0	0.0	0.0	

τ_1	θ_o	$\lambda_o(\tau_1)$	Brewster θ	Brewster $\theta_o - \theta$	Babinet θ	Babinet $\theta_o - \theta$	Arago θ	Arago $\theta_o + \theta$
0.25	87.13	0.095	none		63.4	23.8	68.2	155.4
	84.26	0.162	"		62.4	21.9	71.5	155.8
	81.37	0.191	"		62.4	19.0	76.0	157.4
	78.46	0.186	"		62.3	16.2	80.9	159.4
	76.11	0.171	89.4	- 13.3	61.7	14.4	85.6	161.7
							88.7	164.8
	74.34	0.157	88.5	- 14.1	60.9	13.4	none	
	72.54	0.143	87.4	- 14.9	59.8	12.7		
	71.94	0.138	87.0	- 15.1	-	-		
	71.34	0.134	86.6	- 15.2	59.1	12.2		
	70.73	0.129	86.1	- 15.4	58.6	12.1		

τ_1	θ_o	$\lambda_o(\tau_1)$	Brewster θ	$\theta_o - \theta$	Babinet θ	$\theta_o - \theta$	Arago θ	$\theta_o + \theta$
0.25	66.42	0.102	81.9	- 15.5	55.0	11.4		
	60.00	0.073	75.2	- 15.2	49.0	11.0		
	53.13	0.055	67.5	- 14.4	42.8	10.3		
	45.47	0.044	58.1	- 12.5	36.8	8.8		
	36.87	0.039	45.9	- 9.0	30.6	6.3		
	25.84	0.035	29.6	- 3.8	23.0	2.8		
	19.95	0.035	20.3	- 0.3	19.7	0.2		
	16.26	0.034	none		none			
			neutral points outside of sun's vertical plane					
			θ	$\theta_o - \theta$	$\varphi_o - \varphi$			
	16.26	0.034	16.3	0.0	4.2			
	8.11	0.034	8.1	0.0	8.8			
	0.00	0.034	0.0	0.0	0.0			
			Brewster θ	$\theta_o - \theta$	Babinet θ	$\theta_o - \theta$	Arago θ	$\theta_o + \theta$
0.50	84.26	0.078	none		27.1	57.2	66.4	150.7
	78.46	0.114	"		24.4	54.1	72.8	151.3
	72.54	0.111	"		21.4	51.2	80.8	153.4
	66.42	0.092	87.8	- 21.4	19.2	47.3	none	
	60.00	0.074	82.8	- 22.8	17.3	42.7		
	53.13	0.061	74.8	- 21.6	15.4	37.7		
	45.57	0.052	64.5	- 19.0	13.1	32.5		
	36.87	0.046	51.7	- 14.8	10.2	26.7		
	25.84	0.043	34.8	- 9.0	6.4	19.4		
	16.26	0.042	20.9	- 4.6	3.4	12.9		
	8.11	0.042	9.3	- 1.2	0.2	7.9		
	0.00	0.042	0.0	0.0	0.0	0.0		

into the base of the atmosphere is six-tenths of the downward flux into the top of the atmosphere. The atmospheric reflectivity is 0.20 and 0.05 of the upward flux into the base of the atmosphere for the Fresnel and Lambert models, respectively. This downward flux at the ground augments the flux of unreflected skylight, which is the same for both models, by 0.37 for the Fresnel model but only by 0.09 for the Lambert model. As a result, the zenith intensity is much greater for the Fresnel model than for the Lambert model.

The relative difference between the maximum degree of polarization in the sun's vertical plane for the Fresnel and Lambert models is shown in the center of Fig. 34. The absolute value of the relative difference is less than 10 per cent, except when the sun is at the zenith ($\mu_o = 1.00$) and the optical thickness exceeds 0.50.

The neutral point characteristics that are most sensitive to changes in the type of ground reflection cannot be compared for the two models, since such characteristics are not present in both models for the same solar zenith angle. For example, when the neutral points lie outside of the sun's vertical plane for the Fresnel model, there is no corresponding characteristic of the Lambert model to make a comparison with. However, the Brewster point for $\mu_o = 0.60$ can be used. This neutral point is moderately sensitive to the nature of the ground reflection. The relative difference in the Brewster point positions for the Lambert and Fresnel models is shown on the top portion of Fig. 34. The relative difference approaches one at $\tau_1 \sim 0.1$ and is not defined for $\tau_1 \leq 0.1$, since the Brewster point does not exist in the Fresnel model. The sensitivity of this one neutral point paramter is comparable to or exceeds the sensitivity of the maximum polarization and of the intensity at an arbitrary optical thickness.

3.1.3 Comparison of Measured and Computed Neutral Points

Measured and computed Arago point positions are compared in Fig. 35. The measurements were made visually without optical filters. In order to find the proper optical thickness of a Rayleigh atmosphere that would correspond to the effective visual optical thickness of the earth's atmosphere,

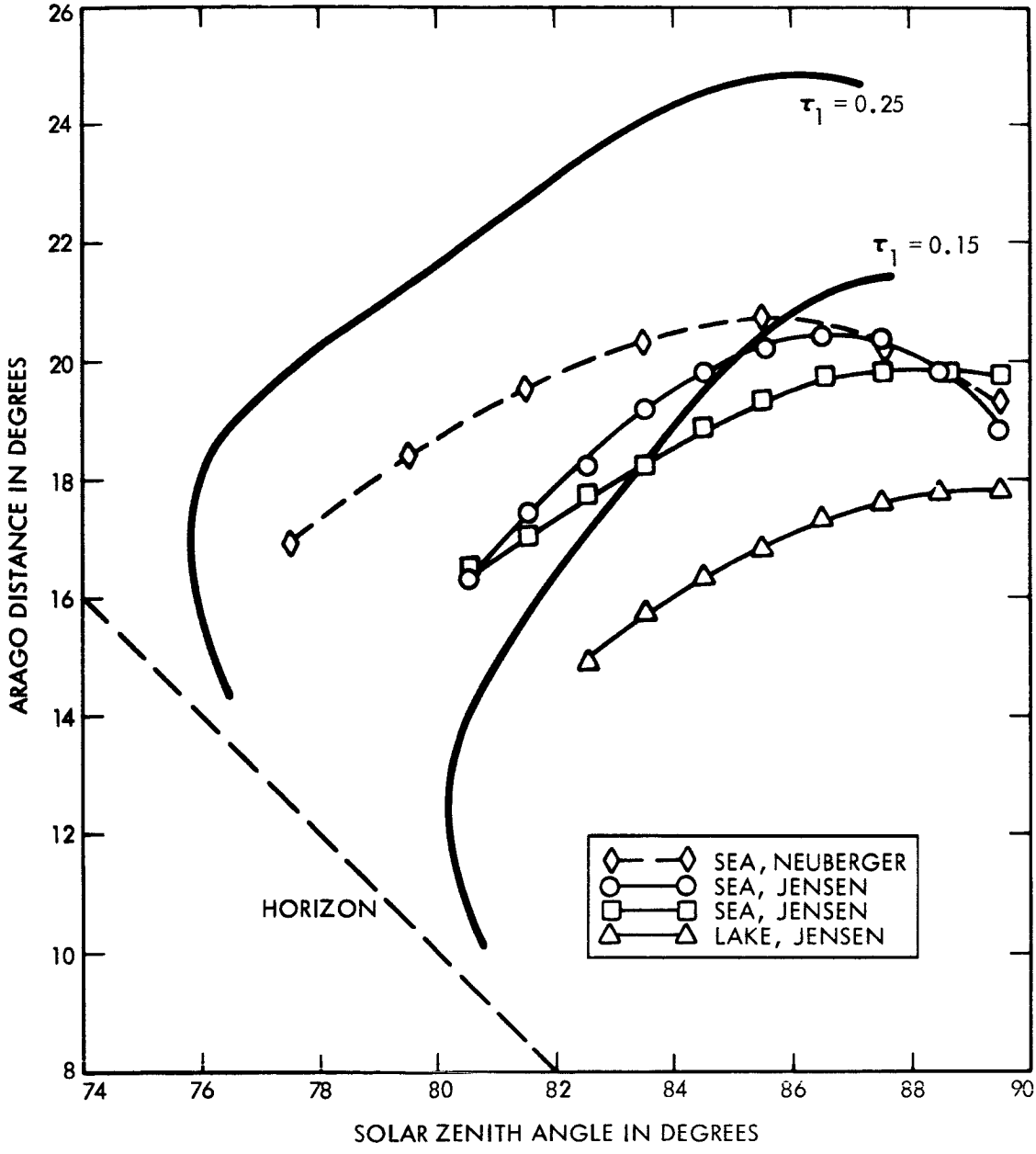

Figure 35. Measured and computed (continuous lines) Arago point distances over seas. The Neuberger and Jensen data are taken from ref. 13 and 11, respectively.

the Arago point positions measured over land were compared with the positions computed for the Lambert model. Measured data by Neuberger[13] indicate an optical thickness of $\tau_1 = 0.15$. Measurements of Arago point positions at $\lambda 5150\text{Å}$, which corresponds approximately to the wavelength of maximum visual acuity, indicate an optical thickness of $\tau_1 = 0.25$.[18] Hence, the computed values for the Fresnel model at $\tau_1 = 0.15$ and 0.25 are given in Fig. 35. The computed Arago point distances for $\tau_1 = 0.10$ would be smaller than those shown for $\tau_1 = 0.15$, but the values for $\tau_1 = 0.10$ were not computed.

The measured data in Fig. 35 have been averaged for more than one day's observations. The averaged data do not show the double Arago point that is shown on the computed curves. However, measurements for a single day have detected the double Arago point (see ref. 11 for a discussion). Only Jensen[11] observed the double Arago point over a sea when haze was not evident. The computed curves show that a double Arago point would occur over smooth water when no haze or aerosol particles are in the atmosphere.

The lack of agreement between the measured and computed curves at large solar zenith angle ($\theta_o > 85^\circ$) depends partially on the fact that the models are plane-parallel. The agreement between the measured and computed curves for $78^\circ \leq \theta_o \leq 85^\circ$ may not be bad, if one realizes that the computed Arago distances for the Lambert model are 21° and 25° ($73^\circ < \theta_o < 84^\circ$) for $\tau_1 = 0.15$ and 0.25, respectively. The relatively small measured values for the lake could be caused if the effective wavelength of the observed radiation is shifted from the yellow towards the red part of the spectrum, where the optical thickness is smaller; and as a consequence, the Arago distance is smaller. The roughness of the water and the aerosol content of the atmosphere will also be the bases for differences between the measured values and the values computed for the model of smooth sea and Rayleigh atmosphere.

Sekera[19] measured the Babinet and Brewster points on one afternoon when the sun was over the sea. He found very good agreement between the measured positions and the positions computed for the Fresnel model while they were present in the sun's vertical plane.

Neutral point positions outside of the sun's vertical plane seem to have been observed only by Cornu[3] and Soret.[20] High altitude air pollution produced by the Krakatowa eruption was present during Cornu's observations. The conditions for these observations do not fit the Fresnel model. However, Soret made observations under conditions that had features in common with the Fresnel model. He made neutral point observations from the shore of a Swiss lake, which extended about 700 - 800 m in the direction of the sun. On several occasions Soret observed in the visual spectrum that the Brewster and Babinet points disappeared from the sun's vertical plane, when the solar zenith angle was about 70°. At the same time a neutral point appeared on each side of the sun, in the solar almucantor, and about 15° - 20° from the sun. Soret said that a pronounced haze lay next to the lake and that the neutral points disappeared when the sun rose from the haze to above it. However, the neutral point data for $\tau_1 = 0.15$ on Fig. 21 indicate that the neutral points are furthest from the sun's vertical plane when $\theta_o = 70^{\circ}$, and also that the neutral points lie in the sun's vertical plane when the sun is higher: $34^{\circ} < \theta_o < 67^{\circ}$. Soret's observations indicate that addition of low-level haze to the Fresnel model would shift the neutral points outside of the sun's vertical plane further from the sun's vertical plane.

3.2 TOP OF ATMOSPHERE

3.2.1 General

The neutral points that would be observed above a Lambert model show a symmetry with the neutral points that would be observed from the ground. This symmetry can be demonstrated with the aid of the schematic representation in Fig. 36. The neutral points for the Lambert model lie in the vertical plane of the sun. Two neutral points are usually present. When the solar zenith angle (θ_o) is not large, one neutral point lies between the anti-solar point and the horizon, and a second one lies between the anti-solar point and the zenith. Neutral points one and two are given the names of Brewster and Babinet points, respectively. These two points are located with respect to the anti-solar direction by the angles Ψ_1 and Ψ_2, as shown on Fig. 36. As the solar zenith angle increases, the Brewster

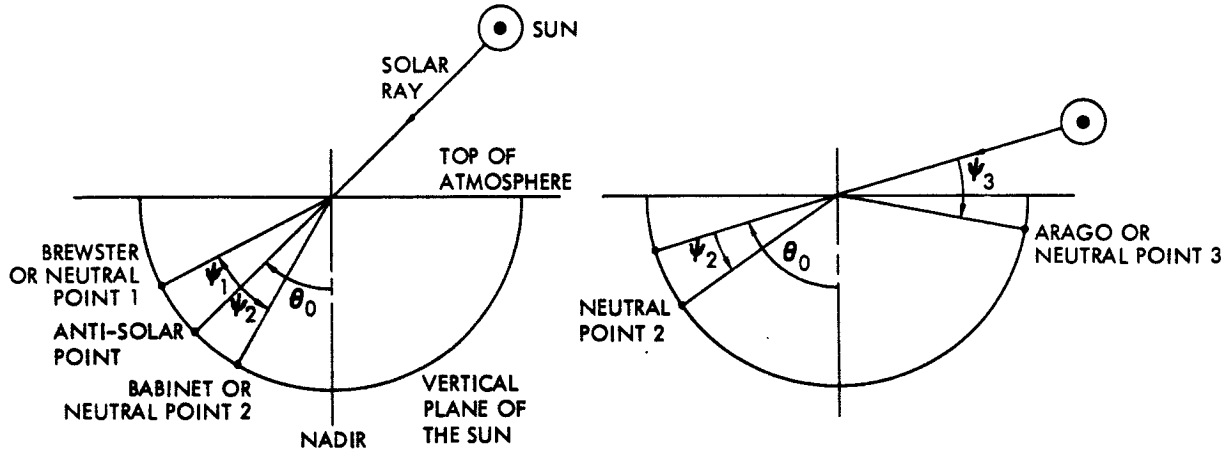

Figure 36. Schematic representation of neutral points at top of atmosphere for Lambert model.

point moves toward the horizon and eventually disappears. Then a third point, which will be called the Arago point, appears at the opposite horizon below the sun. The Arago distance is the angle Ψ_3 between the sun and the Arago point, as shown on the right-hand side of Fig. 36. The neutral point distances on top of the atmosphere are nearly the same as the corresponding ones of the same name on the bottom for the Lambert model, as can be verified by comparing the data on Figs. 18 and 37.

A generalization of these definitions of the Babinet and Brewster points on top of the atmosphere will simplify the discussion of them for the Fresnel model. The generalization is analogous to the one previously made about them for the base of the atmosphere. The Babinet and Brewster points are restricted to the vertical plane of the sun and occur near to the anti-solar point. If the degree of polarization in the sun's vertical plane is positive from the nadir to the anti-solar point and from there to the near horizon, no Babinet or Brewster points occur. If the degree of polarization is positive in the sun's vertical plane along an arc of increasing nadir angle (θ) from the nadir and towards the anti-solar point and then becomes negative at large θ up to the horizon, a Babinet point will be identified with the neutral point that occurs where the sign of the polarization changes. If the degree of polarization is first positive along the arc of increasing nadir angle from the nadir towards the anti-solar point, becomes negative at a larger nadir angle, but becomes positive for a still larger nadir angle that extends to 90°, the neutral point nearest to the nadir will be called a Babinet point, as before, and the neutral point nearest to the horizon will be called a Brewster point. These neutral point definitions do not depend on the solar zenith angle. Since no double Brewster points appeared in the computations for either the Fresnel or Lambert models, no provision is made for such an occurence.

3.2.2 Computed Data

The neutral points in the sun's vertical plane are shown for both the Fresnel and Lambert models in Fig. 37. The neutral points for the Lambert model have been presented previously.[4] The neutral point positions for $\tau_1 = 1.00$ are approximately the same for the two models. The differences

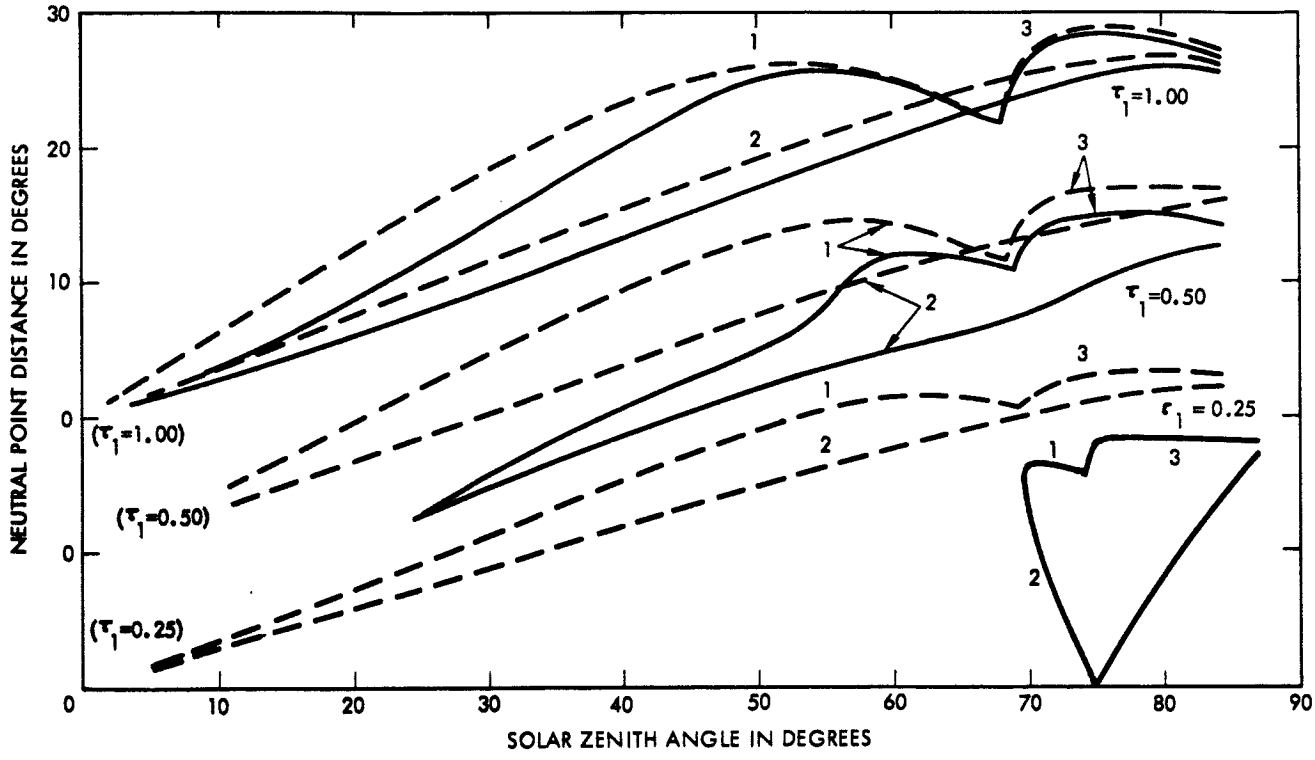

Figure 37. Neutral point positions in sun's vertical plane at top of atmosphere as a function of θ_o. The origin of the ordinate for each succeeding set of curves increases by 10^o and is identified by the appropriate τ_1.

between the neutral points for the two models increase with decreasing optical thickness and become large at $\tau_1 = 0.25$. At the ground the differences are not as large at $\tau_1 = 0.25$ and at smaller optical thickness. Hence, the neutral point characteristics on top of the atmosphere show a greater dependence on the nature of the ground reflection than those at the ground.

Neutral points for the Fresnel model and $\tau_1 = 0.15$ and 0.25 are shown in greater detail on Fig. 38. To explain the meaning of the curves consider just the curves for optical thickness $\tau_1 = 0.15$. The Babinet point is 9.7° from the anti-solar point towards the nadir when the solar zenith angle is $\theta_o = 87^\circ$. As the solar zenith angle decreases, the Babinet point quickly moves towards the anti-solar point, coincides with it when $\theta_o = 82.2^\circ$, and then moves away from the anti-solar point towards the near horizon. The Babinet point lies between the anti-solar point and the horizon when $76.6^\circ \leq \theta_o \leq 82.2^\circ$. The Brewster point appears at the horizon when $\theta_o = 78.5^\circ$. At the same θ_o the Babinet point is 6.8° from the anti-solar point. Both neutral points are between the anti-solar point and the horizon. As θ_o decreases the two neutral points approach each other and merge when $\theta_o = 76.6^\circ$. No neutral points occur in the sun's vertical plane for $0 < \theta_o < 76.6^\circ$, when $\tau_1 = 0.15$.

The behavior of the neutral points as they move out of the sun's vertical plane can be explained by means of the degree of polarization and of the U and Q Stokes parameters. These parameters are given first for the case that the neutral points occur in the sun's vertical plane. Then these parameters are shown for a smaller solar zenith angle, when no neutral points occur in the sun's vertical plane. These parameters will be shown for an optical thickness of $\tau_1 = 0.15$. The sun's zenith angle is $\theta_o = 80.2^\circ$ for the first set of figures, when the Babinet and Arago points occur. Figure 39 shows the degree of polarization of the diffuse radiation flowing outwards from the top of the atmosphere of the Fresnel model. In addition to the Babinet and Arago points, another neutral point is shown outside of the sun's vertical plane at a slightly smaller zenith angle than θ_o. The appearance of this new neutral point will be explained with the next few figures.

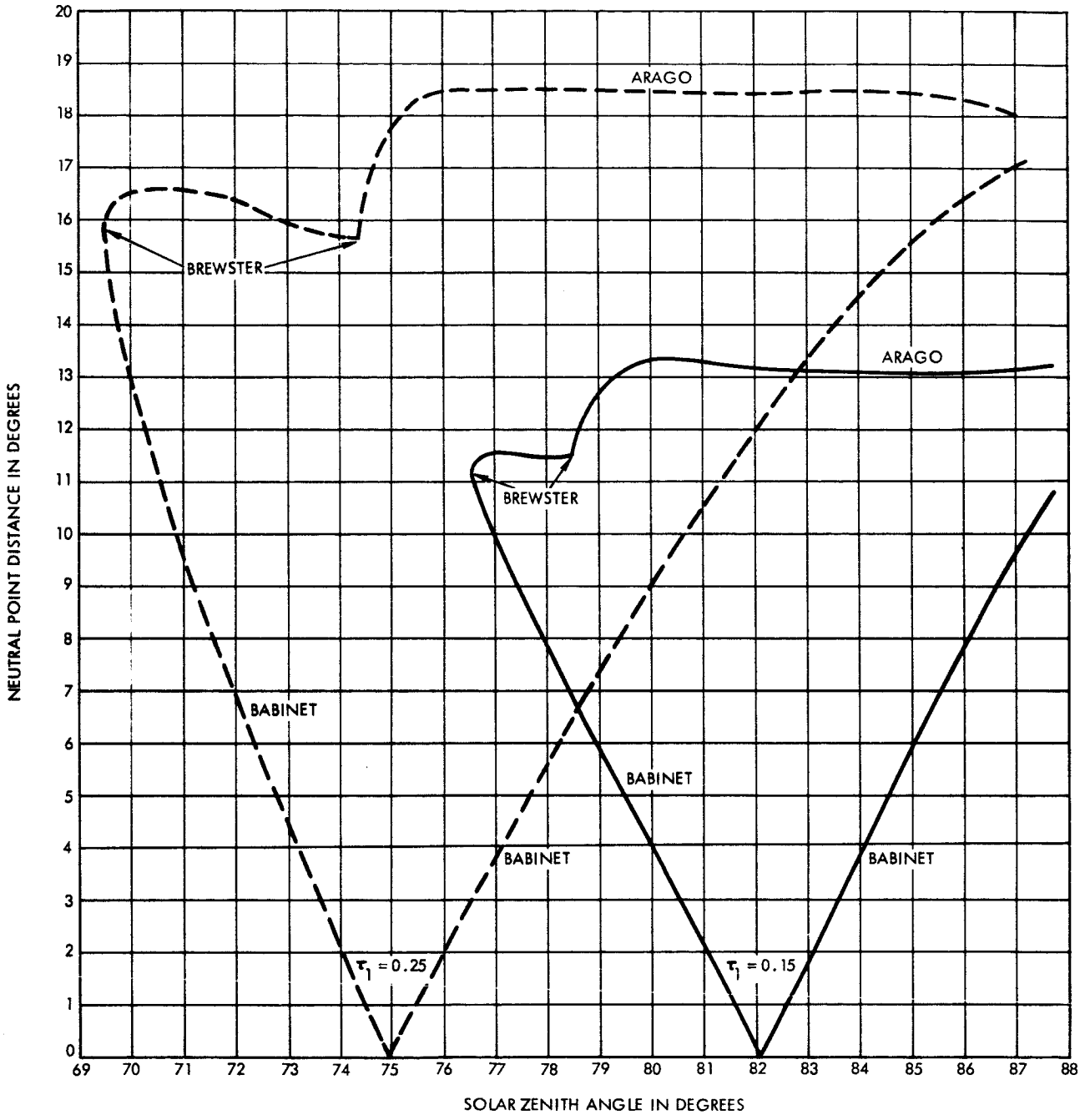

Figure 38. Neutral point positions in sun's vertical plane at top of atmosphere for Fresnel model as a function of θ_o. τ_1 = 0.15 and 0.25.

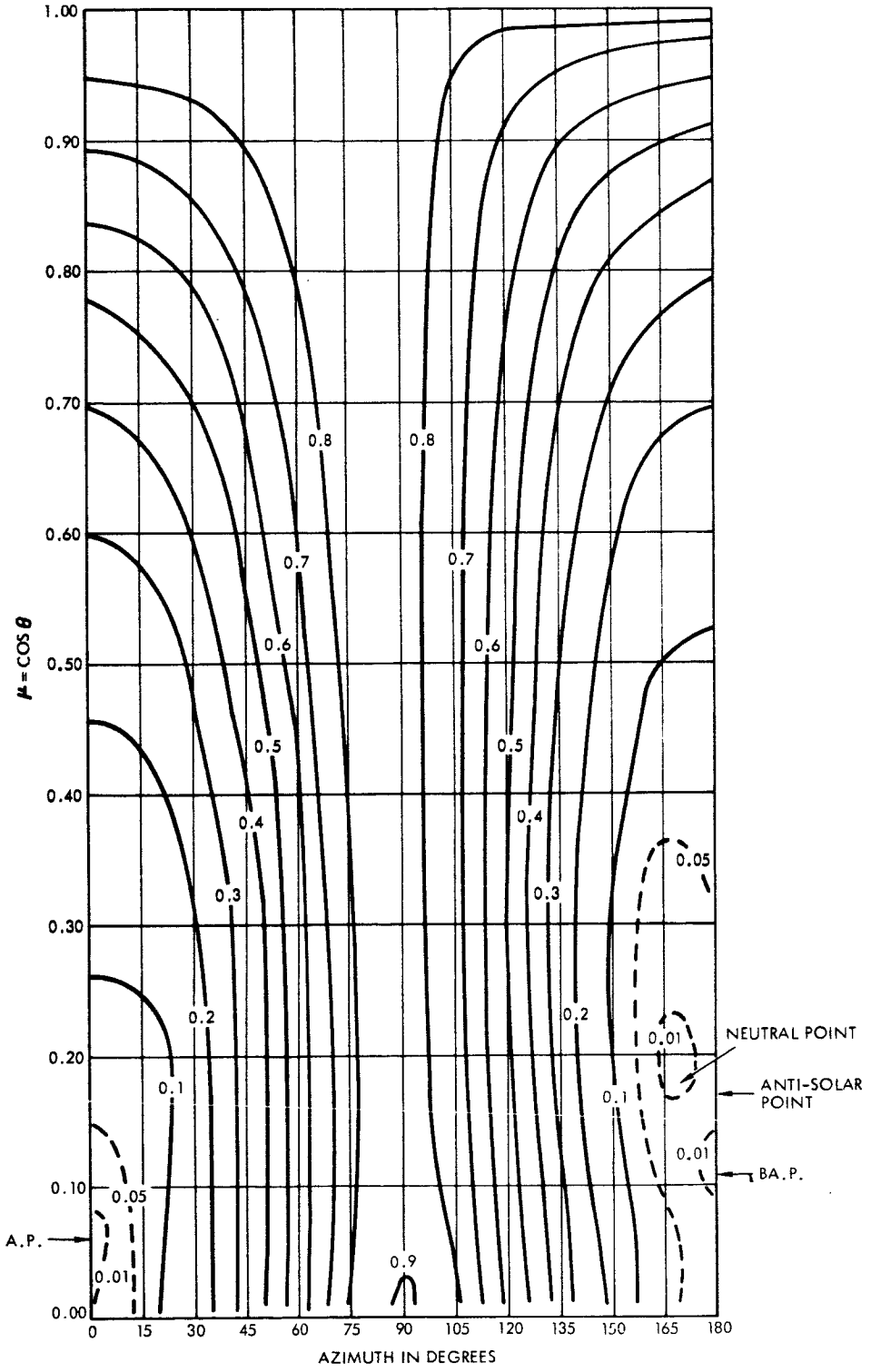

Figure 39. Degree of polarization at top of atmosphere for Fresnel model. $\tau_1 = 0.15$. $\theta_o = 80.2^o$.

The effect of Fresnel reflection at the ground on the degree of polarization of radiation flowing outwards from the top of the atmosphere is shown on Fig. 40. The difference between the polarization of radiation for the model of zero ground albedo and for the Fresnel model is shown. The maximum absolute change is 0.09, which is a greater change than occured at the ground for the same pair of τ_1, θ_o. No unusual changes at the top occur in the vicinity of the neutral points or of the solar image, which is at $\mu = 0.17$ and $\varphi_o - \varphi = 0^o$, except at the solar image where the change is - 0.164. This value is not shown on Fig. 40.

The Q-data for the Fresnel model is shown on Fig. 41. Three neutral points are designated on the zero line. The changes in the Q-values for the airlight alone, for the zero ground albedo model, that are caused by Fresnel ground reflection are shown in Fig. 42. The changes are small and the largest changes occur within 15^o of the horizon.

The U-data for the Fresnel model are shown in Fig. 43. U = 0 in the vertical plane of the sun. A second zero line is restricted to the side of the nadir where the azimuth exceeds 90^o. This second zero line intersects the sun's vertical plane slightly above the anti-solar point. As the solar zenith angle varies the second zero line always intersects the sun's vertical plane near the anti-solar point. The neutral point outside of the sun's vertical plane appears when the solar zenith angle is decreasing and the Babinet point moves from between the nadir and the point where the second U = 0 line intersects the sun's vertical plane to a position between this intersection and the horizon. The zero line of Q, which is tied to the Babinet point as shown in Fig. 41, intersects the second zero line of U outside of the sun's vertical plane when the Babinet point is between the horizon and the point where the second U = 0 line intersects the sun's vertical plane. The changes in the U-data that are caused by Fresnel reflection at the ground are shown in Fig. 44. The changes are not large. The inclination of the plane of polarization is a more familiar parameter than either U or Q, and it depends on these two Stokes parameters (Eq. (42)). The inclination for the Fresnel model is shown in Fig. 45. In the sun's vertical plane, the plane of polarization is parallel to the vertical plane between the Arago point and its nearest horizon, perpendicular to the sun's

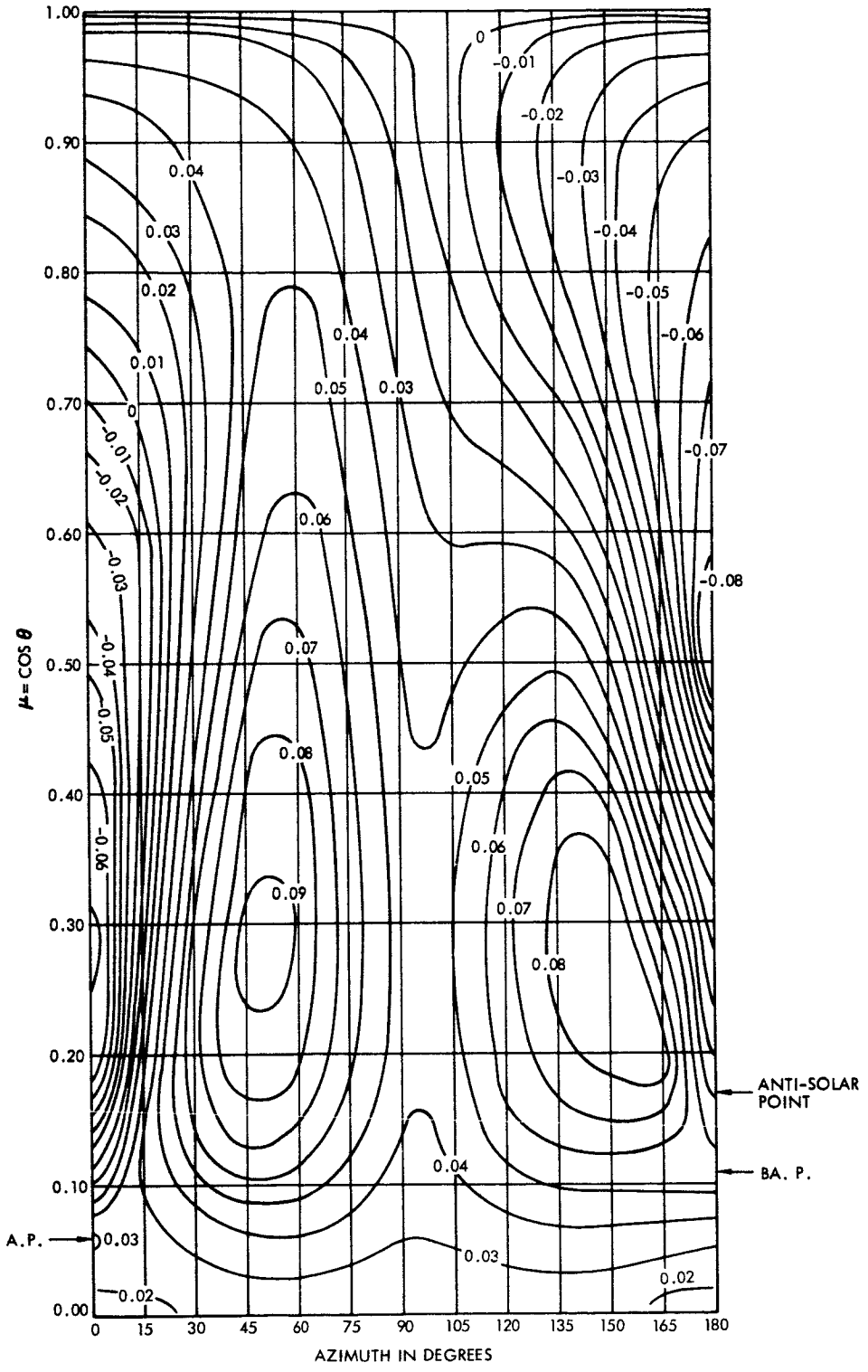

Figure 40. Degree of polarization at top of atmosphere for zero ground albedo model minus that of Fresnel model. $\tau_1 = 0.15$. $\theta_o = 80.2^o$.

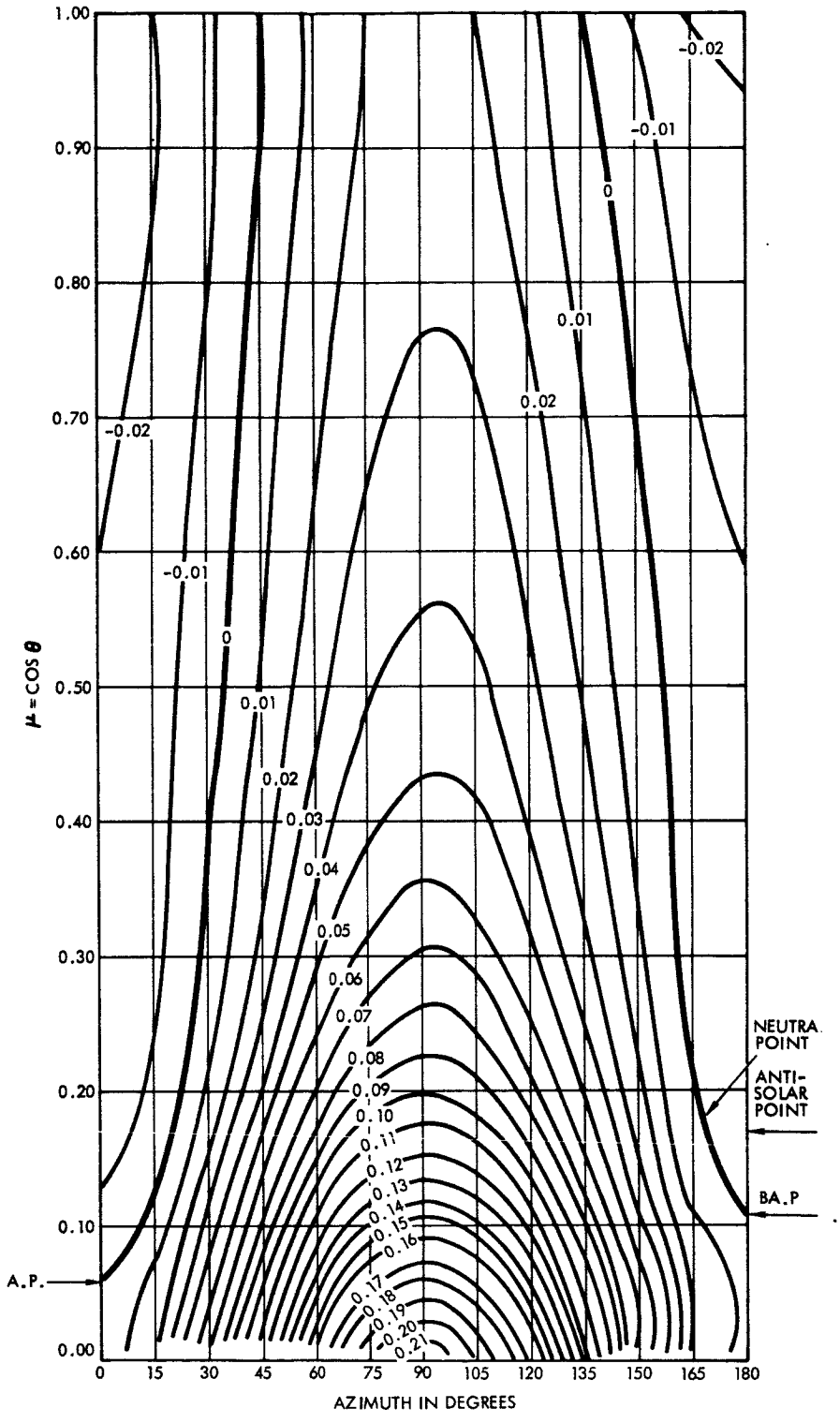

Figure 41. $^{\uparrow}Q$ at top of atmosphere for Fresnel model. $\tau_1 = 0.15$. $\theta_o = 80.2°$.

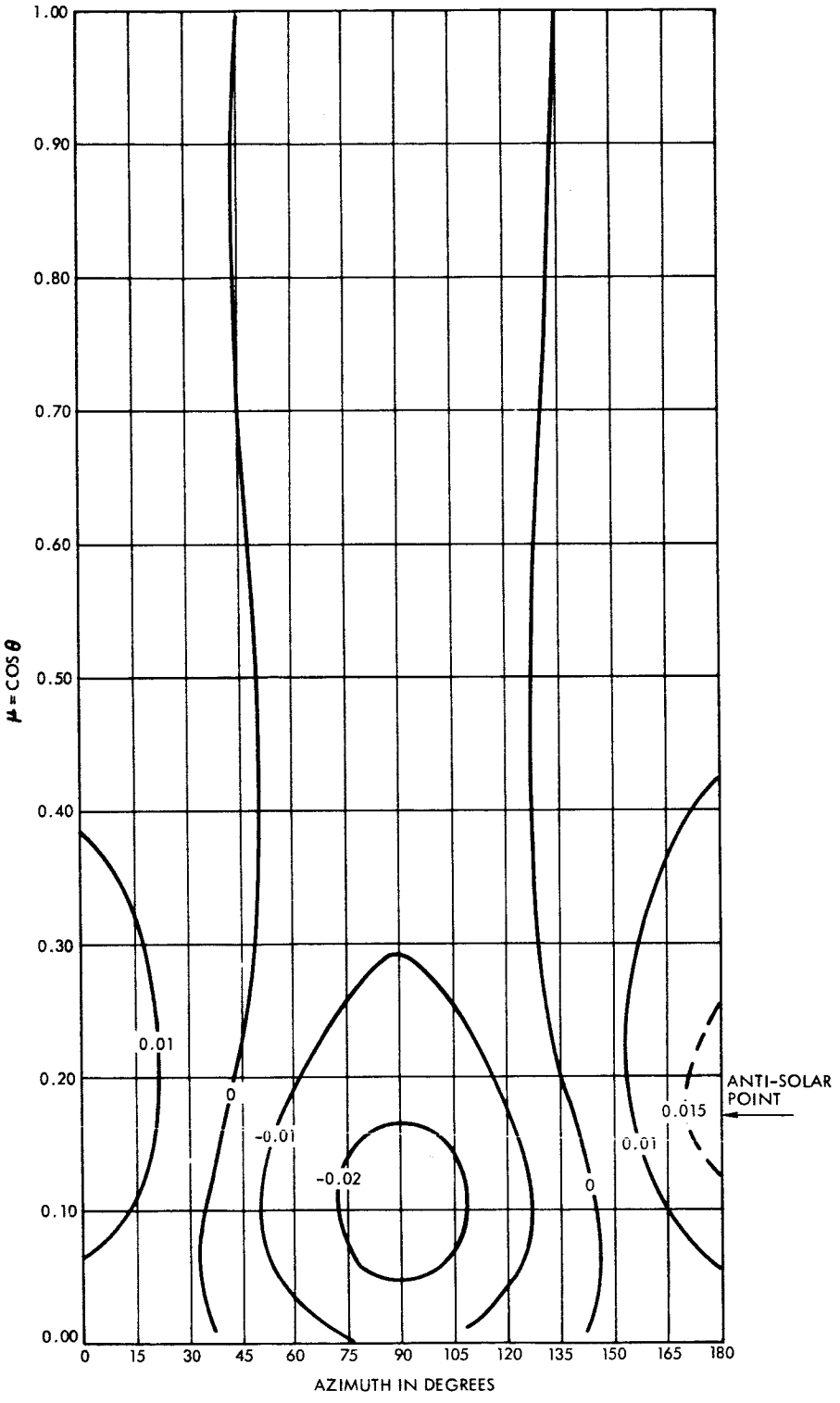

Figure 42. $\uparrow Q$ at top of atmosphere for zero ground albedo model minus that of Fresnel model. $\tau_1 = 0.15$. $\theta_o = 80.2^o$.

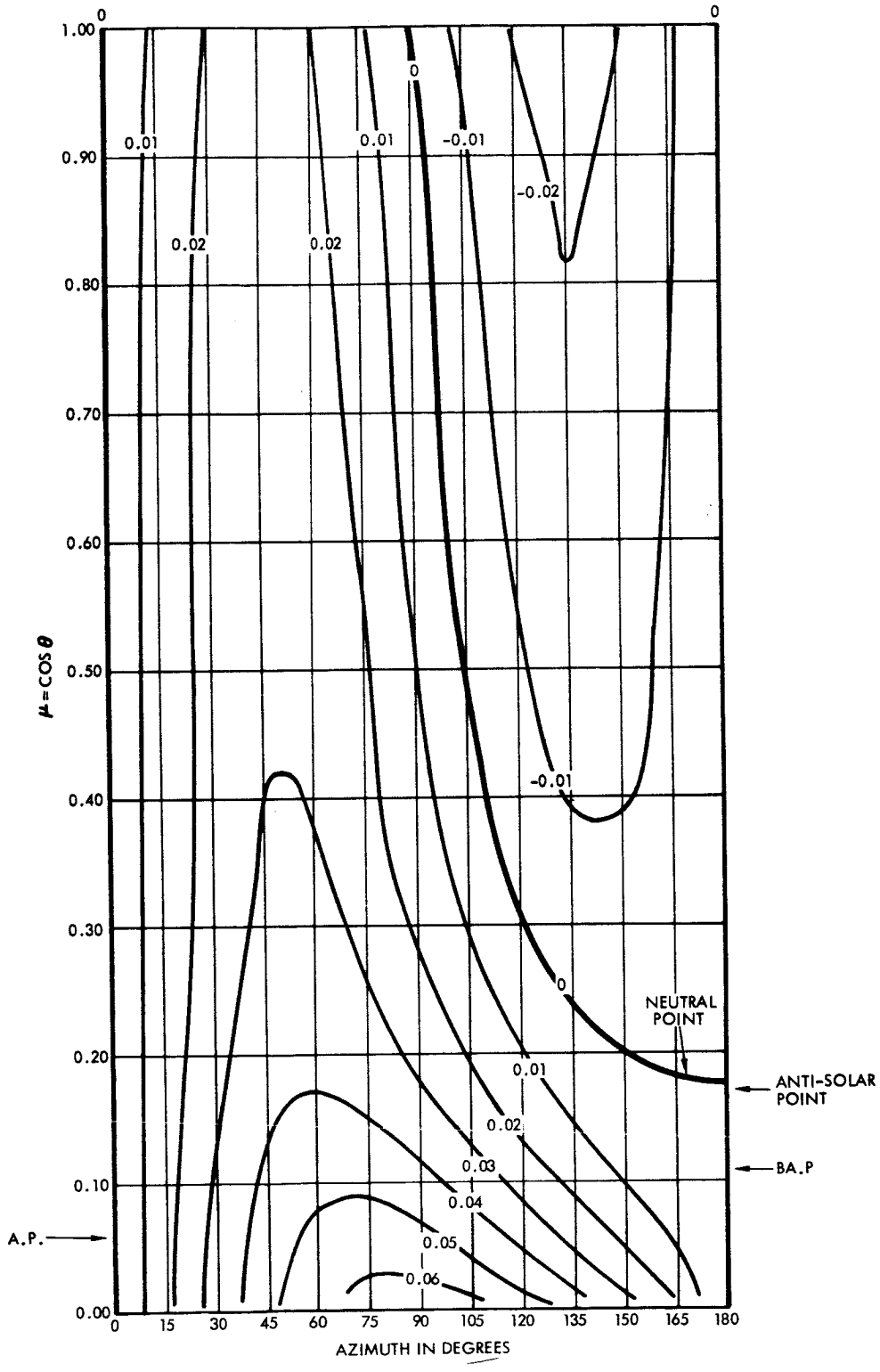

Figure 43. $^{\uparrow}U$ at top of atmosphere for Fresnel model. $\tau_1 = 0.15$. $\theta_o = 80.2^o$.

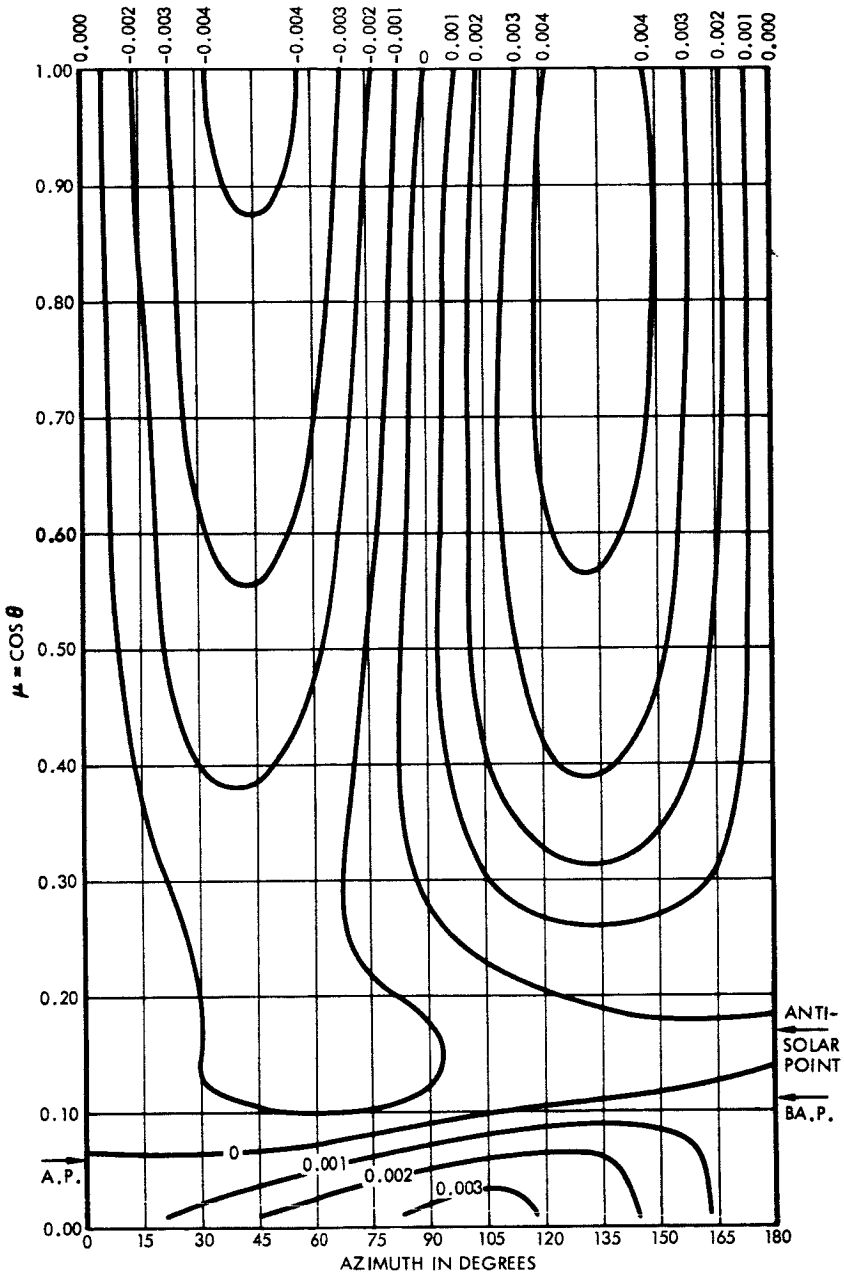

Figure 44. $^{\uparrow}U$ at top of atmosphere for zero ground albedo model minus that of Fresnel model. $\tau_1 = 0.15$. $\theta_o = 80.2^{\circ}$.

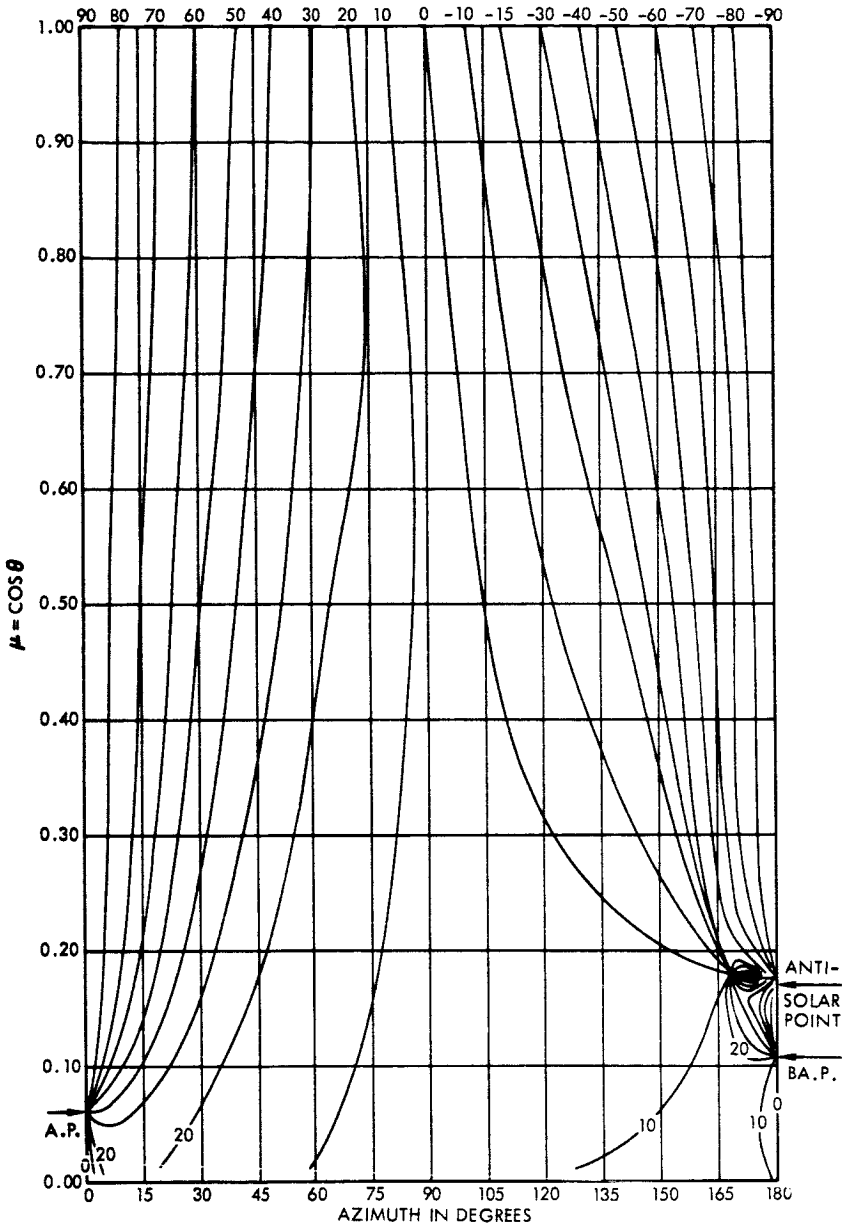

Figure 45. Inclination of plane of polarization (χ) at top of atmosphere for Fresnel model. $\tau_1 = 0.15$. $\theta_o = 80.2^o$.

vertical plane between the Arago and Babinet points, and parallel to the vertical plane between the Babinet point and its nearest horizon. The inclination χ is indeterminate at the neutral points and where the two zero lines of U intersect just above the anti-solar point. The inclination $\chi = -90^{\circ}$ between this intersection and the nadir, and $\chi = +90^{\circ}$ between this same intersection and the Babinet point.

The changes in the inclination χ that are caused by Fresnel ground reflection are shown in Fig. 46. The lines are drawn for the values of both plus and minus 0° $\left[2^{\circ}\right]$ 10° $\left[10^{\circ}\right]$ 30°, 90°. The changes in the inclination are nearly zero where the degree of polarization is largest (Fig. 39). The largest changes in the inclination, say $|\Delta\chi| > 30^{\circ}$, occur where the degree of polarization is less than 10 per cent. The singularities occur at the neutral point positions of both the Fresnel and zero albedo models.

The next two figures will show the Q- and U-data for the Fresnel model for a smaller solar zenith angle ($\theta_o = 69.5^{\circ}$), when no neutral points occur in the sun's vertical plane. The Q-data are shown in Fig. 47. With the decrease in θ_o from Fig. 41 the zero line has been displaced at least 15° in azimuth from the sun's vertical plane that lies between the anti-solar point and the nearest horizon. The effect of Fresnel reflection at the ground on Q and U are not shown, since the effects are quite similar to those already illustrated in Figs. 42 and 44 for $\theta_o = 80.2^{\circ}$.

The data for U are shown in Fig. 48. One zero line coincides with the sun's vertical plane. The second zero line is restricted to azimuths greater than or equal to 90°. Hence, no neutral point can occur outside of the sun's vertical plane for azimuths less than 90°. The second zero line intersects the sun's vertical plane at a nadir angle that is slightly less than θ_o. In order to relate the nadir angle of the neutral point that's found on this line and θ_o, consider a point to move along this second zero line away from the sun's vertical plane. As the azimuth of the point decreases from 180°, its nadir angle decreases, or μ increases. Hence, the difference between the solar zenith angle (θ_o) and the nadir angle of a neutral point on the second zero line is larger, the further the neutral point is from the sun's vertical plane.

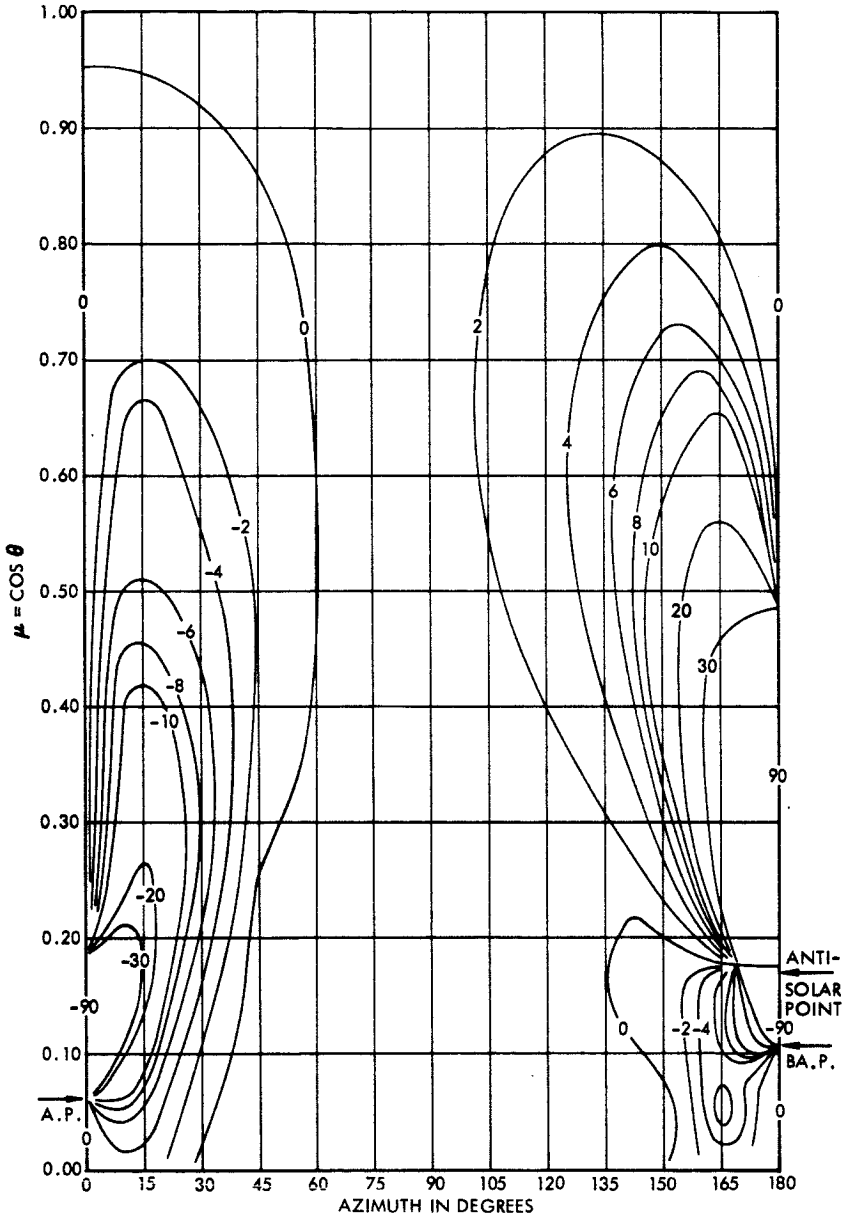

Figure 46. Inclination of plane of polarization at top of atmosphere for zero ground albedo model minus that of Fresnel model. $\tau_1 = 0.15$. $\theta_o = 80.2^o$.

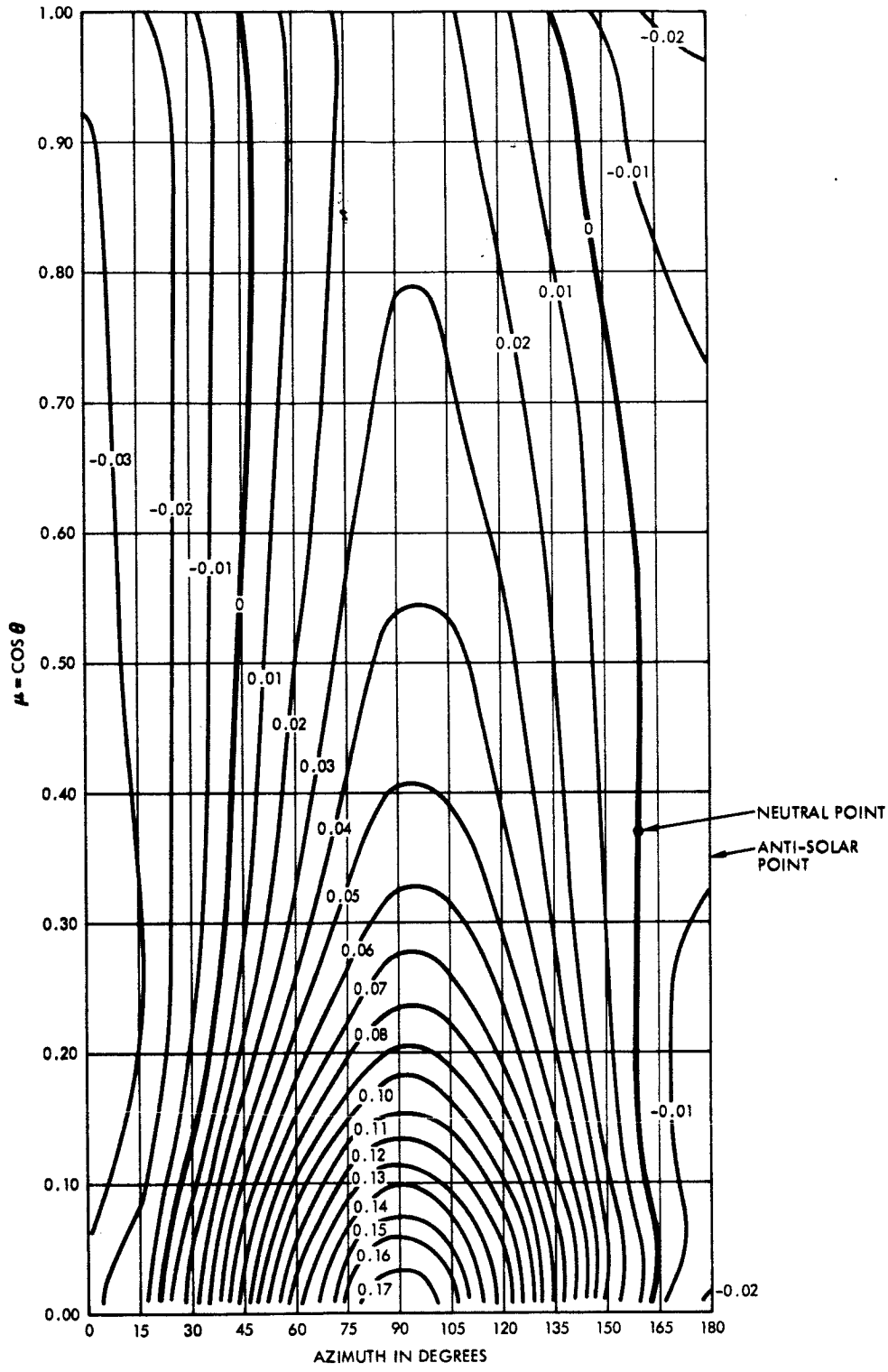

Figure 47. $\uparrow_Q$ at top of atmosphere for Fresnel model. $\tau_1 = 0.15$ $\theta_o = 69.5^o$

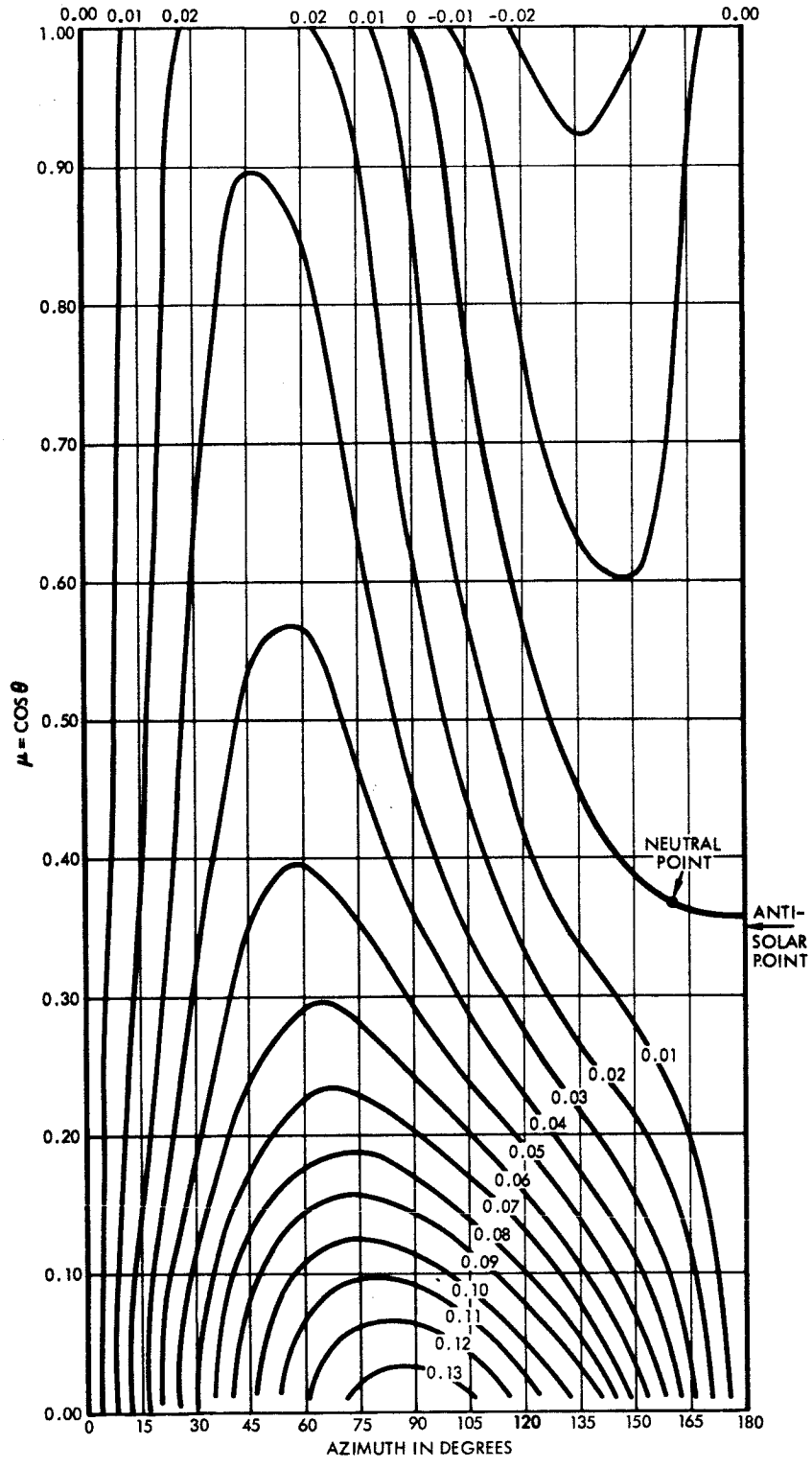

Figure 48. $^{\uparrow}U$ at top of atmosphere for Fresnel model. $\tau_1 = 0.15$. $\theta_o = 69.5^{\circ}$.

The effect that different components of the radiation field have on the neutral points depends on their contribution to the degree of polarization. The relative contributions of several components will be discussed now. The degree of polarization for radiation in the sun's vertical plane can be written as

$$P^F = -Q^F/I^F \tag{46}$$

when Eq. (42) is substituted into Eq. (43). The superscripts F indicate the total value of a parameter for the Fresnel model. Since the Stokes parameters of independent components are additive, Eq. (46) can be written as

$$P^F = -\sum_i Q_i / I^F \ ,$$

where $\sum_i Q_i = Q^F$. If one multiplies and divides each Q_i by I_i/I_i, then Eq. (47) becomes

$$P^F = \sum_i \frac{I_i}{I^F} P_i \tag{48}$$

or

$$\sum_i \frac{I_i}{I^F} \frac{P_i}{P^F} = 1 \tag{49}$$

The relative contribution to the degree of polarization by each component (P_i/P^F) is weighted by its relative intensity (I_i/I^F). Four significant components of the radiation field can be distinguished, as was done in the discussion of the ground albedo. The identifications of the components of radiation at the top and bottom of the atmosphere are slightly different. The most important component at the top generally is the diffuse airlight that has not been reflected from the ground. This component is identical to the diffuse radiation that occurs for the model of zero ground albedo. This component will be called unreflected airlight. A second component is the unreflected airlight after it has been reflected from the ground just once. The second component will be called the reflected airlight.

A third component is the direct sunlight that is reflected from the ground just once. This component is called the reflected sunlight . It may pass directly out of the atmosphere without being scattered, or it may reach the top of the atmosphere after being scattered one or more times by the atmosphere. Some of the reflected sunlight and reflected airlight is scattered by the atmosphere back to the ground, where it is reflected from the ground a second time. The radiation that is reflected from the ground two or more times is called multiply reflected airlight. This component is generally unimportant for the Fresnel model, since roughly 90 per cent of the radiation falling on the ground is lost from the radiation field (at least if $\theta_o < 65^o$).

The total specific intensity of each component is given in Fig. 49. The solar constant is π, or $\pi \cos(72.5^o)$ units of solar flux pass through a horizontal unit area at the top of the atmosphere. The unreflected airlight contributes approximately 80 per cent of the total intensity ($^{\uparrow}I^F$), except where the reflected solar image appears, as indicated on the left-hand side of the figure at $\theta = 72.5^o$. The reflected sunlight and reflected airlight contribute about 20 per cent of the total and are of the same order of magnitude, except where the reflected solar image appears. The multiply reflected intensity is about one per cent of the total.

The degree of polarization of each of the components is shown in Fig. 50. The total polarization (P^F) is quite close to that of the unreflected airlight. The total polarization (P^F) is positive everywhere. As a result, the denominator of Eq. (49) is positive and not zero for this particular example being considered. Although the relative intensity of the unreflected airlight is about 80 per cent, this component will make a small contribution to the total polarization (P^F) where the polarization of the unreflected component is small, if the polarization is large for the other components of weaker intensity. The degree of polarization of the reflected sunlight is greater than or equal to the value of 0.57 that it has upon leaving the ground. The degree of polarization of the reflected airlight exceeds 0.4 in the region where the Babinet and Brewster points have disappeared from the sun's vertical plane, except within 15^o of the horizon. The degree polarization of the multiply reflected radi-

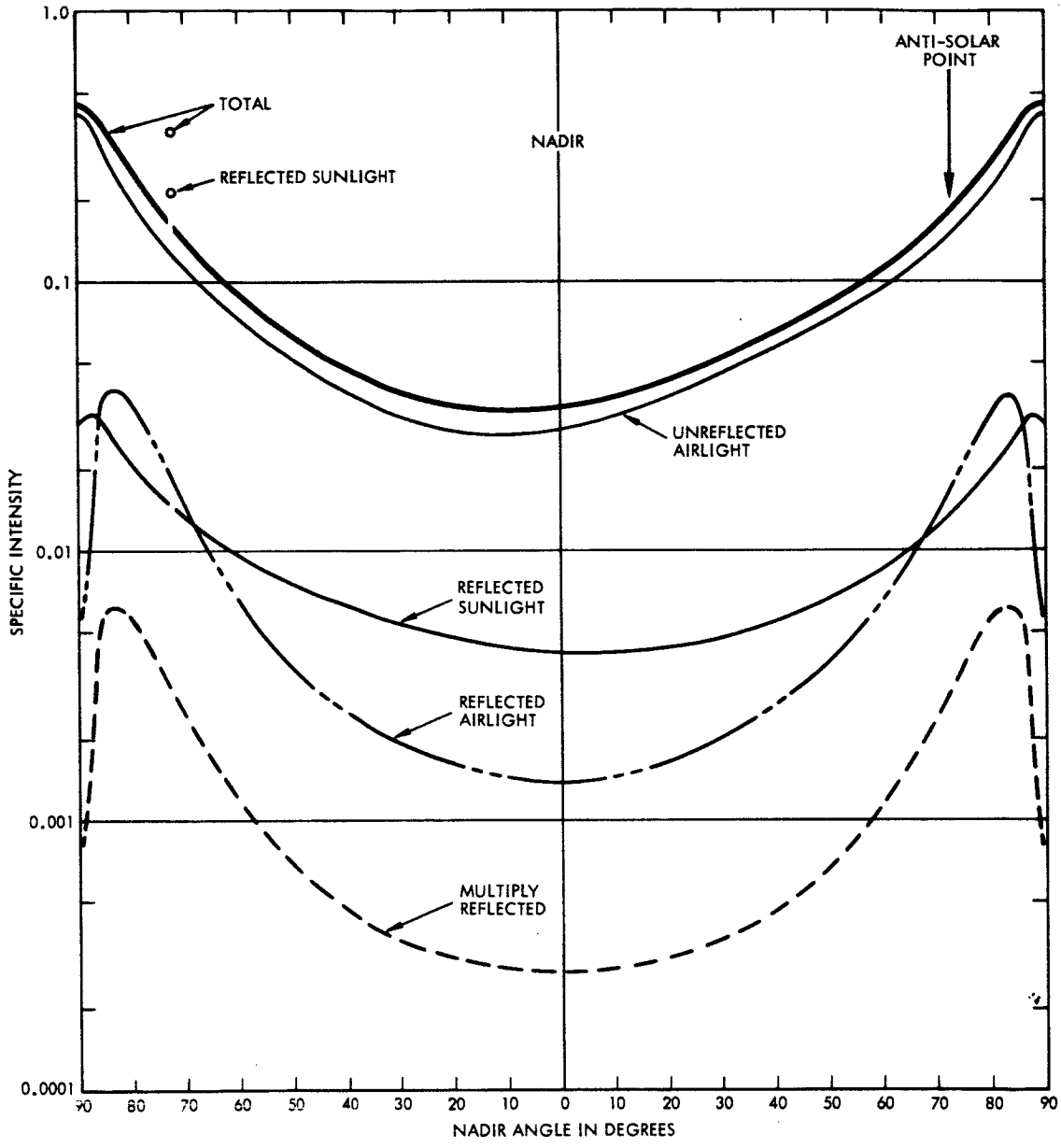

Figure 49. Total specific intensity ($^{\uparrow}I$) at top of atmosphere in sun's vertical plane for different components of radiation field. Fresnel model. $\tau_1 = 0.15$. $\theta_o = 72.5^{\circ}$.

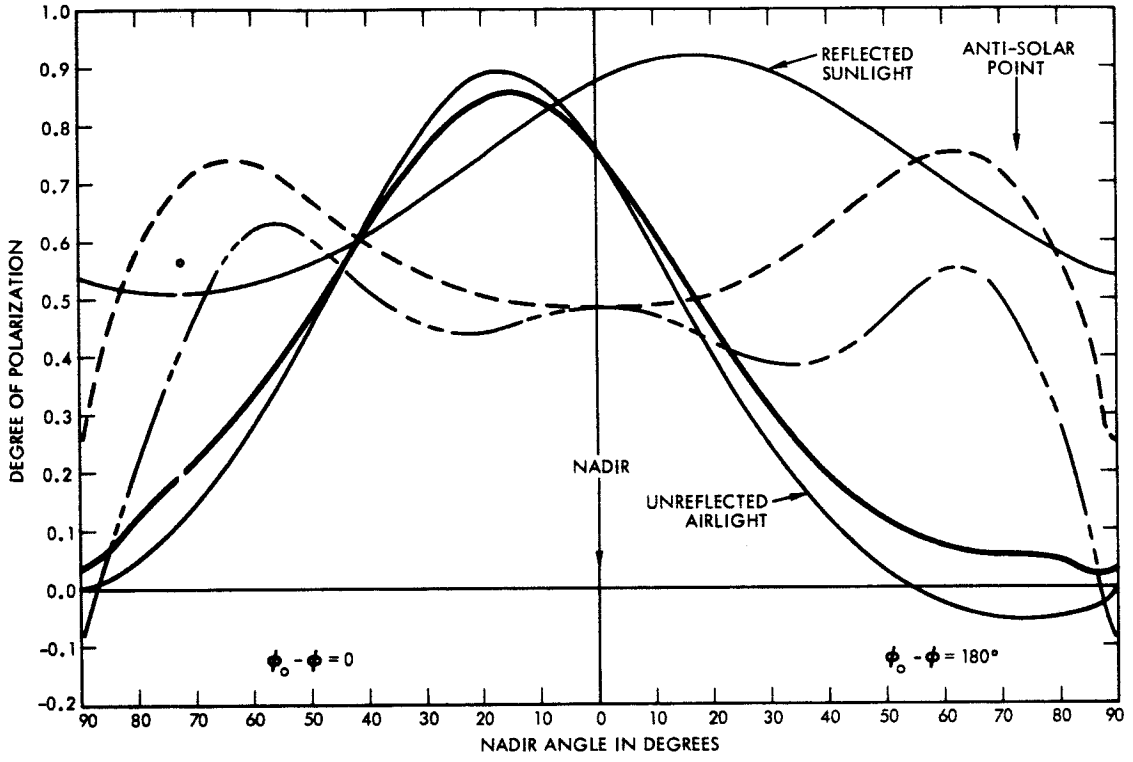

Figure 50. Degree of polarization for different components of radiation field at top of atmosphere in sun's vertical plane. The various components have the same line representation as on Fig. 49. Fresnel model. $\tau_1 = 0.15$. $\theta_o = 72.5^o$.

ation exceeds 0.6 in the same region.

The relative contribution to the degree of polarization of each of the components is given in Fig. 51. In the region where the total degree of polarization (P^F) is large the principal contribution is made by the unreflected airlight. The other components contribute less than 20 per cent in the same region. The unreflected airlight makes a large negative contribution in region where the positions of the Babinet and Brewster points are strongly altered. Both the reflected airlight and reflected sunlight are needed to introduce sufficient positive polarization to make the total polarization (P^F) positive where the unreflected airlight is negatively polarized. The multiply reflected radiation contributes less than 0.25 of the total polarization. The computed Babinet and Brewster points would still disappear from the sun's vertical plane, if this component were neglected. Hence, the disappearance of the Brewster and Babinet points from the sun's vertical plane depends about equally on the reflected sunlight and the reflected airlight.

The azimuthal distance of the neutral points from the sun's vertical plane is shown in Fig. 52. The distance of a neutral point from the sun's vertical plane and the range of θ_o for which the neutral point exists outside of the sun's vertical plane are larger at the top than for a corresponding optical thickness at the bottom (Fig. 21). The computed neutral point positions for the Fresnel model are also given in Table VII.

The degree of polarization in the vicinity of a neutral point that lies outside of the sun's vertical plane is shown for an optical thickness of $\tau_1 = 0.15$ in Fig. 53. The azimuth of the neutral point is $\varphi_o - \varphi = 159.6^o$, and the nadir angle $\theta = \cos^{-1} 0.389 = 67.1^o$. The degree of polarization in the nearest solar vertical plane at the same nadir angle is 0.054. If zero degree of polarization is measured with an absolute uncertainty of 0.01, then the neutral point coordinates would be determined with an angular uncertainty of about 2^o.

The degree of polarization in the vicinity of a neutral point for a larger optical thickness of $\tau_1 = 0.25$ is shown in Fig. 54. The neutral point

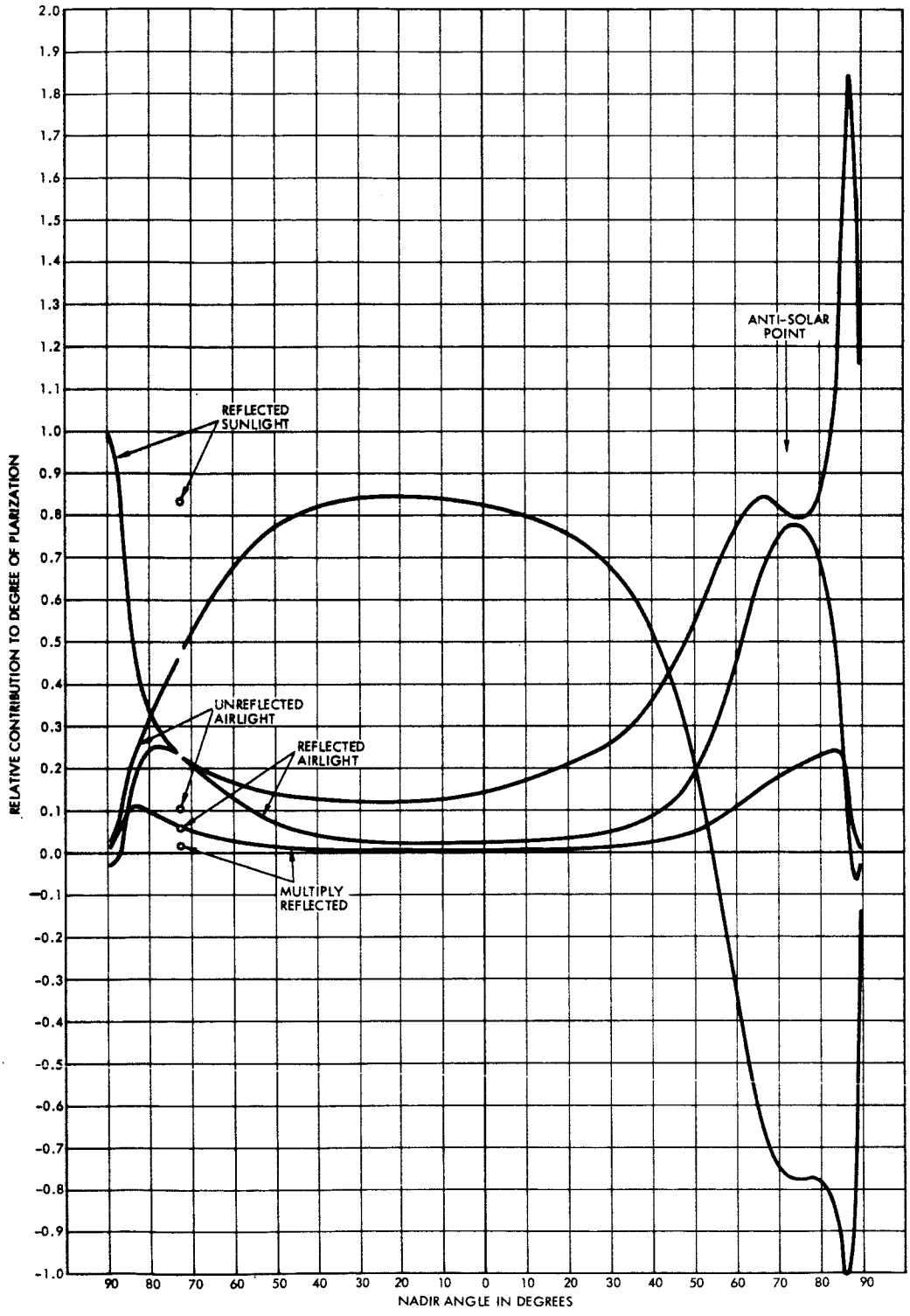

Figure 51. Relative degree of polarization for different components of radiation field at top of atmosphere in sun's vertical plane. $\tau_1 = 0.15$. $\theta_o = 72.5^o$.

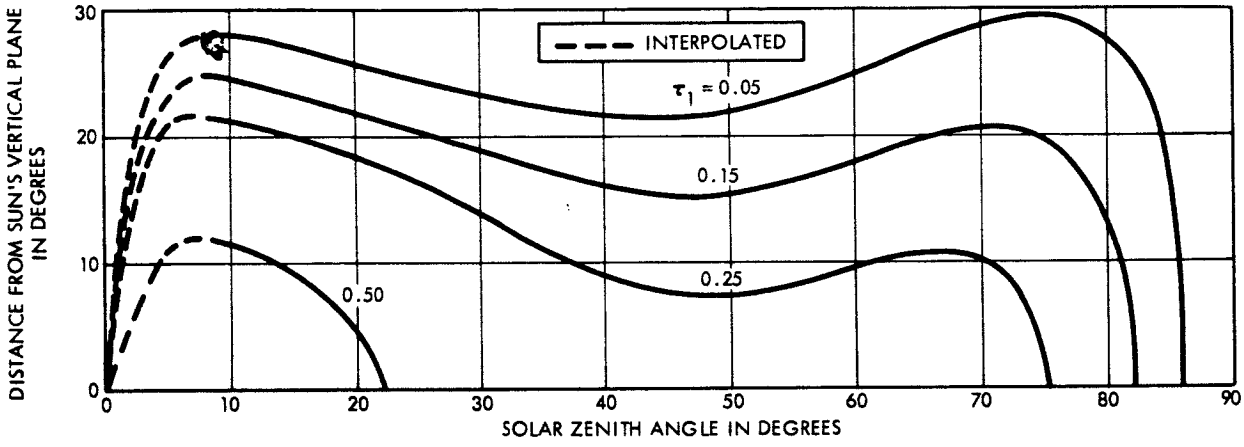

Figure 52. Azimuthal distance of neutral points from sun's vertical plane at top of atmosphere.

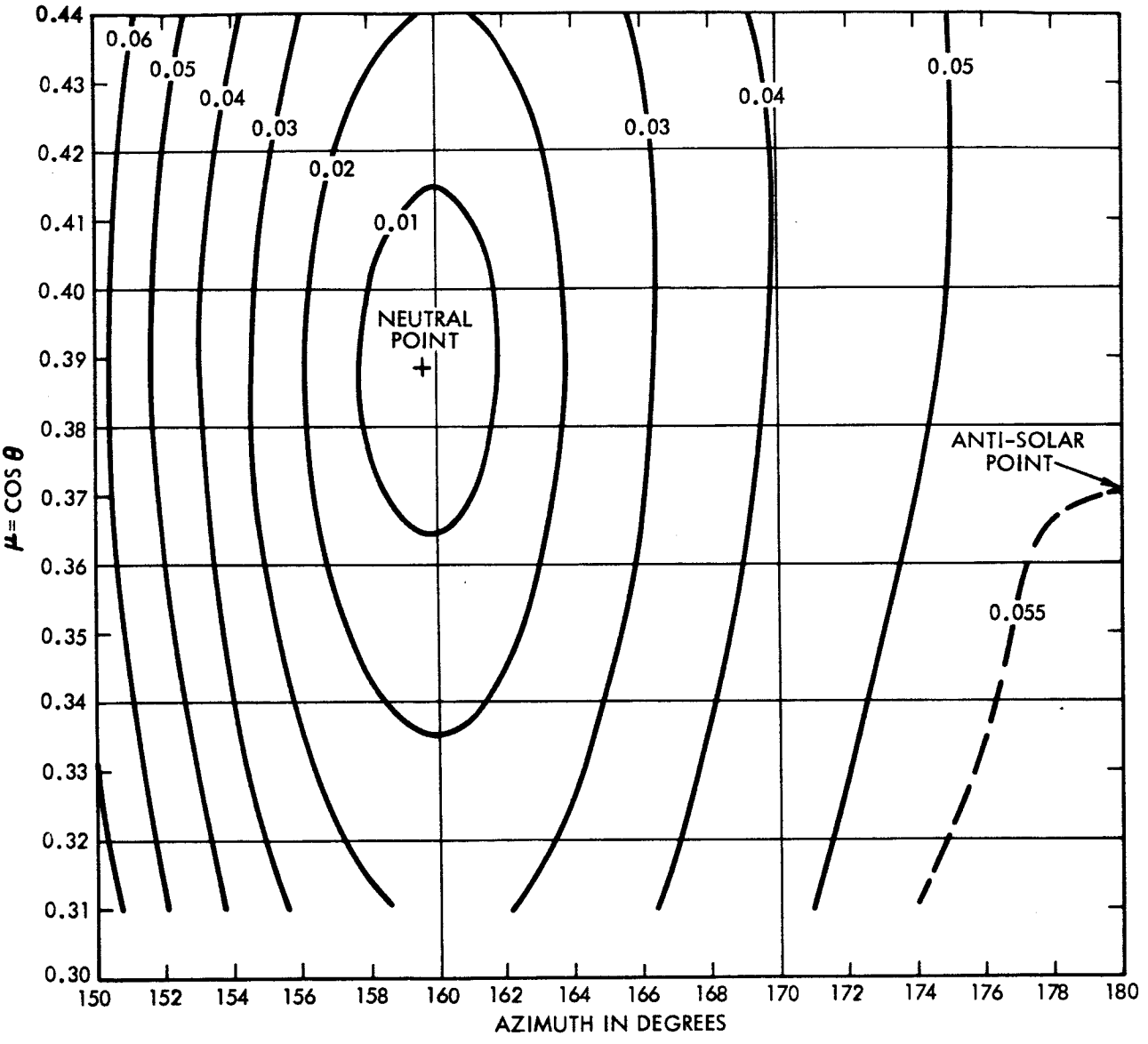

Figure 53. Degree of polarization at top of atmosphere in vicinity of a neutral point that is exterior to the sun's vertical plane. $\tau_1 = 0.15$. $\theta_o = 68.3^\circ$.

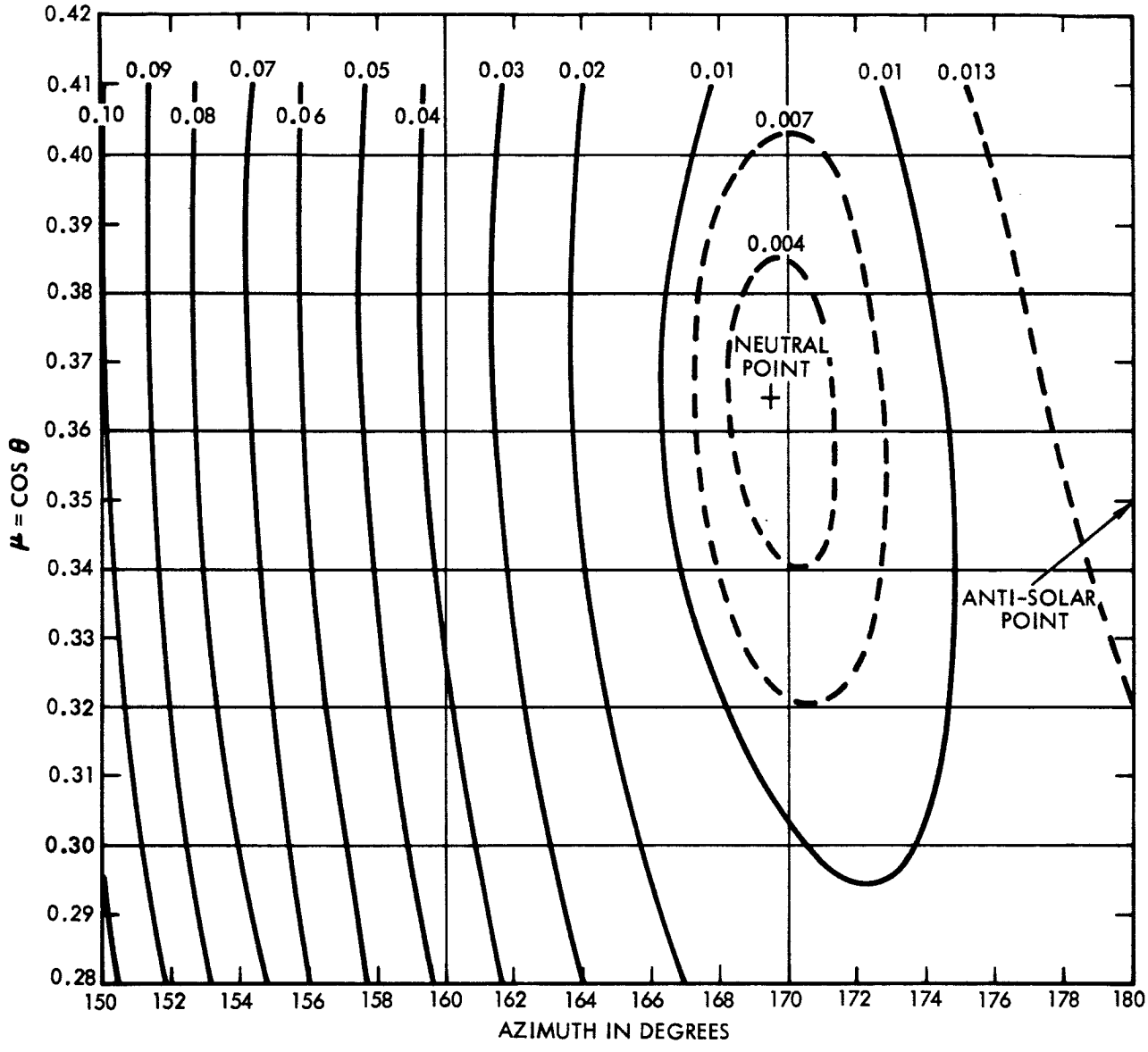

Figure 54. Degree of polarization at top of atmosphere in vicinity of a neutral point that is exterior to the sun's vertical plane. $\tau_1 = 0.25$. $\theta_o = 69.5^o$.

TABLE VII

Computed neutral point positions at top of atmosphere of Fresnel model. Index of refraction is m = 1.34. The word none or a blank means that the neutral point does not exist. A dash means that the neutral point exists, but that its position was not computed.

τ_1	θ_o	Brewster		Babinet		Arago	
		θ	$\theta_o - \theta$	θ	$\theta_o - \theta$	θ	$\theta_o + \theta$
0.05	87.13°	none		87.2°	- 0.1°	-	-
	84.26	"		none		none	

neutral points outside of sun's vertical plane

θ	$\theta_o - \theta$	$\varphi_o - \varphi$
84.26	83.6	0.7	159.7
78.46	77.2	1.3	151.6
75.52	74.0	1.5	150.6
72.54	71.0	1.5	150.7
66.42	65.1	1.4	152.5
60.00	59.3	0.7	155.0
53.13	53.1	0.0	157.3
45.57	46.0	- 0.4	158.4
36.87	37.4	- 0.5	157.8
25.84	26.0	- 0.2	155.6
18.19	18.1	- 0.1	154.1
8.11	8.1	0.0	152.0
0.00	0.0	0.0	180.0

		Brewster		Babinet		Arago		
		θ	$\theta_o - \theta$	θ	$\theta_o - \theta$	θ	$\theta_o + \theta$	$180 - (\theta_o + \theta)$
0.15	87.71	none		76.9	10.8	79.1	166.8	13.2
	84.26	"		79.8	4.50	82.6	166.9	13.1
	83.11	"		81.0	2.1	83.8	166.9	13.1
	82.53	"		81.6	0.9	-	-	-
	80.79	"		83.3	- 2.5	85.9	166.7	13.3
	80.21	"		83.8	- 3.6	86.4	166.6	13.4

		Brewster		Babinet		Arago	
τ_1	θ_o	θ	$\theta_o - \theta$	θ	$\theta_o - \theta$	θ	$\theta_o + \theta$ 180 - $(\theta_o + \theta)$
0.15	78.46	-	-	85.4	- 6.9	none	
	77.88	89.4	- 11.5	85.9	- 8.0	none	
	77.29	88.8	- 11.5	86.6	- 9.3		
	72.54	none		none			

neutral points outside of sun's vertical plane

θ	$\theta_o - \theta$	$\varphi_o - \varphi$
80.8	0.6	171.1
80.1	0.7	169.0
79.5	0.7	167.2
78.8	0.8	165.8
76.9	1.0	162.9
76.3	1.0	162.2
74.3	1.2	160.6
72.6	1.8	160.0
70.1	1.3	159.3
67.1	1.2	159.6
64.2	1.0	160.3
58.2	0.5	162.4
51.6	0.1	164.2
44.1	- 0.2	164.4
35.1	- 0.2	162.4
33.0	- 0.1	161.9
30.8	- 0.1	161.3
28.4	0.0	160.5
25.8	0.0	159.7
19.8	0.1	158.1
13.8	0.3	156.5
11.2	0.3	155.8
7.9	0.2	155
0.0	0.0	180.0

		Brewster		Babinet		Arago		
τ_1	θ_o	θ	$\theta_o - \theta$	θ	$\theta_o - \theta$	θ	$\theta_o + \theta$	$180 - (\theta_o + \theta)$
0.25	87.13	none		70.0	17.1	74.9	162.0	18.0
	84.26	"		69.4	14.8	77.2	161.5	18.5
	81.37	"		70.3	11.0	80.2	161.6	18.4
	78.46	"		72.1	6.4	83.0	161.5	18.5
	76.11	"		73.9	2.2	85.4	161.5	18.5
	75.52	"		74.4	1.1	-	-	-
	74.34	-	-	75.7	- 1.3	none		
	72.54	88.7	- 16.1	78.1	- 5.6	none		
	71.94	88.3	- 16.4	79.0	- 7.1			
	71.34	87.9	- 16.5	80.0	- 8.6			
	70.73	87.3	- 16.6	81.1	- 10.4			
	66.42	none		none				

<u>neutral points outside of sun's vertical plane</u>

	θ	$\theta_o - \theta$	$\varphi_o - \varphi$
75.52	none		
74.34	73.6	0.8	174.5
71.94	71.1	0.9	170.9
70.73	69.8	0.9	170.1
69.51	68.6	0.9	169.5
66.42	65.6	0.8	169.2
63.26	62.5	0.8	169.5
60.00	59.5	0.5	170.4
53.13	53.0	0.1	172.3
45.57	45.8	- 0.2	172.3
36.87	37.1	- 0.2	169.9
25.84	25.6	0.2	163.8
19.95	19.6	0.4	161.7
16.26	16.0	0.3	160.4
8.11	8.1	0.0	158.4
0.00	0.0	0.0	180.0

		Brewster		Babinet		Arago		
τ_1	θ_o	θ	$\theta_o - \theta$	θ	$\theta_o - \theta$	θ	$\theta_o + \theta$	$180 - (\theta_o + \theta)$
0.50	84.26	none		61.5	22.7	71.6	155.8	24.2
	78.46	"		57.2	21.3	76.5	154.9	25.1
	72.54	"		53.8	18.7	83.0	155.5	24.5
	66.42	87.8	- 21.4	49.8	16.6	none		
	60.00	82.0	- 22.0	45.1	14.9			
	53.13	69.6	- 16.5	40.1	13.0			
	45.57	58.6	- 13.1	34.9	10.6			
	36.87	46.3	- 9.4	29.4	7.5			
	25.84	29.1	- 3.3	22.8	3.1			
	23.07	24.6	- 1.5	21.6	1.5			
	19.95	none		none				

<u>neutral points outside of sun's vertical plane</u>

	θ	$\theta_o - \theta$	$\varphi_o - \varphi$
19.95	19.6	0.4	175.4
16.26	16.0	0.3	171.6
8.11	7.9	0.2	168.2
0.00	0.0	0.0	180.0

is closer to the sun's vertical plane and the change in polarization from the solar vertical plane to the neutral point is smaller than for $\tau_1 = 0.15$ (Fig. 53). If the neutral point were located by measuring the degree of polarization, the measured position would be more uncertain at the larger optical thickness, since the spatial gradients of the polarization are weaker in the vicinity of the neutral points at the larger optical thickness.

The sensitivity of the total specific intensity and the maximum degree of polarization in the sun's vertical plane to the nature of the ground reflection is shown in Fig. 55. The value for the Fresnel model is subtracted from that for the Lambert model, and the difference is divided by the value for the Lambert model. The relative difference in the specific intensity of radiation from the nadir is less than 0.1 if $\tau_1 > 0.5$, but the relative difference becomes large at small optical thickness. The intensity of the radiation reflected from the ground towards the zenith is greater for the Lambert model than for the Fresnel model, unless the sun is at the zenith. As a result, the Lambert model is brighter towards the nadir than the Fresnel model, and also brighter the smaller the optical thickness. The relative difference in the maximum degree of polarization is less than 0.2 if $\tau_1 > 0.5$. If the sun is at the zenith, the maximum polarization occurs near the horizon; then the maximum polarization at any optical thickness is insensitive to a change from the Lambert to the Fresnel law of ground reflection. On the other hand, if the sun is near the horizon as it is when $\mu_o = 0.1$, the relative change in the maximum degree of polarization becomes quite large at small optical thickness. In this case the maximum degree of polarization occurs near the nadir, since the direction of the maximum polarization is about 90° from the sun. The optical path length of the atmosphere equals $\tau_1 \sec \theta$, and it approaches a minimum as the nadir angle $\theta \to 0$. As the optical path length in the direction of observation decreases, the characteristics of the reflected radiation at the ground assume increasing importance.

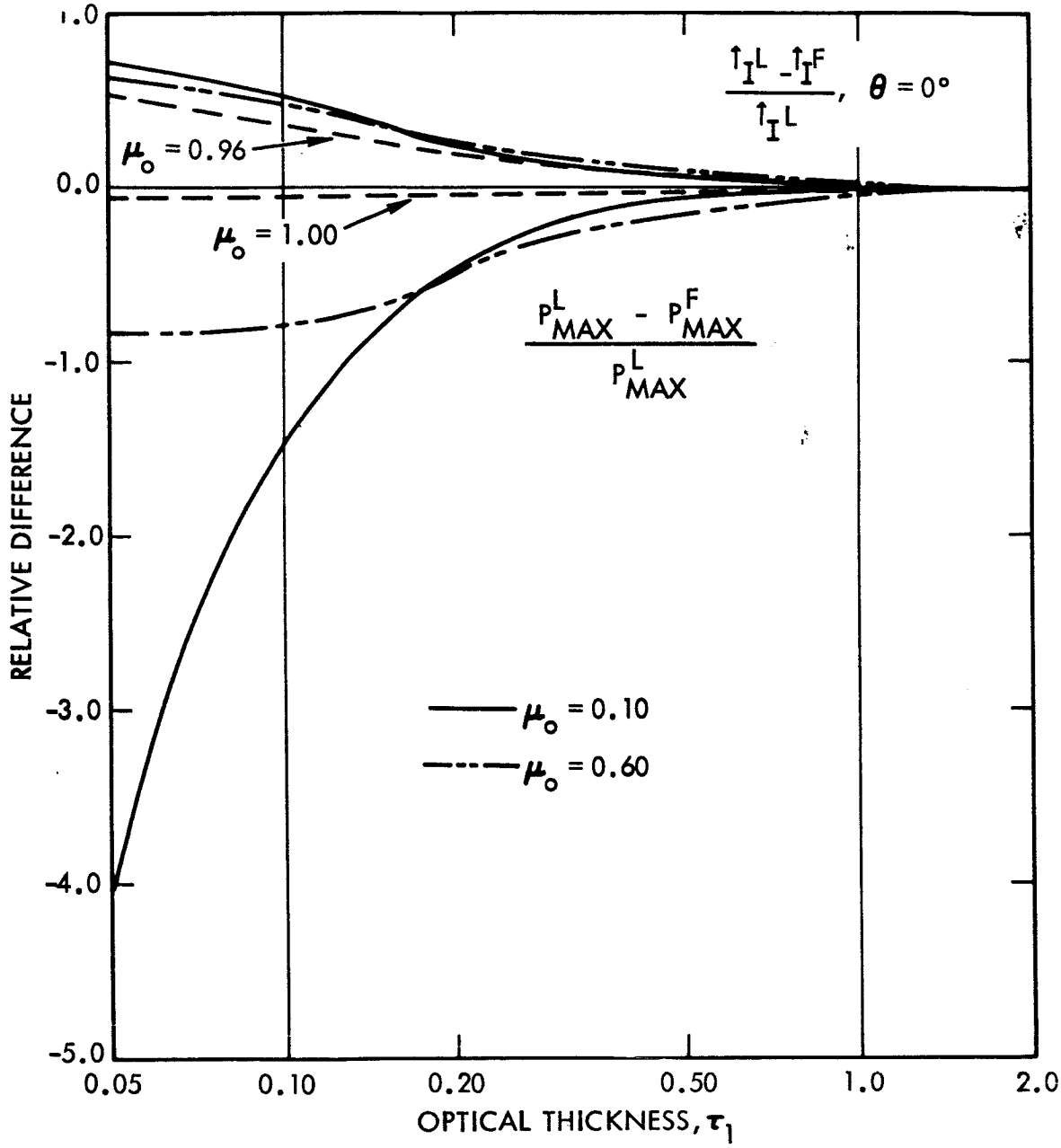

Figure 55. Relative change in total intensity at nadir and in maximum degree of polarization in sun's vertical plane at top of atmosphere from Lambert to Fresnel model.

4. CONCLUSION

The computations of the albedo at a water surface can be simplified considerably by making several assumptions. First, the multiply reflected skylight can be neglected. The resulting relative error in the albedo is less than five per cent. Second, if the polarization of the skylight falling on the water is neglected, the resulting relative error in the total albedo is less than 15 per cent. Third, if the optical thickness is $\tau_1 \leq 0.5$ and the solar zenith angle is $\theta_o < 65^o$, then neglect of the roughness of the sea causes a relative error in the albedo of less than 25 per cent. However, if all three assumptions are made simultaneously, the relative error in the albedo is less than 25 per cent. On the other hand, when computations of the positions of the neutral points are made, only the multiply reflected skylight can be neglected. Displacement of the neutral points from the sun's vertical plane depends on the reflected sunlight and reflected airlight, even though they contribute only a small fraction of the intensity of the radiation emerging from the top of the atmosphere in the vicinity of the neutral points.

The characteristics of commonly used radiation parameters are now known for both the base and the top of the atmosphere of the Fresnel model. The method that is used in this research to find these parameters can be applied to a model of a Rayleigh atmosphere and more general ground reflection characteristics than those specified by the Fresnel law. Examples of surface reflection matrices that could be used are those obtained by Mullamaa[12] for rough sea surfaces. More general atmospheric models of turbid atmospheres, which contain aerosol particles, are difficult to use. The polarization characteristics of radiation scattered from a turbid atmosphere of sufficient optical thickness for multiple scattering to be significant is difficult to compute and has not been done accurately yet.[9]

The application of the results discussed in this report to satellite observations of the earth has two restrictions. The first is that the earth's atmosphere is not homogeneous in spherical shells, principally because dense clouds of condensed water are scattered throughout the troposphere. Only limited portions of the atmosphere can be considered homogeneous. The second restriction is that the earth's atmosphere is not plane-parallel, but spherical. The effect of the sphericity has not been computed yet.

REFERENCES

1. Beckmann, P. and A. Spizzichino, The Scattering of Electromagnetic Waves from Rough Surfaces (The Macmillan Co., New York, 1963).

2. Chandrasekhar, S., Radiative Transfer (Oxford University Press, London, 1950), 1st ed.

3. Cornu, M.A., Observations relatives à la couronne visible actuellement autour du soleil, Comptes Rendus, Acad. Sci., Paris 99, 488 (1889).

4. Coulson, K.L., Characteristics of the radiation emerging from the top of a Rayleigh atmosphere; I - pp. 265 - 276, and II - pp. 277 - 284, Planet. Space Sci. 1 (1959). The information in these reports is given in more detail in The Flux of Radiation from the Top of a Rayleigh Atmosphere (Dept. Meteorology, University of California, Los Angeles, 1959).

5. Dave, J.V. and P.M. Furukawa, Intensity and Polarization of the Radiation Emerging from an Optically Thick Rayleigh Atmosphere, Jo. Opt. Soc. Amer. 56, 394 (1966).

6. Davis, F.J., Surface Loss of Solar and Sky Radiation by Inland Lakes, Wisconsin Acad. Sci., Arts, and Letters 33, 83 (1941).

7. Deirmendjian, D. and Z. Sekera, Global Radiation Resulting from Multiple Scattering in a Rayleigh Atmosphere, Tellus 6, 382 (1954).

8. Feigelson, E.M., M.S. Malkevich, S.Ya. Kogan, T.D. Koronatova, K.S. Glazova, and M.A. Kuznetsova, Calculation of the Brightness of Light - Part 1 (Consultants Bureau, Inc., New York, 1960).

9. Fraser, R.S., Computed Intensity and Polarization of Light Scattered Outwards from the Earth and an Overlying Aerosol 54, 157 (1964).

10. Fraser, R.S., Theoretical Investigation; the Scattering of Light by a Planetary Atmosphere (TRW Space Technology Laboratories, Redondo Beach, Calif., 1964).

11. Jensen, C., Die Polarisation des Himmelslichts, Handbuch der Geophysik 8, 527 (Gebr. Borntraeger, Berlin-Zehlendorf, 1942).

12. Mullamaa, Yu. - A.R., Atlas of the Optical Characteristics of the Disturbed Sea Surface (Akademiya Nauk Estonskoi SSR, Institut Fiziki i Astronomii, Tartu, Russia, 1964). In Russian.

13. Neuberger, H.H., Arago's Neutral Point: A Neglected Tool in Meteorological Research, Bull. Amer. Meteor. Soc. 31, 119 (1950).

14. Neuberger, H.H., The Influence of the Snow Cover on the Position of Arago's Neutral Point, Bull. Amer. Meteor. Soc. 22, 348 (1941).

15. Neuberger, H.H., Studies in Atmospheric Turbidity in Central Pennsylvania (The Pennsylvania State College Studies No. 9, State College, Pennsylvania, 1940).

16. Neumann, G. and R. Hollman, On the albedo of the sea surface, Union Géodésique et Géophysique Internationale Monog. 10, 72 (1961).

17. Powell, W.M. and Clarke, G.L., The Reflection and Absorption of Daylight at the Surface of the Ocean, Jo. Opt. Soc. Amer. 26, 111 (1936).

18. Sekera, Z. Recent developments in the study of the polarization of skylight. In: Advances in Geophysics, v. 3 (Academic Press Inc., New York, 1956).

19. Sekera, Z. The effect of sea surface reflection on the sky radiation, Union Géodésique et Géophysique Internationale Monog. 10, 66 (1961).

20. Soret, J.L., Influence des surfaces d'eau sur la polarisation atmosphèrique et observation de deux points neutres à droite et à gauche du soleil, Comptes Rendus 107, 867 (1888).